INSTITUT DE GEOLOGIE

Thèse de doctorat présentée par Nicolas P. Badertscher à l'Université de Neuchâtel, Faculté des Sciences, Institut de Géologie

-Octobre 2001-

Jury de Thèse:

Prof. Martin Burkhard (Neuchâtel)	Directeur
Dr. Andrew McCaig (Leeds, UK)	Co-directeur
Dr. Rainer Abart (Graz, Autriche)	Examinateur
Prof. Stefan M. Schmid (Bâle)	Examinateur
Prof. Angelika Kalt (Neuchâtel)	Examinateur

IMPRIMATUR POUR LA THESE

Deformation mechanisms and fluid flow along the Glarus overthrust, eastern Helvetic Alps, Switzerland

de M. Nicolas Badertscher

UNIVERSITE DE NEUCHATEL

FACULTE DES SCIENCES

La Faculté des sciences de l'Université de Neuchâtel sur le rapport des membres du jury,

Mme A. Kalt et MM. M. Burkhard (directeur de thèse), R. Abart (Graz A), S. Schmid (Bâle) et A. McCaig (Leeds, UK)

autorise l'impression de la présente thèse.

Neuchâtel, le 9 novembre 2001

Le doyen:

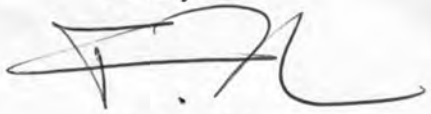

F. Zwahlen

Ce travail est dédié à mes parents

Cover picture : Panorama of the Hausstock with Baba invading the Glarus overthrust area; starship from the Herbie Hancock Album “THRUST”

Remerciements

Une tranche de vie s'achève ! Un voyage géologique international et cosmopolite qui traversa notre belle capitale, la Suisse primitive, l'Autriche orientale, le Grand Nord anglais et le Québec.

Heureux qui comme Ulysse a fait un long voyage….

Merci Martin pour ton enthousiasme, avec toi la géologie devient passion. Merci pour les cafés, le Schappziger, les vertiges sur le Piz Dolf et le Ringelspitz et pour tous ces moments privilégiés partagés sur le terrain et au laboratoire. Merci pour ton enseignement, pour m'avoir apppris que jaune sur bleu valait mieux que blanc sur rouge, il ne me reste qu'à trouver du vin bleu. Si j'étais un Jedi tu serais mon Yoda.

Merci Rainer pour ton enseignement de la géochimie isotopique travesti en discussion par une humilité et une conviavialité infini. Tu as été mon guide dans les couloirs obscurs des fronts isotopiques. Merci aussi pour toutes ces analyses conduites en un temps record. Merci à toi et à toute la Smala de Graz (Lore, Micha, Erwin et sa famille) pour votre merveilleux accueil lors de mon séjour à Graz et pour l'initiation à la Kürbiskernöl.

Merci Andrew et toute ta famille de m'avoir accueilli au pays de 007. Merci pour les matches à Sheffield, ce but marqué restant le dernier de ma carrière, pour le régime forcé involontaire mais si efficace. Merci Andrew de m'avoir accueilli au sein de ton laboratoire et pour les discussions enrichissantes. Merci enfin pour cette excursion aux Pyrénées, qui malgré ma flemme reste un souvenir impérissable.

Merci Georges de m'avoir acueilli et si bien encadré dans ce beau pays, le Québec. Grâce à toi j'ai connu la modélisation mais aussi la poutine, les baleines dans le St-Laurent, les bidochons sur les bateaux sur le Saint-Laurent, la ville de Québec et une équipe de chercheurs conviviaux et efficaces avec lesquels travailler et ne pas travailler a été un plaisir incommensurable. Grazie Mille René, Yan, Jonathan, Pierre and Cie. Vive le Québec libre !!

Merci à toutes les personnes qui ont de près ou de loin participé à l'acquisition de données, l'aide et la gentillesse rencontrée n'ayant d'égale que la Finale de la coupe du Monde de football en 1970 au Mexique: Karl Ramseyer à la cathodoluminescence, Steve Burns au spectromètre de masse, Bob Cliff, Rod Green et Phile Guise au spectromètre de masse aussi, Massoud Dadras au polissage et au E S E M, Michèle Vlymant au S E M, Marco Herrwegh pour l'enseignement de l'utilisation d'un S E M, Thierry Adatte aux RX, Mac Magrandville aux lames minces, Mr Galetti aux XRF, Jean-Mi à la guitare...

Une thèse ce n'est pas que des isotopes, quelques lames minces et 3 analyses XRD, mais aussi des discussions animés pouvant se finir aux poings (pas dans mon cas car je suis trop fort pour les autres), des excursions sur le terrain ou dans le subconscient des étudiants, des moments de gross Rikolade (ein gross bier damit) qui font que finalement on se souvient que avant tout nous sommes des êtres humains voués à partager notre vie avec nos semblables ou à sombrer dans un comportement associal qui génère des scientifiques perdus et ennuyants. Alors pour ceci et cela :

Merci à Didier Marquer pour plein de choses que je me rappelle plus bien de tous les détails, à Gregy pour les grappas, les Schniposaco et son pied au cul qui a su me remettre en place, à T. Adatte dit Sonny RX pour la distraction qu'il sait insuffler par son humour débordant et particulièrement ses gags sur Mr. Piccard et encore désolé pour le gîte dans le Vercors.

Merci à tous les étudiants (même les cancres), assistants et maître-assistant avec qui partager ces quatres années de dure labeur et particulièrememement les séances de musculation du biceps fut une expérience parfois psychédélique mais surtout exceptionnelle. Qu'est-ce qu'on rigole avec vous alors !!!

Merci le clan Challandes, les potes genre Poulmann (inoubliable Ethiopie), Verdâtre (pour les conseils informatiques), Barbsch (pour le foot sur grand écran), l'Apex en Pyrex (quelles belles vacances en Bretagne), Val et Alain et Bébés (ceux qui vendent des sacs qui font qu'on a pas froid la nuit en montagne), Niklette et son épouse de dans deux ans (pour les gilets), Fedy dit la CHICHA, Rapou le gaz qui part, Bast et Karine, DJ enverlent, et les autres dont la liste serait vraiment vachement longue et pour une question d'économie de papier je peux pas tous vous citer sinon je vais me faire taper sur les doigts pour cause de gaspillage; grâce à vous la Vita es bella !!

Enfin last but not least, comment oublier ceux qui connaissent mieux que quiconque la face cachée de la Lune et qui sont et resteront toujours les fondations d'une vie heureuse. Alors Merci à toute ma famille, Willy, Ninja, Lego et Séverine, Kataboulsk, Teufeulzeu et Fofie pour leur soutien si précieux et Merci au Canard qui sait battre des ailes au bon moment, quand son ours de BABA risque de l'écraser.

ABSTRACT

The study of deformation mechanisms and fluid flow associated with the activity of a major alpine fault has been undertaken along the famous Glarus overthrust in the Helvetic Alps of eastern Switzerland. Investigations of deformation mechanism have been concentrated on the Lochsitenkalk (LK) through study of microstructures and microtextures. Fluid-rock interactions have been studied by defining the oxygen, carbon and strontium isotope systematics along the thrust within the LK on more than 50 sampling sites and on 10 vertical profiles across the thrust. The aim of the present work is to solve the mechanical paradox of the Glarus thrust and to define fluid flow pathways and parameters. I propose a new geological history in which deformation mechanisms and fluid flow are intimately linked.

SEM, CL and optical microscopy studies on Lochsitenkalk (LK) document the alternate activity of brittle and ductile deformation mechanisms together with dissolution-recrystallization processes. Plastic intracrystalline deformation mechanisms such as dislocation glide and dislocation creep are associated with dynamic recrystallization. These observations are incompatible with the idea of a dominant superplastic deformation mechanism active in the Lochsitenkalk during thrusting. I propose that the 35 km of northwards thrust translation of the Glarus nappe has been accommodated by a combination of ductile intracrystalline deformation mechanisms in the LK and hangingwall and of brittle deformation concentrated in the LK. Foliated gouge texture in the Lochsitenkalk results of seismic failure triggered by high fluid pressure.

Oxygen, carbon and strontium isotope systematics document two regions of different flow regimes along the Glarus thrust. South of the carbonate-flysch boundary in the footwall, fluids with an $\delta^{18}O$ of about 6‰ (SMOW), an $\delta^{13}C$ of -5‰ (PDB), and a $XCO_2 << 0.1$ were channelized along the thrust in a partly pre-existing carbonate. Northward transport was accomplished by coupled advection and hydrodynamic dispersion processes. A time-integrated fluid flux (TIFF) of 4500-9100 m^3/m^2 has been calculated. This is much larger than the downward cross-thrust flow component documented on vertical profiles for which a TIFF of 3.45 to 5.7 m^3/m^2 has been calculated. This vertical flow corresponds to a lateral downward seepage of channelized fluids. In the northern areas, fluids derived from the dewatering flysch and saturated in calcite flowed upwards and precipitated calcite veins at the thrust contact

before pervasively infiltrating the Verrucano. These fluids are characterized by an $\delta^{18}O$ of about 15‰ (SMOW) and a X_{CO_2} = 0.3-0.4.

A three-dimensional finite-element model that simulates fluid flow, advective-dispersive oxygen isotope transport and reaction in porous media with different hydrologic properties is applied to reproduces regional oxygen isotope zonation in the LK along the thrust plane. In light of these simulations, critical parameters responsible for fluid flow pathways along the Glarus overthrust are inferred. For an oxygen isotope exchange front to develop in the LK in the southern part of the thrust, the contrast of permeability between the LK and the surrounding rocks must be at least 100:1 and a high hydraulic head has to exist for the fluids to be channelized in the LK. In the north, the upward flow component can only exist if fluids are pumped upwards by a drain at the top of the modelled slab.

In the alpine accretionary wedge, the crystalline basement, situated in the root zone of the Glarus thrust, is subject to dehydration that produces large amount of fluids that tend to escape upwards along shear zones. When they reach the Glarus thrust, these fluids are channelized along the thrust contact due to a high permeability contrast (100X) between the LK and its surrounding rocks in the southern portion of the thrust. In the northern part, the flysch sequence is also dehydrating in response to the increasing tectonic load. The advancing thrust pierces the brittle-ductile boundary in the north and in the hangingwall provoking the upwards pumping of fluids from the flysch due to extremely high hydraulic gradients, even if the Verrucano remains much more impermeable than the footwall flysch, thus representing a permeability barrier to the upwards percolation of fluids. In analogy to the fault-valve scenarios, fluid pressure would increase at the thrust contact up to the threshold for hydro fracturing, seismic slip and cataclastic deformation. Due to the opening of fractures, fluid pressure would drop and fracture would heal leading to the formation of veins that progressively seal the fractures, allowing fluid pressure to build up again. Between fracture events, plastic intracrystalline deformation mechanisms occur.

Résumé

L'étude des mécanismes de déformation et des circulations de fluides associés à l'activité d'une faille alpine majeure a été entreprise le long du fameux chevauchement de Glaris dans les alpes helvétiques de Suisse orientale. Les recherches sur les mécanismes de déformation ont été concentrées dans la Lochsitenkalk (LK) par l'étude des microstructures et des microtextures. Les interactions entre roches et fluides ont été étudiées à l'aide des patrons isotopiques de l'oxygène, du carbone et du strontium définis dans la LK le long du chevauchement de Glaris sur plus de 50 sites et sur environ 10 profils verticaux à travers le chevauchement. Le but du présent travail est de proposer une alternative au paradoxe mécanique du chevauchement de Glaris et de définir les patrons et paramètres des circulations de fluides. Je propose aussi une nouvelle histoire géologique du chevauchement de Glaris dans laquelle mécanismes de déformation et circulation de fluides sont intimement liés.

Les observations par microscopie optique, cathodoluminescence (CL) et microscopie électronique à balayage (SEM) sur des échantillons de LK ont révélé une alternance de mécanismes de déformation ductile et cassant ainsi que l'activité de processus de dissolution-recristallisation. Une intense recristallisation dynamique est associée aux mécanismes de déformation ductile intracristallins tels que le glissement de dislocations. Ces faits sont incompatibles avec l'idée d'un mécanisme de déformation superplastique dominant dans la LK lors du chevauchement. Je propose que les 35 km de chevauchement vers le Nord aient été accommodés par une combinaison de mécanismes de déformation plastique intracristallins dans la LK et le toit du chevauchement et de déformation fragile, particulièrement concentrée dans la LK. La texture de gouge foliée typique de la LK résulte d'une fracturation sismique provoquée par une pression de fluides élevée.

Les zonations isotopiques de l'oxygène, du carbone et du strontium révèlent deux régions à régimes de circulations de fluides différents. Au sud de la limite carbonate-flysch dans le mur, des fluides avec un $\delta^{18}O$ de 6‰ (SMOW), un $\delta^{13}C$ de -5‰ (PDB), et un $XCO_2 << 0.1$ ont été canalisés le long du chevauchement dans un carbonate en partie préexistant. Le transport vers le Nord a été accompli par des processus couplés d'advection et de dispersion hydrodynamique. Un flux intégré sur le temps (TIFF) de 4500-9100 m^3/m^2 a été déterminé pour cette composante de flux, ce qui est bien supérieur au TIFF de 3.45 à 5.7 m^3/m^2 qui a été

calculé pour le flux de fluides vers le bas à travers le chevauchement documenté sur les profils verticaux. Ce flux vertical correspond à une perte latérale des fluides canalisés au niveau du chevauchement. Dans la partie Nord du chevauchement, des fluides dérivés de la déshydratation du flysch et saturés en calcite se sont échappés vers le haut et ont précipité des veines de calcite au niveau du contact avant d'infiltrer le Verrucano. Ces fluides sont caractérisés par un $\delta^{18}O$ de 15‰ (SMOW) et un X_{CO_2} = 0.3-0.4.

Une modélisation numérique 3D par éléments finis qui simule la circulation de fluides, le transport par advection et dispersion des isotopes de l'oxygène et les réactions en milieux poreux avec différentes propriétés hydrologiques a été menée afin de reproduire la zonation isotopique régionale de la LK le long du plan du chevauchement. Ainsi, les paramètres critiques responsables des patrons de circulation de fluides peuvent être déduits. Pour qu'un front isotopique se développe dans la partie sud du chevauchement, le contraste de perméabilité entre la LK et les roches en contact direct doit être de 100:1 au minimum et une forte charge hydraulique doit exister au point d'infiltration à l'extrême sud afin que les fluides restent canalisés dans la LK. Dans la portion Nord, la composante de flux vers le haut ne peut exister que si les fluides sont pompés par un drain au sommet de la portion crustale modélisée dans le Verrucano.

Dans le prisme d'accrétion alpin, le socle cristallin du Massif de l'Aar, situé dans la zone de racines du chevauchement de Glaris, se déshydrate et produit ainsi de grandes quantités de fluides qui ont tendance à s'échapper vers le haut le long de zones cisaillement raides. Quand ils atteignent le chevauchement de Glaris proprement dit, ces fluides sont canalisés le long du plan de chevauchement dans sa partie sud grâce à un contraste de perméabilité élevé (100X) entre la LK et les roches environnantes. Dans la portion nord, la séquence de flysch se déshydrate aussi par enfouissement progressif. Lorsque le chevauchement en plein avancement perce la limite fragile-ductile au Nord et dans le toit, les fluides vont être pompés vers le haut à partir du flysch à cause de gradients hydrauliques extrêmes, bien que le Verrucano reste très peu perméable représentant une barrière potentielle à la percolation de fluides. Par analogie au scénario de faille-valve, la pression de fluide augmentait au contact jusqu'au seuil de fracturation, de glissement sismique et de cataclase. L'ouverture de fractures provoque la chute de la pression de fluide dans ces dernières

induisant la précipitation de calcite qui scelle ces fissures permettant une nouvelle montée de la pression de fluides. Entre les événements de fracturation, la déformation ductile intracristalline prend le relais.

RIASSUNTO

I meccanismi di deformazione e il flusso di fluidi associati all'attività di una faglia maggiore sono stati studiati lungo il famoso sovrascorrimento del Glarus, Alpi Elvetiche, nella Svizzera Orientale. I meccanismi di deformazione sono stati studiati specialmente all'interno della formazione del Lochsitenkalk (LK) grazie allo studio di microstrutture e micro testure. Le analisi degli isotopi dell'ossigeno, del carbonio e dello stronzio, effettuate su oltre 50 siti e su 10 profili verticali attraverso il sovrascorrimento, hanno permesso di definire le interazioni tra fluidi e roccia all'interno del LK. Lo scopo di questo studio e' di risolvere il paradosso meccanico del sovrascorrimento del Glarus e di individuare le traiettorie e i parametri che definiscono il flusso dei fluidi. I risultati ottenuti permettono di proporre una nuova "evoluzione" geologica, in cui i meccanismi di deformazioni sono intimamente connessi al flusso dei fluidi.

Analisi di microscopia ottica, SEM et CL indicano che i meccanismi di deformazione, duttile e fragile, hanno agito di pari passo con i processi di dissoluzione e recristallizzazione. I meccanismi di deformazione plastica intracristallina, come la dislocazione sia per "glide" che "creep", sono associati alla ricristallizzazione dinamica. Queste osservazioni sono in contraddizione con la teoria di una deformazione superplastica dominante nel LK durante il processo di raccorciamento. Noi proponiamo che la dislocazione di 35 km verso nord della nappa del Glarus sia stata accomodata attraverso un meccanismo di deformazione duttile intracristallina nel LK e nel tetto, e di deformazione fragile concentrata nel LK. La testura foliata a "gouge" nel LK e' il risultato di collasso sismico innescato dai fluidi ad alta pressione.

La distribuzione degli isotopi dell'ossigeno, carbonio e stronzio indicano l'esistenza di due regioni a differente regime idraulico nella regione del sovrascorrimento del Glarus. A sud del limite carbonati-flysch, i fluidi, caratterizzati da un $\delta^{18}O$ di circa 6 ‰ (SMOW), da un $\delta^{13}C$ di -5‰ (PDB), e da un $XCO_2 << 0.1$, sono canalizzati lungo il sovrascorrimento attraverso i carbonati in parte pre-esistenti. Il trasporto verso nord e' poi realizzato attraverso processi di advezione e di

dispersione idrodinamica. Il flusso idraulico integrato nel tempo (TIFF) e' stato estimato a 4500-9100 m^3/m^2 . Questa stima e' di molto superiore alla componente del flusso discendente attraverso il sovrascorrimento, documentata da profili verticali, per la quale un TIFF variabile tra 3.5 e 5.7 m^3/m^2 e' stato calcolato. Questo flusso verticale corrisponde all'infiltrazione laterale discendente di fluidi canalizzati. Nell'area settentrionale, i fluidi ascendenti, saturi in carbonati e derivanti dalla desidratazione del flysch, prima di infiltrarsi nel Verrucano e al contatto con il sovrascorrimento, precipitano vene di calcite. Questi fluidi sono caratterizzati da un $\delta^{18}O$ di circa 15 ‰ (SMOW) e da un $XCO_2 = 0.3 – 0.4$.

La zonazione regionale che caratterizza gli isotopi dell'ossigeno nel LK lungo il piano del sovrascorrimento sono state riprodotte da un modello tridimensionale a "elementi finiti" che simula il flusso idraulico, il trasporto advettivo-dispersivo degli isotopi dell'ossigeno e le reazioni in mezzi porosi a differenti propietà idrauliche. Queste simulazioni hanno evidenziato i parametri critici responsabili delle traiettorie dei flussi lungo il sovrascorrimento del Glarus. Affinché un fronte di scambio per gli isotopi dell'ossigeno possa svilupparsi nel LK nella regione meridionale del sovrascorrimento, il contrasto di permeabilità tra il LK e le formazioni circostanti deve essere dell'ordine di 100:1 e allo stesso tempo deve esistere un fronte idraulico ad alta pressione affinché i fludi possano canalizzarsi nel LK. Al nord, la componente ascendente del flusso puo' esistere solo se i fludi sono spinti verso l'alto da un drenaggio posto in cima al modello.

Nel prisma di accrezione alpino, la desidratazione che interessa il basamento cristallino, situato nella zona di radice del sovrascorrimento del Glarus, produce larghe quantità di fluidi che tendono a fluire verso l'alto lungo le zone di shear. Nella zona meridionale, raggiunto il sovrascorrimento del Glarus, questi fluidi sono canalizzati lungo la zona di contatto del sovrascorrimento, a causa dell'alto contrasto di permeabilità (100X) tra il LK e le formazioni circostanti. Nella regione settentrionale, anche il flysch e' desidratato a causa dell'aumentato carico tettonico. Il sovrascorrimento, avanzando, supera il limite fragile-duttile al nord e nel tetto.

A causa dell'alto gradiente idraulico, questa situazione provoca una risalita di fluidi dal flysch, anche se il Verrucano, molto meno permeabile del flysch al muro, rappresenta una barriera all'infiltrazione ascendente dei fluidi. Analogamente ad una "faglia a valvola", la pressione dei fluidi aumenta al contatto del sovrascorrimento fino a valori limite che provocano fratturazione idrica, scorrimento sismico e deformazione cataclastica. Le fratture createsi, che inizialmente favoriscono la diminuzione della pressione dei fluidi, vengono in un secondo momento richiuse dalla formazione di vene, permettendo cosi' alla pressione idrica di aumentare di nuovo. Tra due eventi di fratturazione, la deformazione plastica intracristallina e' in atto.

TABLE OF CONTENTS

CHAPTER I: INTRODUCTION

CHAPTER III: FLUID FLOW PATHWAYS ALONG THE GLARUS OVERTHRUST DERIVED FROM STABLE AND Sr-ISOTOPE PATTERNS, paper submitted to American Journal of Science

APPENDIX

Chapter 1: Introduction

Geographical localisation

The studied area is located in the Alps of eastern Switzerland in the Glarus and Grison canton between the city of Glarus in the North and the city of Flims in the south (Fig. 1). It covers an area of 15 km in the N-S direction by about 20 km in the E-W direction and is limited to the West by the Klausenpass and to the East by the Foostock Mountain. The Glarus overthrust is magnificently

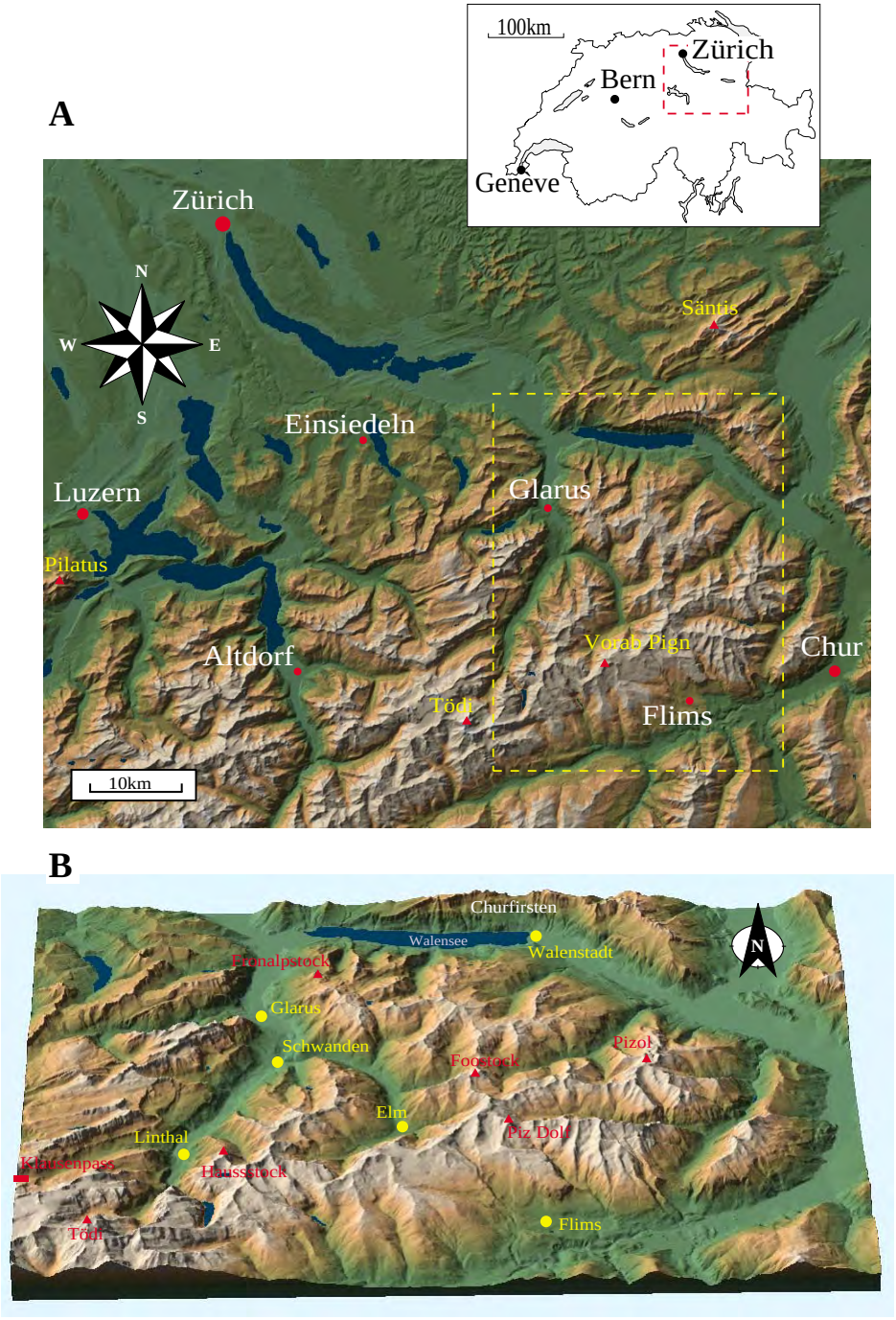

Fig. 1
Localisation and 3D relief of the study area in the Glarus Alps. (A) Hypsometric map of the Helvetic Alps of eastern Switzerland localized on the simplified map of Switzerland by a red rectangle. (B) 3D relief bloc-diagram of the study area. In the southern part, the Glarus overthrust follows approximately the crest between Hausstock and Piz Dolf and further East before plunging toward the North and disappearing below topography at the latitude of Schwanden.

exposed on steep mountainsides, rising from the Valley of the Anterior Rhine to 2600-3000 m and then gently descending northward to about 600 m at Schwanden where it disappears below the topography.

Geological setting

The Helvetic nappes of the Glarus Alps are derived from the Mesozoic passive margin of Europe and from the most internal parts of the Paleogene foreland basin. They represent a perfect example of décollement nappes of which the Glarus overthrust is the basal thrust (Fig. 2). The latter divides the tectonic units in two compartments, the Infrahelvetic complex (Milnes and Pfiffner 1977) below and the Helvetic nappes above (Fig. 2B). From cross-section balancing considerations, a minimum northward displacement of 35 km can be calculated and it is clear that the thrust must extend to mid-crustal levels some 20 km south of the southernmost exposures (Pfiffner 1985). The thrust surface is preserved as an exceptionally sharp horizon that is marked by a calc-mylonite, the so-called Lochsitenkalk, over most of its extent.

In the footwall of the Glarus overthrust, the Infrahelvetic complex consists, from bottom to

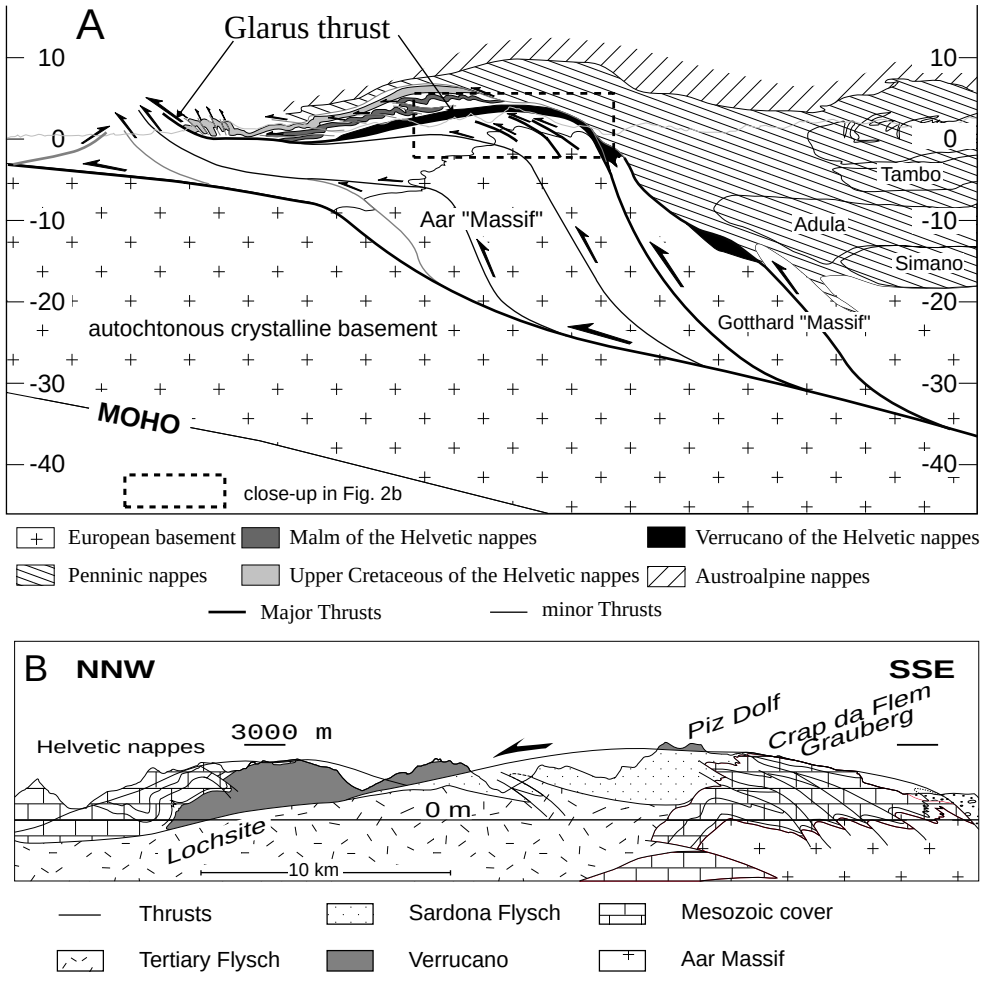

Fig. 2
(A) NNW-SSE crustal cross-section through the eastern Alps of Switzerland (redrawn after cross-section by Pfiffner (1993) and Schmid et al. (1997)). The accessible part of the Glarus overthrust is indicated within the box.
(B) Cross section of the Glarus Alps in eastern Switzerland (according to Oberholzer (1933). Some sampling sites are indicated.

top, of (Fig. 2B/3):

(1) a thick skinned series of imbricates where the Aar massif basement is involved in thrusting and intense folding together with its cover of parautochthonous Mesozoic and Eocene sediments.

(2) the North-Helvetic flysch. The contact between the flysch and the Eocene shales is frequently of tectonic nature (Frey 1965).

(3) South-Helvetic to Penninic "exotic" flysch (Blattengrat and Sardona sheets) that was emplaced over the North-Helvetic flysch during early Oligocene times. The precise paleogeographic origin within the Valais through of the Sardona nappe remains uncertain.

The hangingwall is composed of the Permian Verrucano formation, a clastic series of predominantly siltstones and shales with some conglomeratic units and rare volcanoclastic horizons that were deposited in a Permian graben. This "inverted Verrucano basin" is overlain by a concordant Mesozoic series (Fig. 2/3) overridden by structurally higher Helevtic nappes (Axen and Säntis) composed of Mesozoic limestones and marls. This Helvetic complex is overlain by Penninic and Austroalpine nappes (Fig. 2A). Tectonic structures in the Helvetic nappes are influenced by the paleogeographic pattern: the thickening of the Mesozoic series southward and the replacement of limestones by shales on the one hand (Pfiffner 1993), the existence of a E-W trending late Variscan graben on the other hand, the northern boundary of which acted as a lateral ramp during alpine collision.

Cinematics of the Infrahelvetic and Helvetic complexes have well been defined by the studies of Pfiffner (1977; 1978), Schmid (1975) and Siddans (1979), who named a number of phases:

(1) Pizol phase: emplacement of the "exotic" South Helvetic Blattengrat and Penninic Sardona sheets onto an erosion surface of the North-Helvetic flysch during early Oligocene times.

(2) Calanda phase (including the somewhat earlier Cavistrau phase (Trümpy 1991)): folding and imbrications of the whole Infrahelvetic complex with development of a penetrative cleavage.

(3) Ruchi phase: thrusting of the Glarus nappe and the final emplacement of the different Helvetic nappes. A very penetrative schistosity developed in the Verrucano hangingwall (attributed to the Calanda phase by Pfiffner (1977; 1978)) together with other structures such as shear bands, crenulations, N-S stretching lineation. The cleavage in the Infrahelvetic complex is refolded or reoriented parallel to the thrust in the last 5 meters before the contact.

Despite this out-of-sequence character, the Glarus thrust generally cuts up-section from South to North. In the southernmost exposures, Verrucano is thrust over parautochthonous late Jurassic and Early Cretaceous limestones, whereas further north it overlies an up to 2 km thick sequence of flysch (Fig. 2B).

Regional metamorphic conditions in the Glarus Alps have been reviewed by Frey (1988). Metamorphic grade ranges from anchizonal (about 200°C) in the North and in the footwall flysch to lower greenschist facies conditions in

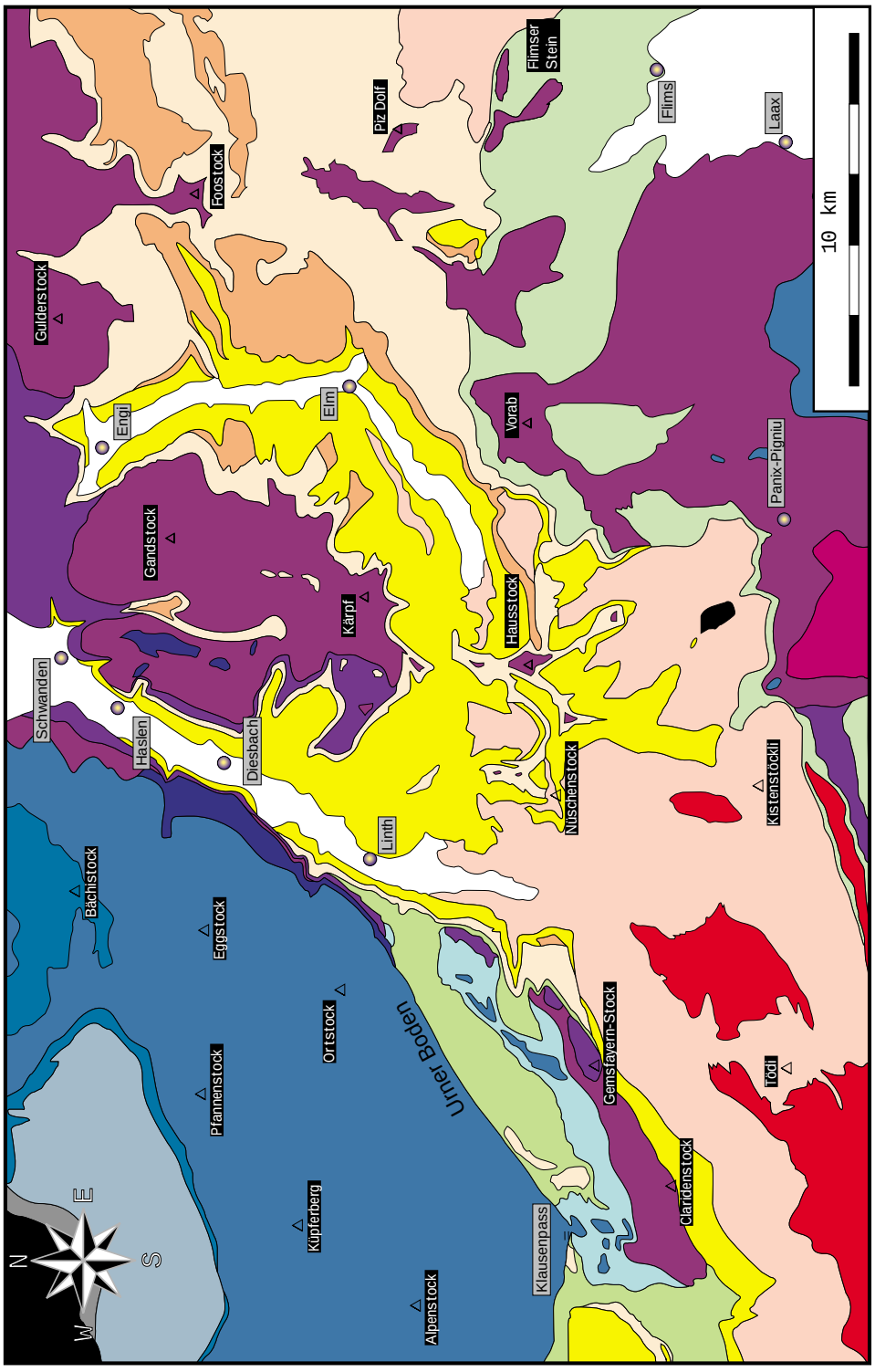
Ultrahelvetic nappes
Sardona Flysch
Blattengratt Flysch
Helvetic and autochthonous nappes
Säntis-Drusberg nappe
Säntis-Drusberg nappe
Richisauer slice
Axen nappe
Silbern-Toralp nappe
Bächistock nappe
Axen s. str. nappe
Braunwald slice
Subhelvetic nappes
Mürtschen and Kammlistock nappe
Basement of the Murtschen nappe
Glarus nappe
Parautochthonous nappes
Claridenring slices
Griesstock nappe
Vorab-Tschepp nappes
Sedimentary cover
Post-Eocene Flysch
Trias-Eocene
Aar Massif
Autochthonous and parautochthonous basement
N
S
W
E
Guldenstock
Engi
Foostock
Piz Dolf
Flimser Stein
Flims
Laax
Elm
Vorab
Gandstock
Kärpf
Hausstock
Schwanden
Haslen
Diesbach
Linth
Nuschenstock
Panix-Pigniu
Kistenstöckli
Bächistock
Eggstock
Pfannenstock
Ortstock
Urner Boden
Gemsfayern-Stock
Tödi
Claridenstock
Küpferberg
Klausenpass
Alpenstock
10 km

Fig. 3
Tectonic map of the Glarus Alps in eastern Switzerland. Modified after Oberholzer (1933).

the south and in the Verrucano, as determined from illite crystallinity, mineral parageneses, vitrinite reflectance and fluid inclusions. The anchizone-epizone boundary is offset by about 2 km along the Glarus thrust due to post-peak metamorphism thrusting (Groshong et al. 1984; Frey 1988). Peak metamorphic conditions were reached after the Calanda deformation phase (Groshong et al. 1984; Pfiffner 1985), based on the post-kinematic growth of chloritoïd within Triassic shales in the footwall of the thrust. The age of peak metamorphism has been determined by Hunziker et al. (1986) and Hunziker (1987) at about 30 Ma within the Verrucano and Helvetic nappes. Translation along the Glarus thrust, as dated from one Lochsitenkalk sample, persisted until at least 23 Ma (concordant K/Ar and Rb/Sr ages of illite<2mm). This late Oligocene age for thrusting of the Glarus nappe is considered older than the final emplacement of the frontal parts of the Säntis thrust sheet, which is thought to represent the frontal emergence of the Glarus overthrust.

Historical review: the Glarus overthrust, a controversy of a century ago

The story of the discovery of nappes in the Glarus Alps has been told several times (Heim 1921; Bailey 1935; Staub 1954; Trümpy 1991). The following lines are strongly inspired from the paper of Trümpy (1991), in which he discusses the controversy between the tenants of nappes as overfolds and those of nappes as thrust sheets. This involves the evaluation of the role of ductile versus brittle deformation that corresponds to the confrontation between two geologists: Albert Heim of lasting fame and August Rothpletz almost forgotten.

Hans-Conrad Escher very early (1809) noted an anomaly in the Glarus Alps: the Grauwacke of the Glarus Alps (Verrucano) was lying above the Alpenkalk (Mesozoic limestones). But Leopold von Buch, the reference geologist called him to order that the Grauwacke must lie below the Alpenkalk, otherwise it is not the Grauwacke. The discovery of the Glarus thrust cannot be attributed to H-C. Escher, but he was certainly the first to realize that the stratigraphic succession in the Glarus mountains was not conform to the accepted model.

Arnold Escher, H. -C. Escher's son and first professor of geology at the ETHZ, began his studies in the Glarus Alps in 1839. By then the biostratigraphic dating of formations had made rapid progress. He recognized that the Verrucano was overlain by Jurassic and Cretaceous formations, and hence must be older than the overridden flysch. He expressed his qualms about accepting the existence of such an outrageous structure in his paper of 1846. In 1848, Escher led Sir Roderick Impey Murchinson over the Segnespass, who produced the clearest statement on the existence of a large overthrust (Fig 4):

"The lowest visible strata are schists and Glarus slates[1] …The flysch continues to be the chief rock of the mountains until you reach the depression in the high ridge, where the track passes into the Grisons……Widening to about 100 feet or more to the southwest of the mountain pass, this flysch is then directly surmounted by a mass of hard grey subcrystalline limestones[2] …This limestone is,…,.continuously superposed to the flysch in irregular thicknesses, and more or less in a tabular position…Now, this limestones is in its turn distinctly overlaid by a zone of talc and mica schist[3] …This uppermost rock...lie beneath the whole secondary series."

And further

"It became necessary to admit that the strata had been inverted, not by frequent folds, as on the sides of the lake of Altorf or in the Hoher Sentis, but in one enormous overthrow; so that over the wide horizontal area above-mentioned, the uppermost strata which might have been lying in troughs or depressions due to some grand early plication[4] were covered by the lateral extrusion over them of older and more crystalline masses."

Murchinson was thus convinced by the existence of a large overthrust. Another geologist, (Theobald 1866; 1869) working in the eastern Glarus Alps, accepted the presence of a single S-N direct overthrust.

But Arnold Escher continued to harbour his doubts, afraid by the consequences of his observations in terms of shortening. At the annual assembly of the Swiss Society of Natural Sciences in Neuchâtel, Escher (1866) finally presented his strange alternative: instead of a single thrust from the south, he imagined two recumbent overfolds, one from the south and one from the north, facing each other above a tobacco-pouch syncline of flysch (Fig.5). This was the origin of the Glarus Double Fold (Doppelfalte), a complete monstruosity since all structures were north facing.

Albert Heim (1839-1937), elected successor to his mentor Escher at the age of 23, became the dominating figure of swiss geology for almost 50 years. Heim had a gift for the understanding of basic mechanisms such as deformation of rocks.

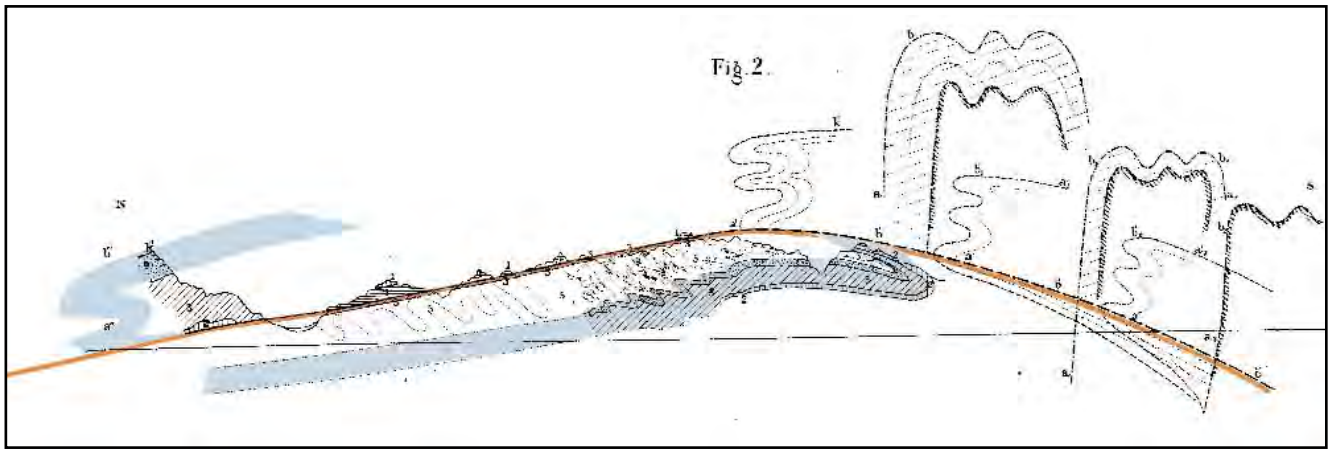

Fig. 4
Geological observations and interpretations of Murchinson along the Glarus overthrust. The blue layer underlines the idea of a big overthrow suggested by Murchinson in 1841. Modified after Murchinson (1841).

[1]Flysch
[2]Lochsitenkalk
[3]Verrucano
[4]Calanda folding

He started his field studies in the upper Reuss Valley, in the proximal part of the Helvetic nappes. In his original study area around the Grosse Windgälle folds, ductile deformation of rocks is very conspicuous. He may later have been led by the experience of his early and most active filed years, as well as by the influence of Escher, to seek the same structural style in areas deformed under less overburden, such as the external part of the Helvetic nappes and the Jura folds.

For the regional structure of the Glarus Alps, Heim (1878) firmly upheld the Double Fold theory. The Lochsitenkalk as well as the subhelvetic slices found at the thrust contact form the inverted limb of these two folds (Fig. 5). Although Eduard Suess, after having read the paper of Bertrand (1884), tried to convince Albert Heim that the Glarus Alps were formed by thrust sheets, Heim maintained his theory.

The 1878 volumes of Heim had a tremendous impact, and the double fold theory was soon widely adopted. Heim's second major work on the problem (1891) brought few new ideas. On Flimserstein he found brownish-weathering beds between the Upper Jurassic and the Verrucano that he attributed to the middle Jurassic, confirmed by the presence of a special oyster. Rothpletz soon proved that these formations are of Cretaceous age, but Heim did not draw the consequences. On the other hand, Heim discarded Bertrand's prophetic paper (see below) and the double fold hypothesis became a dogma.

German participants of a field trip in 1890 signed a protocol attesting the validity of Heim's observations and inferences. This was done eight years after Rothpletz's recognition of thrusts not connected with folds, seven years after Bertrand's great reinterpretation, and 11 years before Heim rallied to the nappe theory.

August Rothpletz worked first in the northern calcareous Alps and then pursued the structures he recognized, westward into the Glarus Alps. Thus, he was more familiar with external parts of the Alps, where brittle deformation was more conspicuous than in the area where Heim had begun to study. While Heim had attached little importance to fault structures, Rothpletz saw faults every-

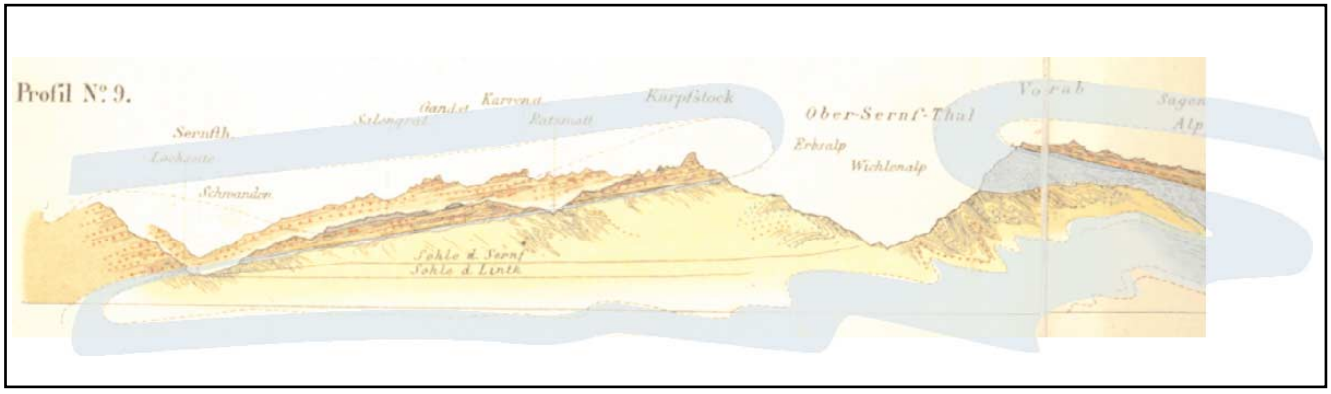

Fig. 5
Cross-section in the Glarus Alps in eastern Switzerland. The blue layer that follows the carbonate layers illustrates the Double Fold (Doppelfalte) interpretation of the Glarus Alps structure that was first proposed by Escher (1848) and then supported by Heim (1878; 1891). Modified after Heim (1891).

where, real and imaginary.

Rothpletz (1883) showed that the subhelvetic slices were more often in upright position and described the Lochsitenkalk as a fault gouge, recognizing but also exaggerating the effects of brittle deformation. He accepted the "South Fold" as a north directed recumbent fold, but interpreted the "North Fold" as a slab thrust toward the South. He saw no contradiction between the north-facing folds and the south-directed thrust movement, as he always considered the folds to predate the thrust (Rothpletz 1883; 1894).

Heim's reaction was instantaneous and virulent (1895). He attacked the weak points of Rothpletz's theory, but did not discuss the crucial observations in Bützistock and Schilt.

In a fourth book, Rothpletz (1898) combined the "South Fold" and the "North Fold" into one great overthrust sheet, but he thought that this thrust sheet had travelled from the East, inspired by the presence of almost N-S fold axis. In spite of these errors, his tectonic map looks surprisingly modern (Fig. 6).

Heim made free use of his authority to crush Rothpletz, by insisting on the weakness of some of his arguments. In fact, the views of Heim, who overemphasized ductile deformation, and the view of Rothpletz, who overemphasized brittle deformation, are complementary.

Marcel Bertrand became professor at the Ecoles des Mines in 1866. In his paper of 1883, Bertrand reinterpreted Heim's descriptions and profiles (Fig. 7), demonstrating that the obvious solution

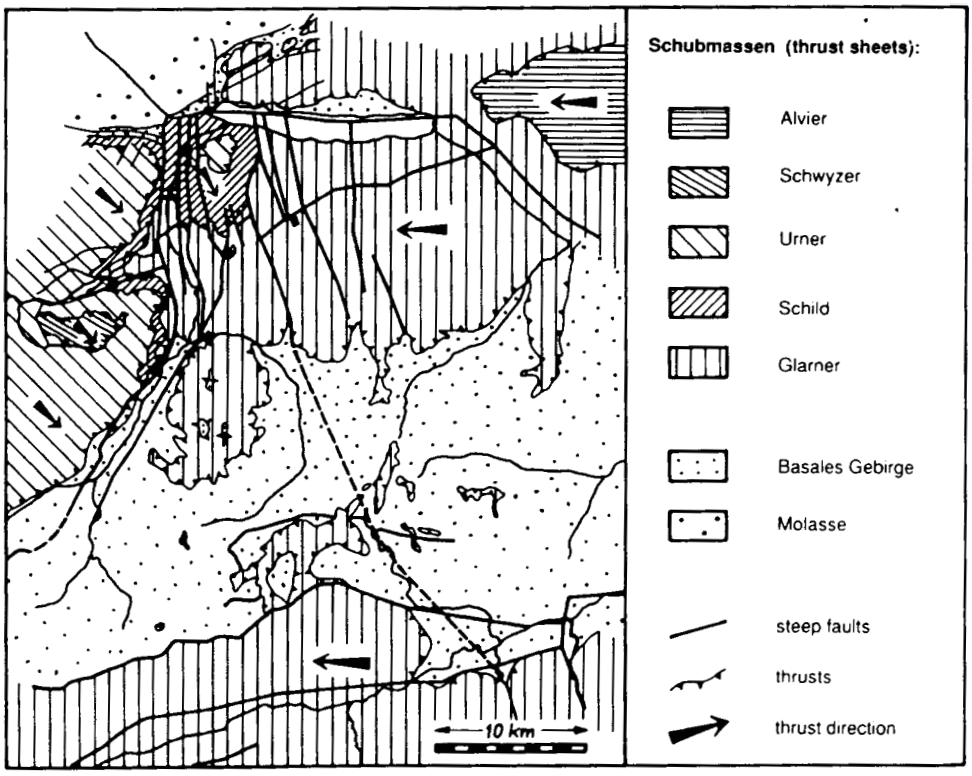

Fig. 6
Tectonic map of the Glarus Alps, copied from Rothpletz, 1898, plate 10. Compare with Fig. 3.

of the problem was to admit only one great overthrust from south to north, Murchinson's overthrow of 1849. It is hard to understand why Heim and Rothpletz took no notice of Bertrand's truly innovative paper: germanophone provincialism?? The breakthrough of the nappe theory in the Alps had to wait for another decade.

The next act of this drama was played in the Prealps by Hans Schardt who became the successor of Albert Heim in 1911. In his first paper, Schardt (1884) regarded the Prealps as autochthonous with some local thrusts toward the north and the south. Schardt (1893) realized that the Hornfluh breccias were of Jurassic age and that they were resting on Tertiary flysch. In a grand sweep, this phenomenon was extended to the entire Prealps and eventually to the northern flank of the Alps. At the same time, great thrusts had been identified in the Scottish Highlands and in Scandinavia. The nappe theory was born and applied to the Glarus thrust. In the third volume of Suess' magnificent Antlitz der Erde, which was published in 1901, the nappe theory is firmly established. Heim rallied to the new theory. This has had drastic consequences on shortening calculations and on tectonic theories.

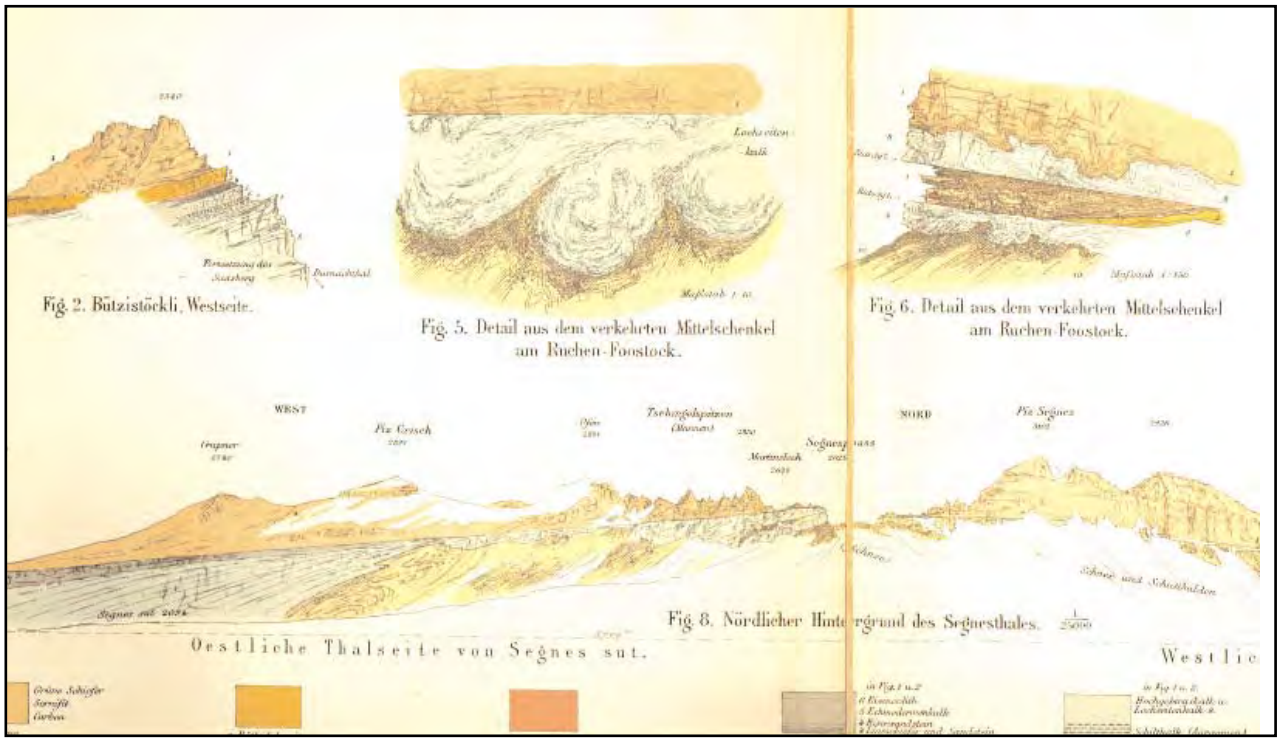

Fig. 7

Geological observations of Heim (1891) in the Glarus Alps. From left to right and top to bottom: (1) Panorama of the Bützistock, view from the West (2) Detail of the Glarus overthrust contact at Ruchen-Foostock, note the very lobate contact between the Lochsitenkalk and the flysch in the footwall. (3) Detail of the Glarus overthrust contact at Ruchen-Foostock; note the sandwiched layer of flysch or Verrucano in between two layers of Lochsitenkalk. Both upper and lower contacts of the Lochsitenkalk are cuspate-lobate. (4) Panorama of the Glarus thrust on both sides of the Segnespass, view from the south. Reproduced from Heim (1891)

Previous works: Oberholzer, Schmid, Pfiffner and Cie

The Glarus thrust has been subject of so many studies, that it is impossible to quote all of them. Only those works that contain crucial information related to the problem investigated in this study will be discussed below.

Nevertheless, it seems virtually impossible not to mention the work of Jakob Oberholzer, a schoolteacher that was married to a tiresome woman (Trümpy 1991). To escape this situation, he spent his summers in the Glarus Alps and did a tremendous job in mapping the whole region at the scale of 1:50'000. His reference book, Geologie der Glarner Alpen (Oberholzer 1933), is infinitely rich with wonderful panoramas (Fig. 8), cross-sections, maps (Fig. 3) and very detailed lithological descriptions. In his first work, Oberholzer (1908) upheld the overfold theory of his mentor Heim, but in his main work Oberholzer (1933) expressed some reservations.

A long series of studies that investigating the mechanics of the Glarus overthrust began at the end of the sixties with the paper of Hsü (1969). In order to test the hypothesis of Hubbert and Rubey (1959), who first proposed that a very high fluid pressure was necessary to allow large overthrusts to move (Fig. 9), Hsü made a mathematical analysis of the statics and kinetics of the Glarus overthrust. He concluded that the thrust translation was accomplished in two stages at least. The earlier phase of main movement was related to the flowage of the Lochsitenkalk within the thrust zone associated with a fluid pressure equal or nearly equal to lithostatic pressure and due to a horizontal push from behind. Hsü considered that the whole thrust-related deformation was concentrated within the Lochsitenkalk. The late stage of frictional sliding produced the fault gouge within the Lochsitenkalk related to an uplift of the Aar massif under normal fluid pressure in order to avoid the sliding of the block under its own weight on a downward slope. This last conclusion

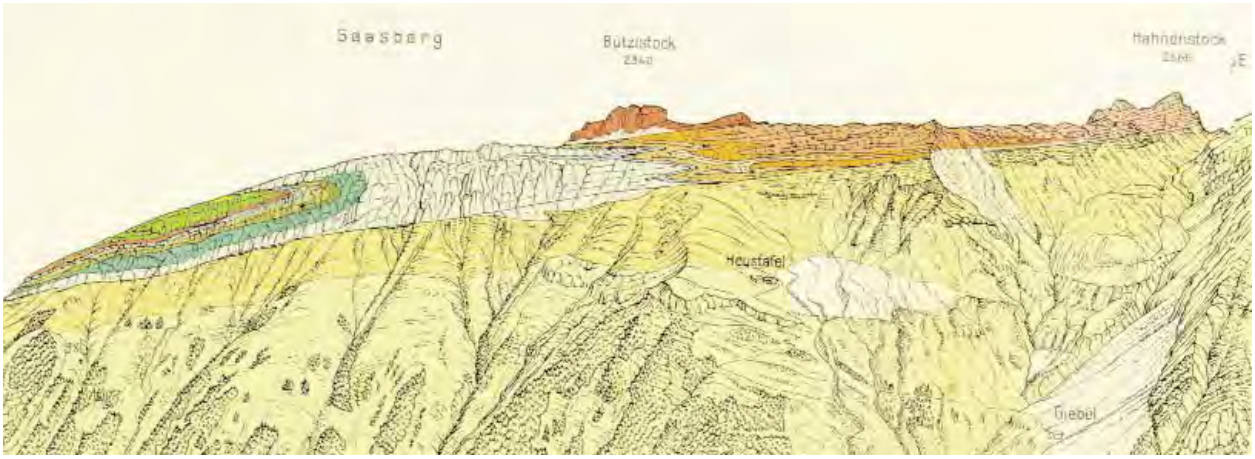

Fig. 8
Panorama of the Bützistock, view from the Southwest. Note the lateral transition from Verrucano to Mesozoic carbonates in the hanginigwall towards the west. Reproduced from Oberholzer (1933)

was based on the wrong assumption, that the arc shape of the Glarus thrust was a syn-thrust feature. Hsü calculated a movement rate of 0.2 cm/year during the first phase of translation. This paper contains some very interesting ideas such as the necessity of a very high fluid pressure to allow thrust translation along a climbing slope. But the model is complicated by the idea that part of the thrust movement took place along a downward slope due to the arc shape of the Glarus overthrust.

Schmid (1975; 1982) and Schmid et al. 1977; 1981) investigated the textures and microstructures of the Lochsitenkalk in order to assess which of the possible deformation mechanisms accommodated the thrust translation. In his first important contribution, Schmid (1975) concluded that "on the whole, the idea of an extremely ductile mylonite layer along the interface between two

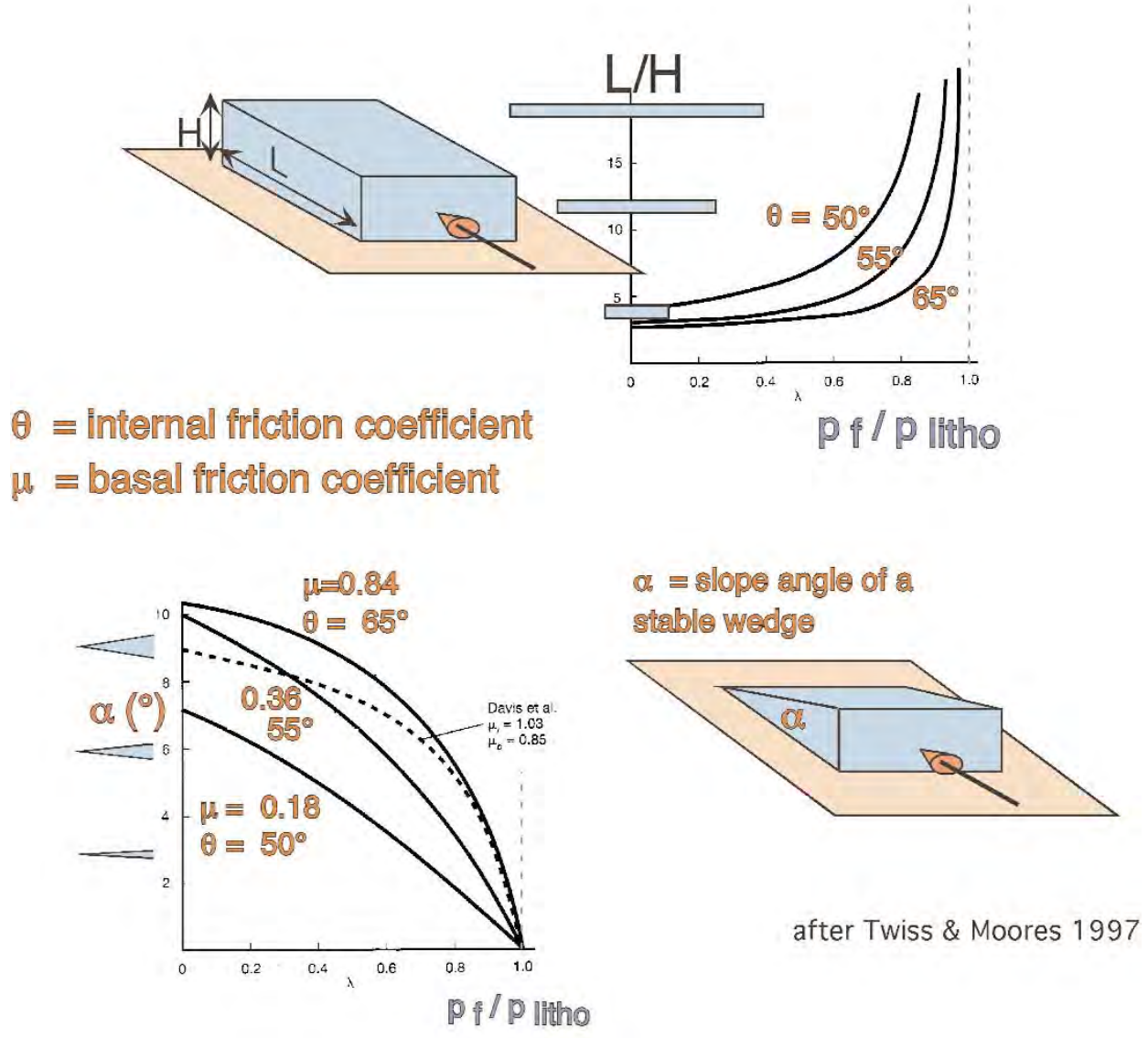

Fig. 9

Permissible geometry of thrust sheets as a function of the pore fluid pressure ratio l. Upper part: Maximum possible ration of width (L) to height (H), for a thrust sheet taped like a rectangular block, plotted a function of l. Lower part: Equilibrium surface slope (α) for a wedge-shaped thrust sheet with a horizontal décollement plotted a function of l. Modified after Twiss and Moores (1992)

more or less rigid blocks taking up all differential movement along the base of the of the upper block is correct". This conclusion is in part based on the idea that the mylonitic foliation observed in the Verrucano hangingwall predates thrusting and that thrust related structures are very weak within the footwall and hangingwall. He also calculated a thrust related strain rate of $10^{-10}sec^{-1}$. The comparison with an experimentally deformed sample of Solnhofen limestone, with a grain size similar to that of Lochsitenkalk, revealed that these rocks are much too strong to flow at such a fast strain rate. Schmid (1975) concluded that the deformation mechanisms occurring in nature and experiments must be different.

In his paper of 1977, Schmid studied the deformation mechanisms that occurred in experimentally deformed limestones. He found three regimes of creeps, the third one designed as superplastic regime that is characterized by a strong grain-size dependence, by a dominance of grain-boundary sliding, by a much weaker lattice preferred orientation and very weak shape preferred orientation compared to the two other dislocation-creep regimes. In the superplastic regime, the strain rate increases markedly with decrease in grain size at a given stress. At that time no natural occurrence of superplastic flow had been identified, but Schmid et al. (1977) states that "the fine-grained calcite mylonite …from the Glarus overthrust in the Swiss Alps…is currently being studied from this point of view."

In Schmid et al. (1981), the crystallographic orientations of calcite grains of some tectonites from the Glarus overthrust have been determined by X-ray texture goniometry. Most of the Lochsitenkalk samples were characterised by very weak textures and Schmid et al. (1981) suggest superplastic flow with grain boundary sliding as the dominant deformation mechanism, the latter being favoured by the extremely small grain size (Fig. 10). In one sample, a strong lattice preferred orientation has been identified in fine-grained matrix. Schmid et al. (1981) attributed this feature to the inheritance of a texture acquired by twinning of large intraclasts that later syntectoni-

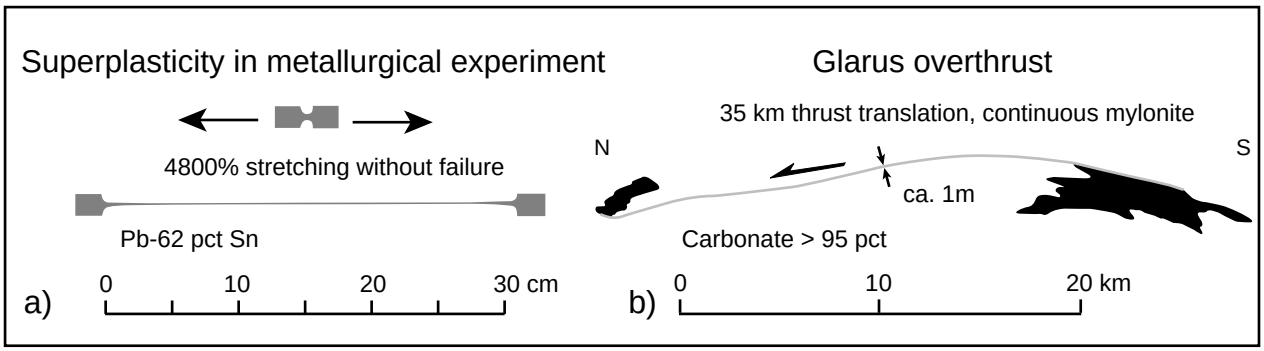

Fig. 10

Superplasticity has been proposed as an explanation for the extreme strain localization in the Lochsiten calc-mylonite (Schmid et al. 1977) a) Superplastically deformed Pb-62%Sn alloy in a metallurgical stretching experiment from Langdon (1982). b) Schematic cross section of the Glarus thrust. A metre thick calc-mylonite connects Mesozoic carbonates in the foot- and hanging-wall over a total thrusting distance of about 30 km north-south, drawn to scale, the calc-mylonite would measure less than 2 µm thin in this figure

cally recrystallized into a small-grained matrix. This led Schmid et al. (1981) to conclude that such a "recrystallisation-induced change in deformation mechanism in the Lochisten mylonite would have dramatically weakened this lubricating layer (Schmid et al. 1977) and could explain the observation that shear was confined to this extremely thin mylonite horizon in the Glarus region".

Schmid (1982) confirmed and refined these deformation processes. He produced pictures illustrating the mechanism of dynamic recrystallisation by subgrain rotation, which induces changes in grain size of the material. As the initial grain size is reduced, grain size sensitive creep may or may not take over depending on the size of the new grains and the position of the boundary between power law creep and grain size sensitive creep (superplatic flow) mechanisms (Fig. 11). He concluded that "instantaneous recrystallisation is a very unreasonable assumption from what may occur in nature. The evolution of an equiaxed fine-grained aggregate of recrystallised grains will lead to a bimodal grain size distribution: some fabric domains will be fully recrystallised while the original grain size will be preserved in other domains. This may lead to a situation where both power-law creep and superplasticity occur simultaneously in different fabric domains." Such a situation cannot be described by a single point in Fig. 11. Initially the fully recrystallised domains will be isolated and will make a small fraction of the volume of the rock. Flow will remain stable. "As the volume of recrystallised material grows, the bulk strain rate will increase and/or the bulk stress will drop due to the increasing contribution of superplastic flow to the overall deformation in the rock…In conclusion, dynamic recrystallisation will induce a change in microstructure which in turn induces a change in deformation mechanism leading to work softening… The similarity between the final microstructure of the Lochsiten mylonite and microstructure of superplastically deformed Solnhofen limestone is striking. The texture of totally recrystallised domains of the mylonite is very weak (Schmid et al. 1981). This suggests a change in mechanism into superplastic flow." **Since then, the Lochsiten mylonite will be classically considered as extremely smeared out Helvetic carbonates from the footwall or hangingwall that deformed in the superplastic regime by grain boundary sliding.**

Pfiffner (1982) investigated the textures and microstructures of the Lochsitenkalk and the Mesozoic carbonate of the underlying footwall by transmission optical microscopy and transmission electron microscopy. He noted a decrease in shape fabric toward the thrust fault that he interpreted as an increasing contribution of grain boundary sliding to the bulk deformation processes. However he distinguished between the northern and the southern section of the thrust. In the north, the absence of crystallographic texture and of shape fabric points toward grain boundary sliding in superplastic flow regime. In the southern section, the possible presence of shape preferred orientation and the absence of crystallographic texture, led Pfiffner to conclude that superplastic flow was restrained to certain portions of the mylonite, while the rest of the Lochsitenkalk

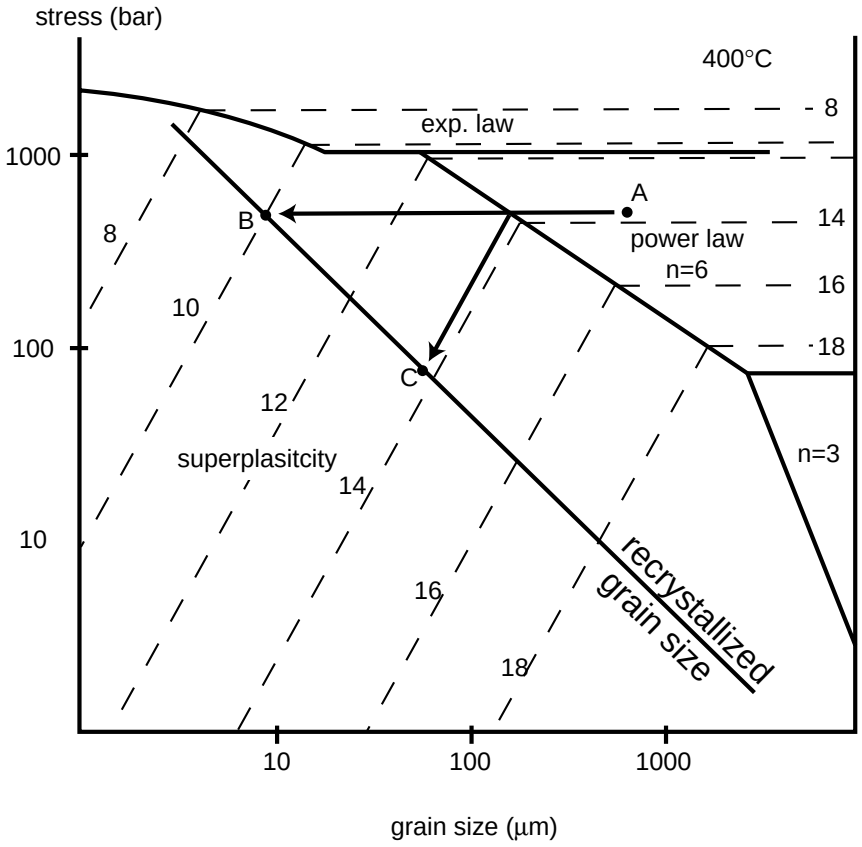

Fig. 11

Deformation regime map for calcite at a temperature of 400°C presented in different stress vs. grain size coordinates. The strain rate contours are labelled with the negative exponent of the strain rate in s^{-1}. In the superplastic regime, the equation for grain size sensitive creep of Solnhofen limestones was used (Lange 1968). The flow laws for the exponential and power law regimes are taken from data on Carrara marbles (Rutter 1974; Schmid et al. 1980). Surimposed on this deformation map is the curve labelled recrystallized grain size. A calcite aggregate deforms by a strain rate and under stress indicated by point A. The position of this point A indicates that the materials has a grain size which is larger than the size of the subgrains and recrystallized grains expected to form with increasing strain. The material deforming by dislocation creep at point A will eventually recrystallise to a grain size along a curve, which comes to lie within the field of superplasticity. The paths to point B and C indicate two extreme possibilities of what could occur if the production of a new grain size by rotation recrystallisation would be instantaneous. The case B illustrates that under boundary conditions of constant stress acceleration of strain rate will occur as a consequence of the change in grain size. The case C illustrates a stress drop under the opposite boundary conditions of constant strain rate. Once the change in mechanism has occurred, the curve of recrystallised grain size vs. stress becomes meaningless. Modified after Schmid (1982)

deformed by power-law dislocation creep.

A late twinning event recognized in the Lochsitenkalk (see also Groshong et al. 1984) affected even the smallest grains pointing toward very high differential stress (Pfiffner 1982).

This late high stress event is also documented by Briegel and Goetze (1978) who measured the dislocation density in Lochsitenkalk samples by transmission electron microscopy. They deduced a stress of about 2 kbar. Based on experimental data on flow and fracture of fine-grained limestones, it was concluded that the last deformation, which is recorded in the microstructures, occurred below 300°C in a region in which mechanical

properties are comparatively temperature-insensitive, possibly as the fault motion "froze" during cooling (Briegel and Goetze 1978). In the contrary, Schmid (1982) attributes the high stress event to the initial deformation within the power-law creep regime.

The large-scale structures of the Glarus Alps, perfectly described by Oberholzer (1933), have been largely studied in the last three decades. Pfiffner (1977; 1978) has investigated the Infrahelvetic complex structures, defining the different deformation phases (see above). Further works of Pfiffner (1980; 1981; 1985; 1993) mostly deal with thrust geometry, chronology between the different thrusts, displacement along each thrust fault and the structures resulting from movement along thrust in the eastern Helvetic Alps, including the Glarus overthrust. This allowed palinspatic reconstructions, deductions on thrust localisation in the Helvetic Alps and brought new insights into the different stages of deformation across the Alps. The Tertiary flysch of the Glarus Alps has been the subject of a very detailed structural mapping by Lihou and Mange Rajetzky (1996). This work has confirmed the out-of–sequence character of the Glarus overthrust and has evidenced strike-slip faulting in the Infrahelvetic complex during thrusting of the Glarus nappe.

The works of Burkhard and Kerrich (1990) and Burkhard et al. (1992) add a new angle to the Glarus thrust deformation history. Inspired by a work in the western Helvetic Alps (Burkhard and Kerrich 1988) in which fluid flow along basal thrust was documented by the analysis of stable isotope systematics in the Mesozoic carbonates, Burkhard and Kerrich (1990) and Burkhard et al. (1992) determined the stable and Sr isotope composition of Lochsitenkalk in five sites along the

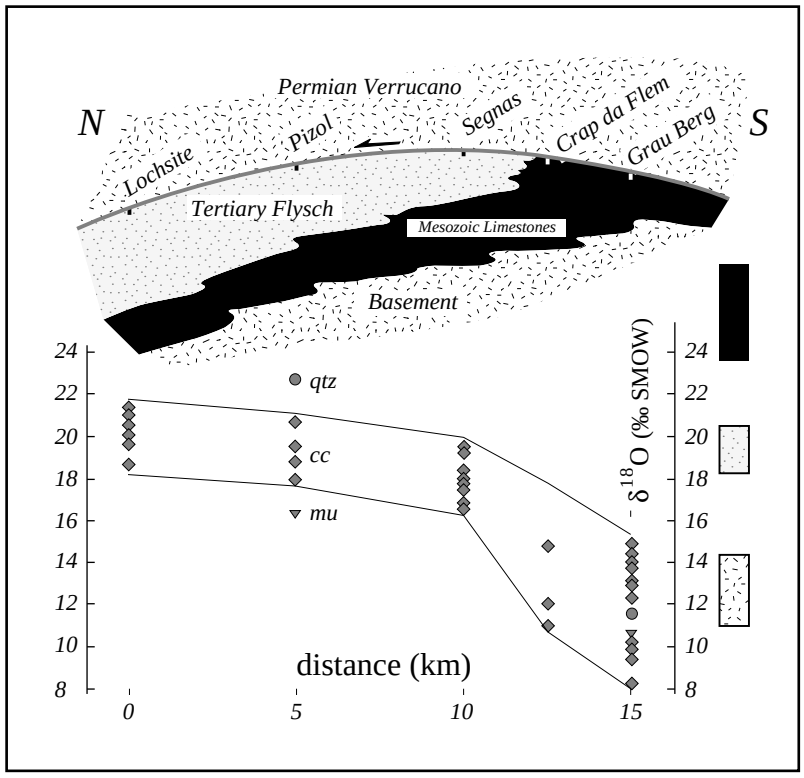

Fig. 12
Plot of calcite $\delta^{18}O$ values from the Lochsitenkalk mylonite on a schematic N-S cross section of the Glarus thrust. The range of whole rock isotopic composition for different potential fluid reservoirs are indicated to the right of the $\delta^{18}O$ scale using the corresponding shading. Modified after Burkhard and Kerrich (1990).

thrust and of Mesozoic, Lochsitenkalk and Verrucano samples on one vertical profile across the thrust. Simultaneously, XRF analysis of major and trace elements have been conducted in a vertical profile in the Verrucano: apart from a clear carbonate and minor quartz addition to the Verrucano and some minor changes (chlorite and albite dissolution), no marked geochemical anomalies associated with the Glarus overthrust had been identified. The isotope systematics, however, revealed much more interesting features (Fig.12): the $\delta^{18}O$ of the Lochsitenkalk is invariably lowered (10-20‰ SMOW) compared to its Helvetic marine carbonate protolith (25-27‰ SMOW) following an increasing trend from 10‰ in the south to 20‰ in the north. Burkhard and Kerrich (1990) and Burkhard et al. (1992) interpreted this feature as due to the northward advection of ^{18}O depleted fluids along the thrust coming from the dehydration reactions in the basement in the root zone of the thrust. They calculated Water/Rock (W/R) ratios based on the secular model of Taylor (1977) (multi pass and one pass model) (Fig. 13).

This kind of calculation has been strongly critized: the W/R varies along the thrust because the fluid composition evolves while advecting towards the north by interaction with the rock. Bowman et al. (1994), based on the data of Burkhard and Kerrich (1990) and Burkhard et al. (1992), proposed a much more solid calculation by applying transport theory (Bickle and Baker 1990; Baumgartner and Rumble 1988; Baker and Spiegelman 1995) for the fluid flow that occurred

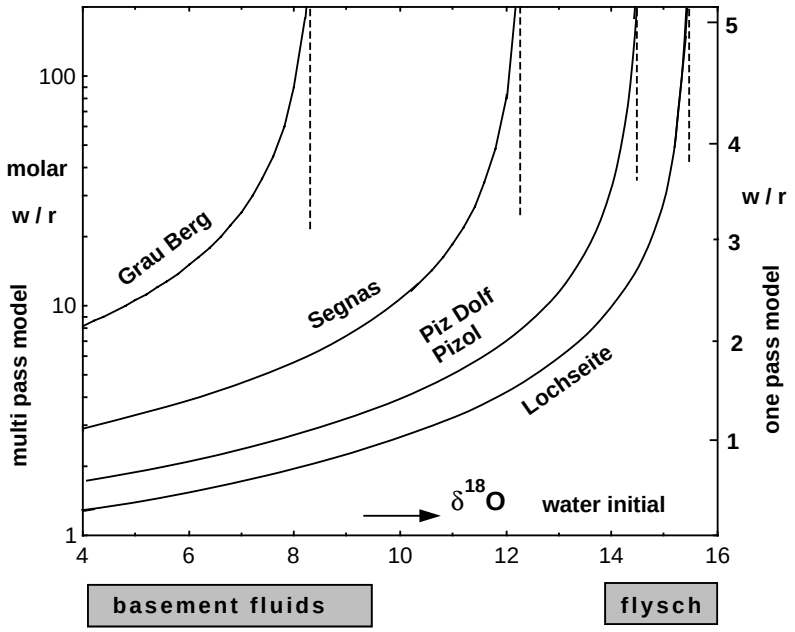

Fig. 13
Calculated molar Water/Rock ratios for the different calc-mylonite sites along the Glarus thrust. W/R ratios (logarithmic scale!) are plotted vs. the unknown initial water composition at T=300°C, resulting in a given $\Delta^{18}O_{cc\text{-}H_2O}$ of 5%. A mean initial $\delta^{18}O$ value of 25.4% is assumed for the limestone protolith (Burkhard and Kerrich 1988). W/R ratios are calculated using Taylor's closed system formula (e.g. Ohmoto 1986). This "multi pass model" W/R ratio is plotted on the left axis, whereas the corresponding W/R for a "single pass model" is plotted on the right axis. Modified after Burkhard et al. (1992)

along the thrust. A time-integrated fluid flux of 2950-5900 m^3/m^2 and a Peclet number of about 10 were derived (Fig. 14). Unfortunately, the latter paper mathematics was too strong and the true geological problem was forgotten.

This new approach to the Glarus thrust was the occasion for Burkhard and Kerrich (1990) and Burkhard et al. (1992) to reconsider the role of fluids in the deformation along the Glarus thrust. They proposed that the Lochsitenkalk could in part or in whole be formed of secondary calcite precipitated from fluids circulating along the thrust (Burkhard and Kerrich 1990). The role of brittle deformation was emphasized (Burkhard

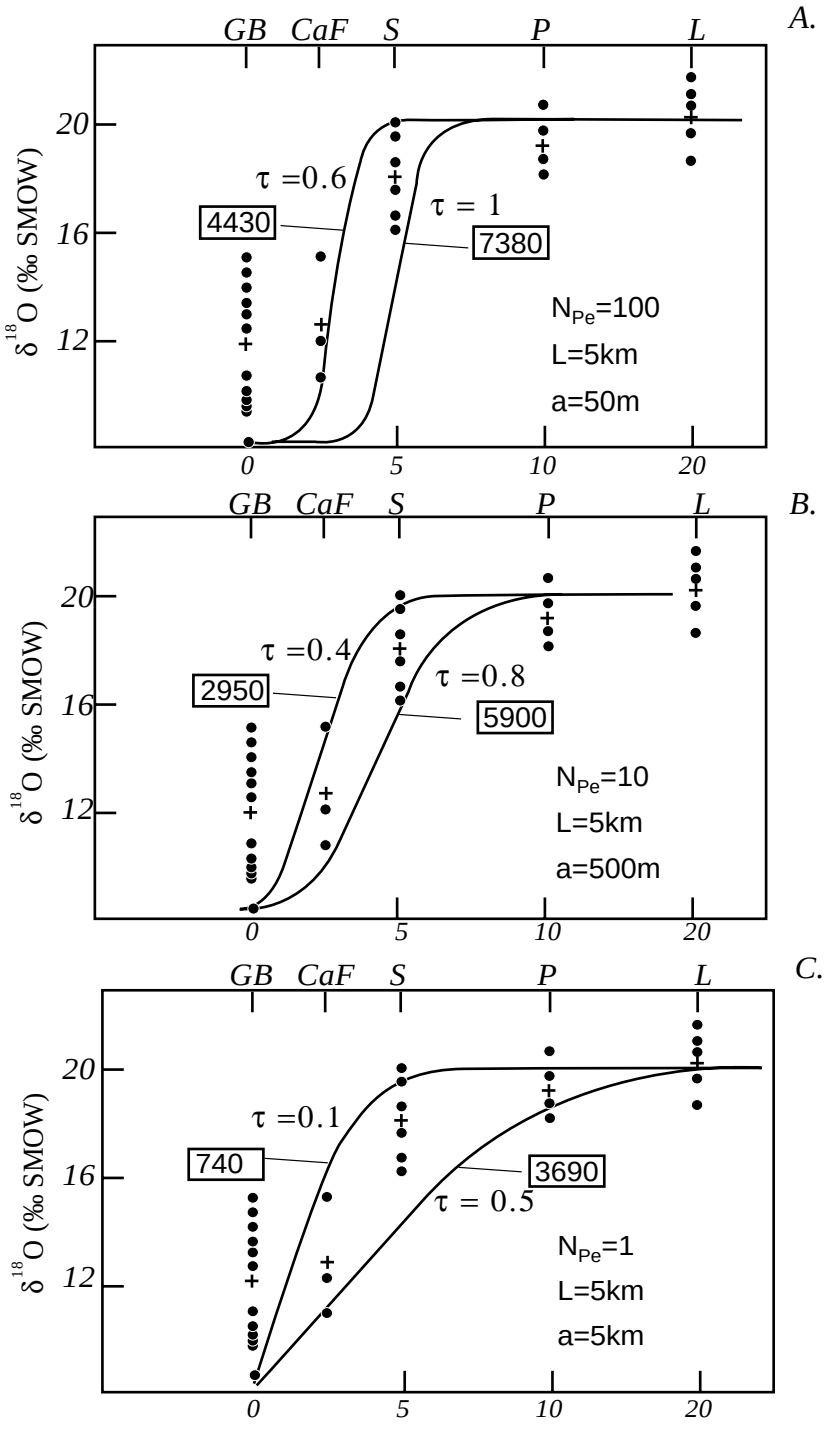

Fig. 14

Model oxygen isotope exchange fronts, computed with an $\delta^{18}O$ value of 4.5 per mil for the infiltrating fluid and at different value of N_{Pe}, are surimposed on the oxygen isotope data measured by Burkhard and Kerrich (1990) from the Glarus thrust. Exchange fronts developed at N_{Pe} in the vicinity of 10 and at values of non-dimensional time (t) ranging from 0.4 to 0.8 (B) appear to provide the best fit to the geometry and position of the oxygen isotope front (defined by the maximum average $\delta^{18}O$ values at Crap da Flem and Segnas). Surimposed on the model exchange fronts are the time-integrated fluid fluxes (m^3/m^2) defined by the transport models. Abbreviations of sample locations: GB= Grau Berg, CaF= Crap da Flem, S= Segnas, P= Pizol and L=Lochsite. L is a non-dimensional distance, a is the dispersion coefficient. Modified after Bowman et al. (1994).

and Kerrich 1990) and a cycle between ductile and brittle deformations due to the variation of fluid pressure was proposed. Unfortunately, no real arguments were presented to support this idea.

Aim of this study

Since the works of Schmid (1975; 1982) and Schmid, et al. (1977; 1981), the Lochsitenkalk of Glarus thrust was classically considered as a natural example of rock deforming by grain boundary sliding in the superplastic flow regime. Burkhard and Kerrich (1990) and Burkhard et al. (1992) proposed an alternate activity of brittle and ductile deformation mechanisms related to a cyclic variation of fluid pressure to account for the 35 km of northward thrust translation.

Burkhard and Kerrich (1990) and Burkhard et al. (1992) document an anomaly in the oxygen isotope composition of the Lochsitenkalk on a N-S profile of the Glarus thrust that was interpreted as an exchange isotope front due to the northward advection of abnormally ^{18}O depleted fluids along the thrust. The data of Burkhard and Kerrich (1990) and Burkhard et al. (1992) have been used by Bowman et al. (1994) to calculate the fluid flow parameters by applying transport theory. But this calculation was based on a very restrained data set and the isotopic variations across the thrust have not been considered.

Here I will try to solve two problems linked to the thrusting of the Glarus nappe. First, the deformation mechanisms active in the Lochsitenkalk during thrusting will be investigated by analysing Lochsitenkalk sample with transmission optical microscope, scanning electron microscope and cathodoluminescence. This should give new insights into the role of brittle (hydrofracturation) and ductile (superplastic flow, dislocation creep) deformation mechanisms in the formation and evolution of the Lochsitenkalk, by analysing microstructures, crystallographic textures on mm-scale zones, grain shape and size.

Secondly, the oxygen, carbon and strontium isotope systematics will be precisely defined. More than forty sites along the Glarus thrust have been chosen for precise sampling in the Lochsitenkalk and across the thrust in the footwall and hanging-wall. The resulting isotopic zonation will allow us to determine the geometry of the different fluid flow systems and to define some fluid flux parameters such as the time-integrated fluid flux, the Peclet number and the diffusion distance of the different flow systems. Finally, the veracity of these assumptions will be checked by simulating them with a finite element calculation model developed at the Université Laval, Québec, in order to constrain precisely which could have been the parameters that have determined the fluid flow pathways during the thrusting of the Glarus nappe.

Work description and partition

This work is the result of an intense international collaboration and this is why I will provide below some detailed information about my own contribution with respect to input from co-authors in the various papers.

Chapter II deals with the deformation mechanisms active in the Lochsitenkalk during thrusting. The alternate activity of brittle and ductile intracrystalline deformation mechanisms in the Lochsitenkalk are documented through structural observations on ordinary and ultra-thin sections, augmented by cathodoluminescence and SEM observations on Lochsitenkalk samples. Some far reaching, original and somewhat provocative interpretations of thrust-translation in terms of seismic slip in a background ductile deformation regime are proposed at the end of this chapter. Apart from cathodoluminescence analyses which have been conducted at the University of Bern in collaboration with Dr. K. Ramseyer, all the remaining preparations and analyses were conducted by myself at the University of Neuchâtel. Ultra-thin section preparation and SEM observations benefitted from help by the staff of the ancient “Institut de Métallurguie Structurale" and the new "Comlab at CSEM”, especially Dr. M. Dadras. The paper was initially written by myself, its english was corrected by "Word's Spell checker" and by Martin Burkhard and Rachel Hosein. Subsequently it went through a serious round of review/revision before going published in Terra Nova. While most of my original ideas have been preserved in this process, I experienced this reviewing procedure as a delicate balance act of negociation between parties (authors, reviewers, editor).

Chapter III and IV present two alternative interpretations of the carbon, oxygen and strontium isotope data, measured in detailed profiles along and across the Glarus overthrust. In chapter III, channelized fluid flow along the thrust in the south and vertical upward flow across the thrust from the flysch into the Verrucano in the north are advocated. Calcite oxygen, carbon and strontium isotope values have been measured in over 30 sites along the Glarus thrust in the Lochsitenkalk and in 10 detailed vertical profiles across the thrust. Field work and sampling was conducted almost exclusively by myself during summer 1998 and 1999, on occasions in the company of field assistants and friends and Professor M. Burkhard. One joint field visit was organized together with R.Abart and A.Mc.Caig (3 days) in early summer 1998. R.Abart conducted his own sampling campaign at Grau Berg and Lochsite in 1998/99. In total, about 800 samples of Lochsitenkalk, Verrucano, flysch and footwall carbonates have been analysed in order to define their $\delta^{18}O$ (SMOW) and $\delta^{13}C$ (PDB) on calcite. Most of these analyses have been conducted at the University of Graz (ca. 75%, R. Abart) and at the University of Berne (ca. 25%, S. Burns) on automatic extraction lines. My own contribution consisted in the preparation of rock-powders from pre-cleaned samples. More than fifty $^{87}Sr/^{86}Sr$ ratios have also been determined on three pre-cleaned rock-slabs of Lochsitenkalk at the University of Leeds under the direction of Dr. A. M. McCaig and Dr. Bob Cliff. During a stay at the University of Leeds, I prepared some 50 aliquots of rock powder for analysis on an automatic Mass Spectrometer. An indepth discussion of the strontium data with Dr. A. M. McCaig is largely reflected in chapter III. The latter was prepared in collaboration with Rainer Abart. My personal contribution to this chapter has been to prepare

the figures and to write the paper apart from the mathematics of the flow modelling section, which is Rainer Abart's. A first draft of this manuscript benefitted from comments and corrections by Rainer Abart, Martin Burkhard and Andrew McCaig. . Nevertheless, this paper represents my analyses and interpretations of the isotopic data and I evaluate my own contribution to it at over 80%.

In chapter IV, an alternative interpretation of flow pathways along the Glarus thrust is discussed in detail. Downward flow across the thrust from the Verrucano into the footwall carbonates in the south and upward flow from the flysch into the Verrucano in the north are advocated in order to explain very detailed vertical profiles across the thrust, where calcite oxygen, carbon and strontium isotope data are combined with quartz oxygen isotope data and mineralogical information (H_2O and CO_2 contents). In contrast to chapter III, only two vertical profiles across the thrust are considered, i.e. Grauberg and Lochseite. Most of the samples used in this study were collected and processed independently by R. Abart.

Chapter IV is mostly elaborated and written by R.Abart. His preferred interpretation, i.e. vertical isotope exchange, constrasts with my own preference for chanellized flow along the thrust. My contribution to this paper is restricted to background information about the regional geology and participation in the interpretation of the overall and regional trends, I estimate that my contribution represents some 10%.

In chapter V, I present finite-element numerical simulations of fluid flow along the Glarus thrust that allow me to constrain the parameters responsible for the flow pathways that have been deduced from the isotopic zonation. During a stay at the University of Laval (Québec, Canada), I learned to use the code of simulation FRAC3D developed by Therrien and Sudicky under the direction of Professor Georges Beaudoin and Professor René Therrien. I did some 10 simulations there, and then I continued to do up to 100 simulations from Neuchâtel through Telnet protocol, some of them being presented in the appendixes. These simulations were designed to reproduce the calcite oxygen isotope zonation in the Lochsitenkalk along the Glarus thrust. I show that the fluid flow pathways are mainly controlled by the configuration of sources and drains and by the piercing of the lithostatic-hydrostatic boundary by the advancing thrust. This paper is the result of very effective collaboration between Georges Beaudoin, Martin Burkhard and my-self, and my contribution has been first to do the simulations, then to choose the figures and best simulations, and finally to write the paper. Of course, Georges Beaudoin, Martin Burkhard and René Therrien brought some very constructive corrections.

In Chapter VI, the conclusion of chapter II-V are reviewed and critized from a more philosophical point of view. This chapter underlines pros and cons of the conclusions of the different chapters. For example it gives a large discussion on the unsolved problem of channelized flow vs. vertical downwards flow in the southern part of the Glarus overthrust (comparison of chapter III and IV). It

also provides larger explanations on the contribution of seismic vs. ductile deformation in the total displacement of the Glarus nappe. In other words, this chapter emphasizes some points that have only been slightly discussed or avoided because of the restricted number of pages allowed for each paper.

Finally, the appendixes are displayed in order to support the observations presented in each part of this work. Additional information is given in a short caption for each table or figure presented.

Chapter 1: Introduction, version française

Situation géographique

La zone d'étude se situe dans les Alpes de Suisse orientale à cheval sur les cantons de Glaris et des Grisons, entre la ville de Glaris au nord et la cité de Flims au sud (Fig. 1). Elle couvre une surface qui s'étend sur 15 km du sud au nord et sur 20 km d'est en ouest et est limitée à l'ouest par le Klausenpass et à l'est par l'arête du Foostock. Le chevauchement de Glaris, parfaitement visible sur

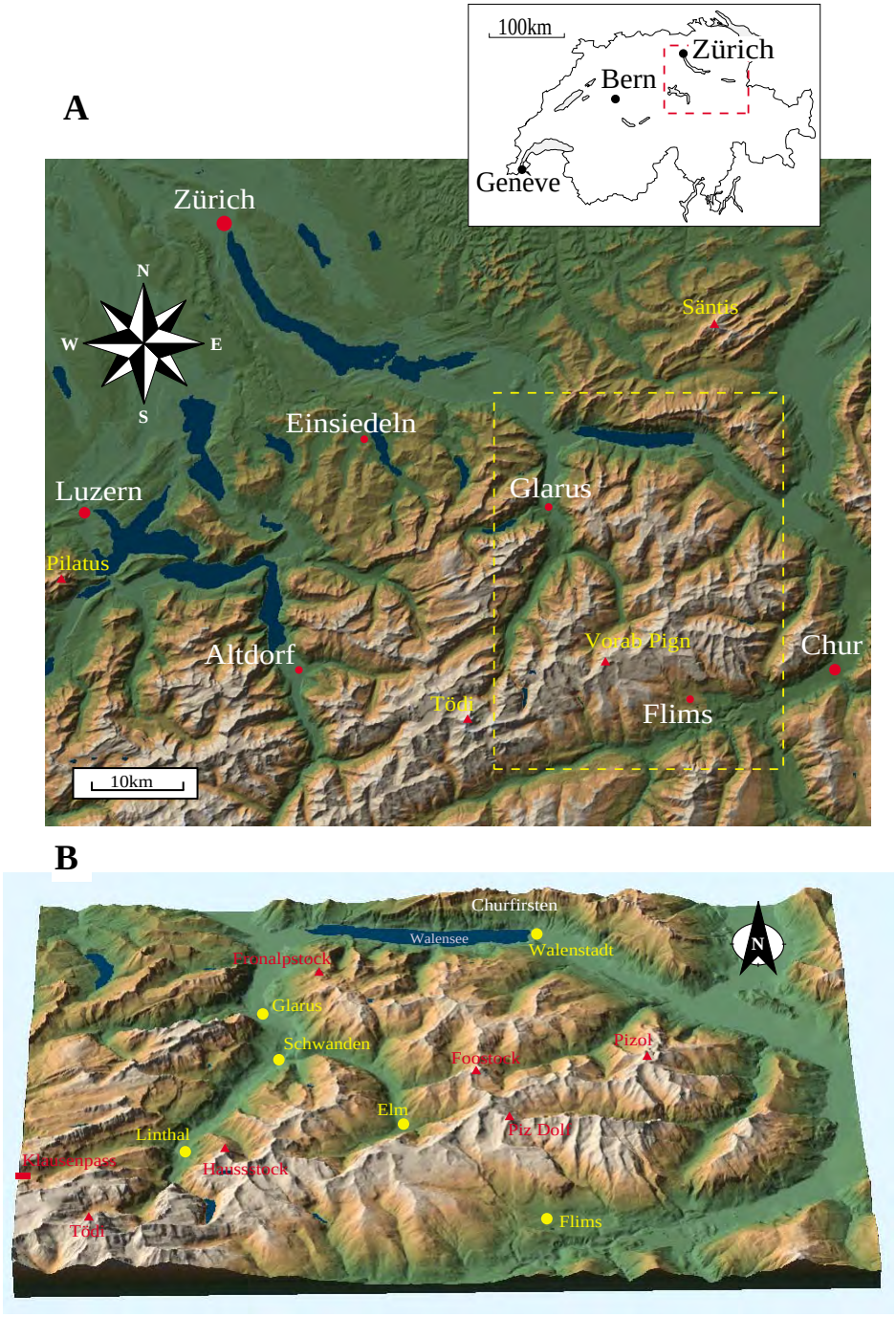

Fig. 1
Situation et relief 3D de la zone d'étude dans les Alpes glaronnaises. (A) carte hypsométrique de l'Helvétique des Alpes de Suisse orientale localisée sur la carte simplifiée de la Suisse par un rectangle rouge. (B) Bloc-diagramme du relief 3D de la zone d'étude. Au sud, le chevauchement de Glaris suit approximativement la crête entre le Hausstock et le Piz Dolf puis continue vers l'est avant de plonger en direction du nord et de disparaître sous la topographie au niveau de Schwanden.

les faces raides des montagnes, monte depuis la vallée antérieure du Rhin jusqu'à une altitude de 2600-3000 m avant de redescendre et de disparaître sous la topographie à une altitude de 600 m au niveau de Schwanden.

Contexte géologique

Les nappes helvétiques qui forment les Alpes glaronnaises proviennent de la marge passive mésozoïque de l'Europe et des parties les plus internes du bassin d'avant-pays paléogène. Elles constituent un parfait exemple de nappes de décollement, dont le chevauchement de Glaris représente le chevauchement basal (Fig. 2). Ce dernier subdivise les unités tectoniques en deux ensembles, le complexe infrahelvétique rencontré sous le chevauchement (Milnes and Pfiffner 1977) et les nappes helvétiques situées au-dessus du chevauchement (Fig. 2B). Par les techniques d'équilibration des coupes, un déplacement minimal de 35 km le long du chevauchement de Glaris est calculé et il devient clair que le chevauchement doit s'enraciner dans la croûte moyenne environ 20 km au sud des affleurements les plus méridionaux (Pfiffner 1985) (Fig. 2A). Le chevauchement est exceptionnellement bien préservé dans le paysage comme un horizon plat souligné par la présence d'une mylonite calcaire, la bien nommée

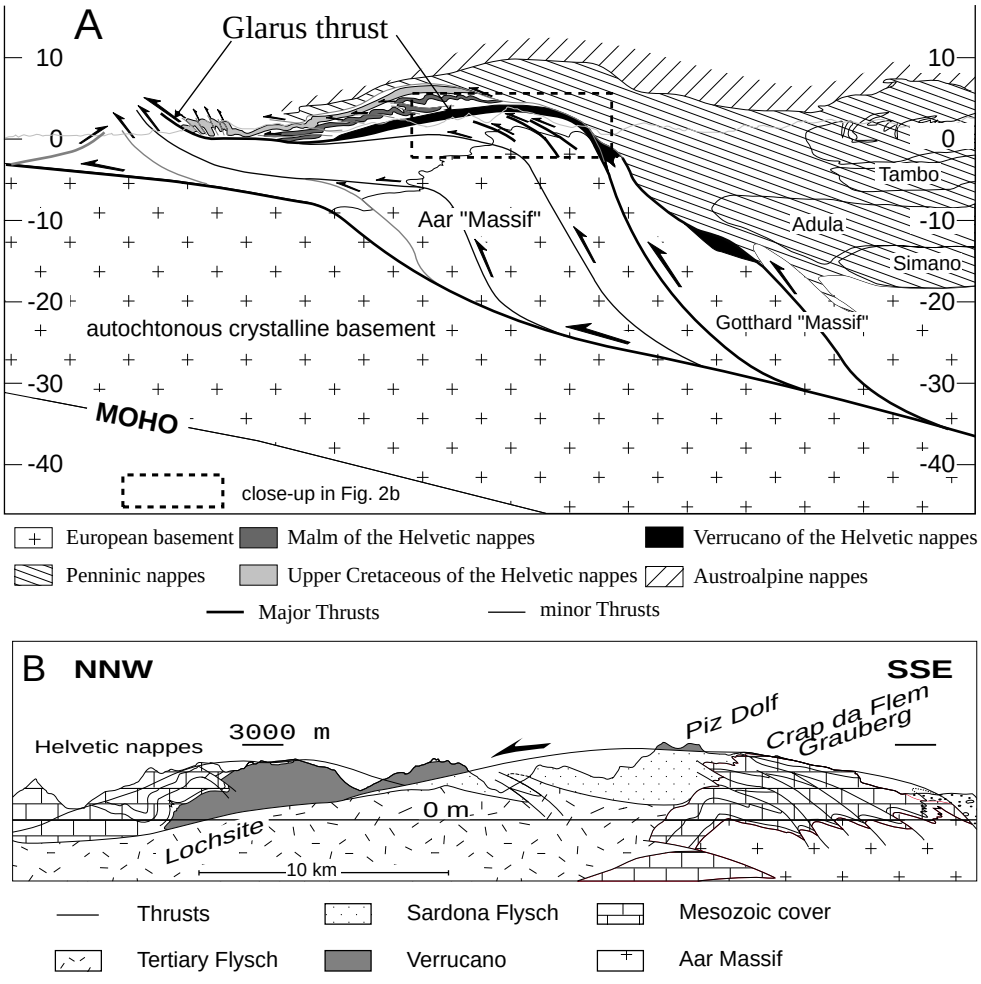

Fig. 2
(A) Profil géologique NNW-SSE à l'échelle crustale à travers les Alpes de Suisse orientale (modifiée d'après les coupe de Pfiffner (1993) et Schmid et al. (1997)). La partie accessible du chevauchement de Glaris est indiquée par le rectangle.
(B) Coupe géologique des Alpes glaronnaises en Suisse orientale (d'après Oberholzer 1933). Quelques sites d'échantillonage sont indiqués.

Lochsitenkalk.

Le complexe infrahelvétique dans le mur du chevauchement de Glaris est consituté de la base au sommet (Fig. 2b/3):

(1) d'une série de blocs imbriqués chevauchés et plissés constitués de socle cristallin du Massif de l'Aar et de sa couverture paraautochtone d'âge Mésozoïque et Eocène

(2) de flysch nord-helvétique. Le contact entre le flysch et les argilites eocènes est souvent de nature tectonique (Frey 1965)

(3) de flysch «exotiques» d'origine sud-helvétique et pennique (nappes de Blattengratt et de Sardona) qui ont chevauché le flysch nord helvétique à l'Oligocène précoce. L'origine paléogéographiqe précise de la nappe de Sardona dans la dépression valaisanne reste toutefois sujet à controverse.

Le toit lui est constitué de la formation permienne du Verrucano, une série détritique à dominance pélitique et limoneuse alternant avec quelques niveaux conglomératiques et quelques rares horizons volcanoclastiques qui se sont déposés dans un graben. Ce bassin «inversé» est surmonté d'une série mésozoïque concordante elle-même surmontée par les nappes helvétiques supérieures (Axen et Säntis) consitituées d'alternances marno-calcaires mésozoïques (Fig. 2/3). Les nappes penniques et austroalpines reposent sur ce complexe helvétique (Fig. 2A). La structuration des nappes helvétiques a fortement été influencée par la paléogégraphie anté-alpine: l'épaississement des séries mésozoïques vers le sud et le remplacement de calcaires par des marnes d'une part, et l'existence d'un demi-graben tardi-varisque E-W d'autre part, la limite nord de ce dernier jouant en rampe latérale lors de la collision alpine.

La cinématique des complexes infrahelvétique et helvétique a été précisément définie par les travaux de Schmid (1975), Pfiffner (1977; 1978) et Siddans (1979) qui ont déterminé 3 phases principales de déformation:

(1) La phase Pizol correspond à la mise en place à l'Oligocène des nappes sud-helvétique de Blattengratt et pennique de Sardona sur une surface d'érosion du flysch nord-helvétique.

(2) La phase Calanda décrit le plissement et l'imbrication du complexe infrahelvétique impliquant le développement d'un clivage très pénétratif.

(3) La phase Ruchi marque le chevauchement de la nappe de Glaris et la mise en place finale des différentes nappes helvétiques. Une schistosité mylonitique se développe dans le toit du chevauchement de Glaris, de même qu'une très intense linéation d'étirement, des bandes de cisaillement ainsi que de la crénulation. Le clivage dans le complexe infrahelvétique est crénulé ou réorienté parallèlement au chevauchement dans les 5 mètres sous le contact.

Bien qu'il soit hors séquence, le chevauchement de Glaris recoupe la série stratigraphique du bas vers le haut. Dans les affleuremements les plus méridionaux, le Verrucano repose sur des calcaires datant du Jurasssique tardif au Crétacé précoce, alors que plus au nord, le Verrucano a été chevauché sur du flysch tertiaire.

Les conditions métamorphiques enregistrées dans les Alpes glaronnaises ont été réexaminées par Frey (1988). Le degré de métamorphise régional s'étale de l'anchizone (environ 200°C) au nord et

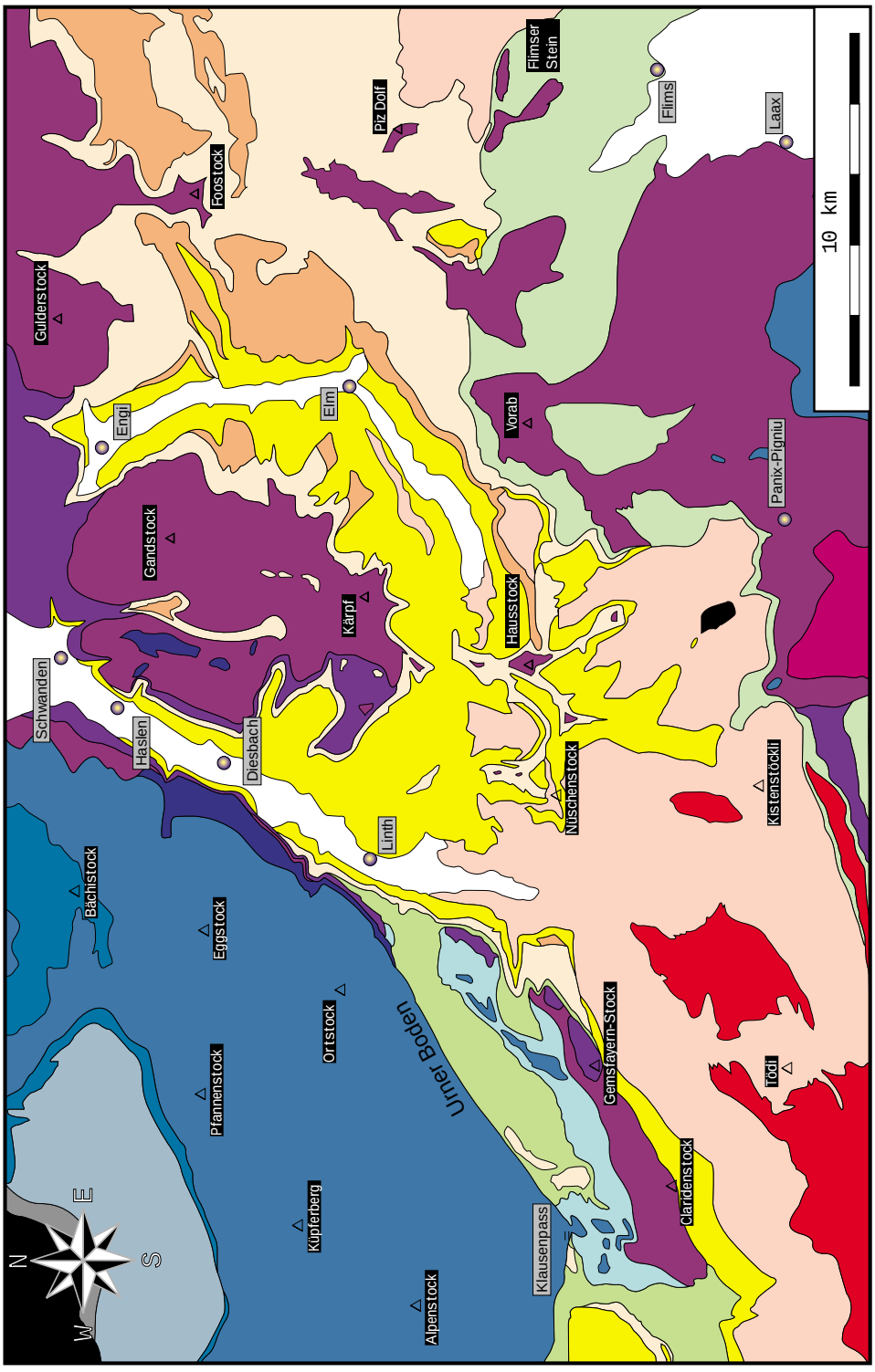
Ultrahelvetic nappes
Sardona Flysch
Blattengratt Flysch
Helvetic and autochthonous nappes
Säntis-Drusberg nappe
Säntis-Drusberg nappe
Richisauer slice
Axen nappe
Silbern-Toralp nappe
Bächistock nappe
Axen s. str. nappe
Braunwald slice
Subhelvetic nappes
Mürtschen and Kammlistock nappe
Basement of the Murtschen nappe
Glarus nappe
Parautochthonous nappes
Claridenring slices
Griesstock nappe
Vorab-Tschepp nappes
Sedimentary cover
Post-Eocene Flysch
Trias-Eocene
Aar Massif
Autochthonous and parautochthonous basement
N
S
W
E
Guiderstock
Engi
Gandstock
Schwanden
Haslen
Diesbach
Bächistock
Eggstock
Pfannenstock
Ortstock
Küpferberg
Alpenstock
Klausenpass
Linth
Kärpf
Elm
Foostock
Piz Dolf
Flimser Stein
Vorab
Hausstock
Nuschenstock
Gemsfayern-Stock
Claridenstock
Tödi
Kistenstöckli
Panix-Pigniu
Flims
Laax
Urner Boden
10 km

Fig. 3
Carte tectonique des Alpes glaronnaises en Suisse orientale. Modifiée d'après Oberholzer (1933)

dans le flysch aux conditions du faciès des schistes verts au sud et dans le Verrucano, cette zonation étant basée sur la cristallinité de l'illite, les paragenèses minérales, le réflectance de la vitrinite et les inclusions fluides. La limite anchizone-épizone est décalée de 2 km au niveau du chevauchemant de Glaris car le chevauchement postdate le pic du métamorphisme (Groshong et al. 1984; Frey 1988). La croissance post-cinématique de chloritoïde dans les pélites triasiques indique que le pic du métamorphisme a pris place après la phase Calanda (Groshong et al. 1984; Pfiffner 1985), ce dernier étant daté à 30 Ma dans le Verrucano et dans l'Helvétique (Hunziker et al. 1986; Hunziker 1987). Une datation effectuée sur un échantillon de Lochsitenkalk montre que les mouvements le long du chevauchement de Glaris ont persisté jusqu'à 23 Ma (âges K/Ar et Rb/Sr concordants). Cet âge tardi Oligocène pour le chevauchement de la nappe de Glaris reste considéré comme plus vieux que la mise en place finale du front de la nappe de Säntis, qui est pressentie comme l'émergence nord du chevauchement de Glaris.

Découverte du chevauchement de Glaris: l'histoire d'une controverse de la fin du 19ème siècle.

L'histoire de la découverte de nappes de charriage dans les Alpes glaronnaises a souvent été relatée (Heim 1921; Bailey 1935; Staub 1954; Truempy 1991). Les lignes qui vont suivre sont fortement inspirées du papier de Trümpy (1991) dans lequel il retrace la controverse qui a opposé les défenseurs des nappes en tant que plis couchés et les défenseurs des nappes comme corps charriés. Ceci impliqe l'évaluation des rôles relatifs de la déformation ductile et de la déformation fragile, ce qui correspond à la confrontation de deux géologues: Albert Heim, de renommée mondiale et August Rothpletz, presque oublié.

Hans-Conrad Escher nota très tôt (1809) une anomalie dans les Alpes glaronnaises: le Grauwacke des Alpes glaronnaises (Verrucano) repose sur l'Alpenkalk (calcaire mésozoïque). Léopold von Buch, la référence géologique de l'époque, l'appela pour lui expliquer avec diplomatie que le Grauwacke doit se trouver sous l'Alpenkalk, sinon ce n'est pas du Grauwacke. Sans pouvoir attribuer la découverte du chevauchement de Glaris à H-C. Escher, ce dernier fut certainement le premier à réaliser que la succession stratigraphique dans les Alpes glaronnaises ne collait pas au modèle communément accepté.

Arnold Escher, fils de H.-C. Escher et premier professeur de géologie à l'ETHZ, commença ses études sur les Alpes glaronnaises en 1839. Les datations biostratigraphiques de formations avaient alors fortement progressé. Il reconnut rapidement que le Verrucano est surmonté de formations jurassiques et crétacées et qu'il devait donc être plus vieux que le flysch sur lequel il

repose. Il exprima pourtant des doutes sur l'existence d'une telle structure dans son papier de 1846. En 1848, il conduisit Sir Roderick Impey Murchinson à travers le col du Segnas qui décrivit d'une manière parfaitement clair l'existence d'un grand chevauchement (Fig. 4):

"The lowest visible strata are schists and Glarus slates[1] …The flysch continues to be the chief rock of the mountains until you reach the depression in the high ridge, where the track passes into the Grisons……Widening to about 100 feet or more to the southwest of the mountain pass, this flysch is then directly surmounted by a mass of hard grey subcrystalline limestones[2] …This limestone is,…,.continuously superposed to the flysch in irregular thicknesses, and more or less in a tabular position…Now, this limestones is in its turn distinctly overlaid by a zone of talc and mica schist[3] …This uppermost rock...lie beneath the whole secondary series."

Et plus loin

"It became necessary to admit that the strata had been inverted, not by frequent folds, as on the sides of the lake of Altorf or in the Hoher Sentis, but in one enormous overthrow; so that over the wide horizontal area above-mentioned, the uppermost strata which might have been lying in troughs or depressions due to some grand early plication[4] were covered by the lateral extrusion over them of older and more crystalline masses."

Murchinson était donc convaincu de l'existence d'un grand chevauchement. Theobald (1866; 1869), qui lui aussi travaillait dans les Alpes glaronnaises, accepta la présence d'un chevauchement de direction N-S.

Mais Arnold Escher continua d'exprimer ses doutes, effrayé par les conséquences de ses observations en terme de raccourcissement. A l'assemblée annuelle de la Société Suisse des Sciences Naturelles à Neuchâtel en 1866, Escher présenta même une étrange alternative au chevauchement venant du sud. Il imagina deux plis couchés, l'un à vergence sud et l'autre à vergence nord se faisant face autour d'un synclinal de flysch en blague à tabac (Fig. 5). Cette présentation annonçait la naissance du double pli de Glaris (Doppelfalte), une infamité totale puisque toutes les structures

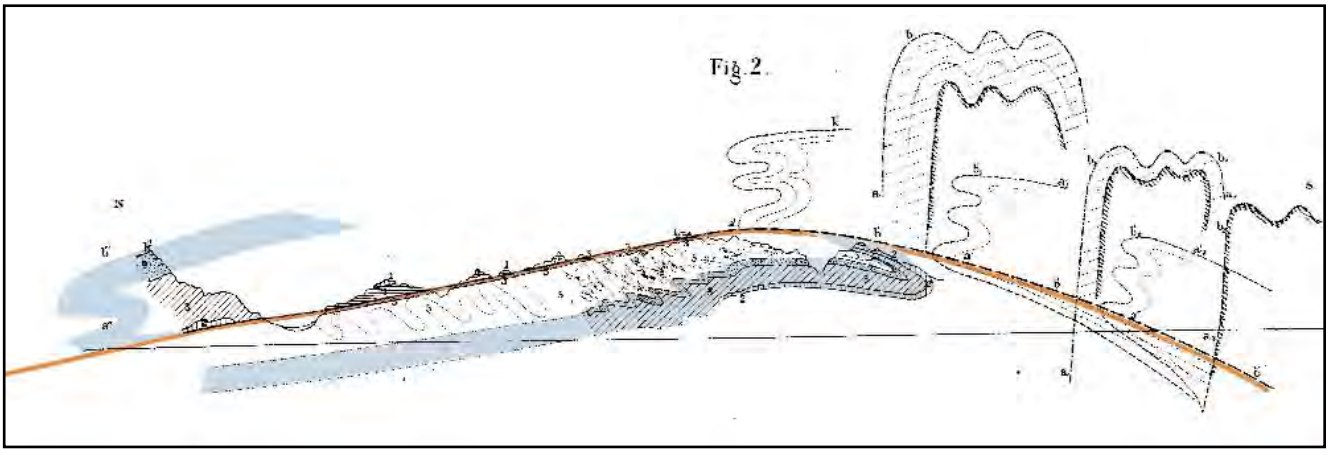

Fig. 4
Observations et interprétations géologiques des Alpes glaronnaises de Murchinson. Le niveau bleu souligne l'idée d'un grand charriage suggéré par Murchinson en 1841. Modifié d'après Murchinson (1841).

[1] Flysch
[2] Lochsitenkalk
[3] Verrucano
[4] Calanda folding

présentent une vergence nord.

Albert Heim (1839-1937), qui fut élu successeur de Escher à l'âge de 23 ans, devint la figure de proue de la géologie suisse pendant près de 50 ans. Heim, qui avait un don pour la compréhension des mécanismes basiques telles que la déformation des roches, commença ses études de terrain dans la vallée supérieure de la Reuss, dans les parties internes des nappes helvétiques. Or, dans la région de la Grosse Windgälle, la zone d'étude originale de Heim, la déformation est majoritairement de nature ductile. Heim peut avoir été influencé par cette expérience originelle de ses années de terrain les plus actives et par les vues d'Escher dans sa recherche d'un style structural identique dans des régions déformés sous un couvert moins important, telles que les parties externes de l'Helvétique et les plis du Jura.

Heim (1878) défendit fermement la théorie du double pli pour expliquer la structure géologique des Alpes glaronnaises, la Lochsitenkalk de même que les écailles subhelvétiques présentes au contact en formant les flancs inverses (Fig. 5). Bien qu'Eduard Suess, après avoir lu le papier de Bertrand (1884), ait essayé de convaincre Albert Heim de la présence d'un grand chevauchement, le grand Heim maintint fermement ses positions.

Les livres de Heim de 1878 eurent un énorme impact, et la théorie du double pli fut bientôt largement adopté par la communauté scientifique. Le second travail de Heim (1891) sur le sujet apportera peu de nouvelles idées. A Crap da Flem, il décrivit des lits à patine d'altération brunâtre entre le Jurassique du mur et le Verrucano qu'il attribua au Jurassique moyen, renforcé dans ses convictions par la présence d'une huître particulière. Rothpletz reconnaîtra rapidement que ces formations sont d'âge Crétacé, mais Heim n'entra pas en matière et par la même rejeta le papier prophétique de Bertrand (1884). L'hypothèse du double pli devint alors un dogme.

En 1890, des participants allemands à une excursion dans les Alpes glaronnaises signèrent un protocole attestant de la validité des observations et des interprétations de Heim. Ceci se passait 8 ans après l'identification par Rothpletz du chevauchement, 7 ans après la grande réinterprétation de

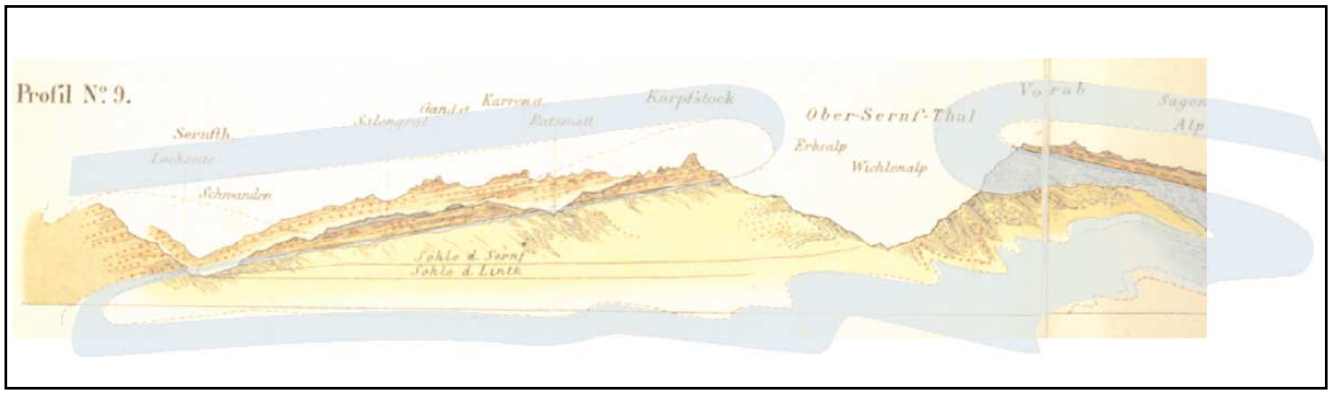

Fig. 5
Profil géologique dans les Alpes glaronnaises en Suisse orientale. Le niveau bleu qui souligne les niveaux de carbonates mésozoïques illustre l'interprétation en Double Pli (Doppelfalte) de la structure des Alpes glaronnaises proposée par Escher (1848) puis défendue par Heim (1878; 1891). Modifié d'après Heim (1891)

Bertrand et 11 ans avant que Heim ne se rallie a la théorie des nappes.

August Rothpletz commença de travailler dans les Alpes calcaires nord et par la suite rechercha dans les Alpes glaronnaises les structures qu'il avait reconnues plus à l'est. Il était donc plus familier avec les parties externes des Alpes, où la déformation fragile est plus importante que dans les zones où Heim avait débuté ses recherches de terrain. Alors que Heim attachait peu d'importance aux failles, Rothpletz, lui, en voyait partout, réelles ou imaginaires.

Rothpletz (1894) prouva que les écailles subhelvétiques sont majoritairement en position normale et il décrivit la Lochsitenkalk comme une «fault gouge», reconnaissant et exagérant les effets de la déformation cassante. Alors qu'il acceptait le «pli sud» comme un pli couché à vergence nord, il réinterpréta le «pli nord» comme un bloc chevauché vers le sud. Il ne voyait aucune contradiction entre un pli à vergence nord et un chevauchement dirigé vers le sud, puisqu'il considérait le pli comme précédant le chevauchement (Rothpletz 1883; 1894). La réaction de Heim fut immédiate et virulente (1895) : il attaqua les point faibles de la théorie de Rothpletz mais ne discuta pas les observations cruciales faites au Bützistock et au Schilt.

Dans un quatrième livre, Rothpletz (1898) combine le «pli sud» et le «pli nord» en une grande nappe de charriage, mais, basé sur l'observation d'axes de pli N-S, il conclut que cette nappe avait bougé d'est en ouest. Malgré ces erreurs d'inter-

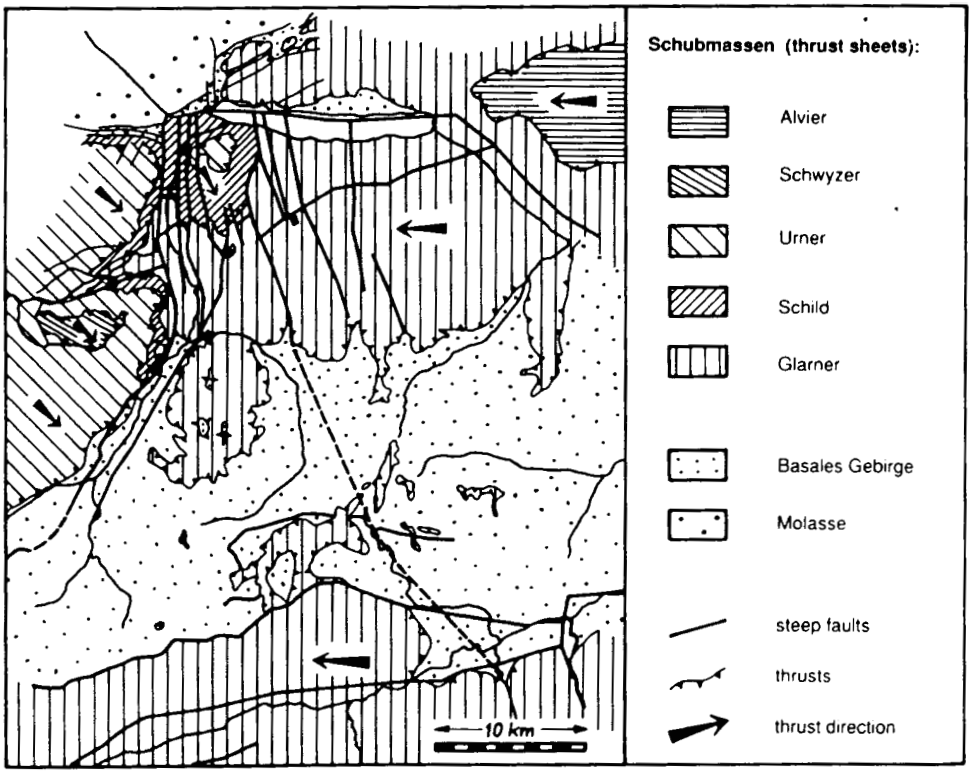

Fig. 6
Carte tectonique des Alpes glaronnaises, copié de Rothpletz, 1898, planche 10. Comparez avec la Fig. 3.

prétation, sa carte tectonique ressemble étonnemment à une carte moderne (Fig. 6).

Heim ne se priva évidemment pas de faire usage de son autorité et de son charisme pour écraser Rothpletz, en insistant bien sur la faiblesse de certains de ses arguments. Pourtant, les idées de Heim, qui surévaluait le rôle de la déformation plastique, et les vues de Rothpletz, qui lui surévaluait le rôle de la déformation fragile s'avèrent complémentaires.

Marcel Bertrand devint professeur à l'Ecole des Mines en 1866. Dans sa publication de 1884, Bertrand réinterprète les observations ponctuelles et les profils géologiques de Heim (Fig. 7), démontrant que la seule solution possible était d'admettre la présence d'un unique grand chevauchement N-S, reprennant l'idée que Murchinson exposa en 1849. Il est dès lors difficile de comprendre pourquoi Heim et Rothpletz ont négligé les travaux innovateurs de Bertrand. La découverte de nappes dans les Alpes devait attendre encore une décennie.

Le prochain acte de cette comédie dramatique se joua dans les Préalpes et l'acteur principal en fut Hans Schardt. Ce dernier devint le successeur de Heim en 1911. Dans sa première publication, Schardt (1884) considère toujours les Préalpes comme autochtones bien que recoupées de quel-

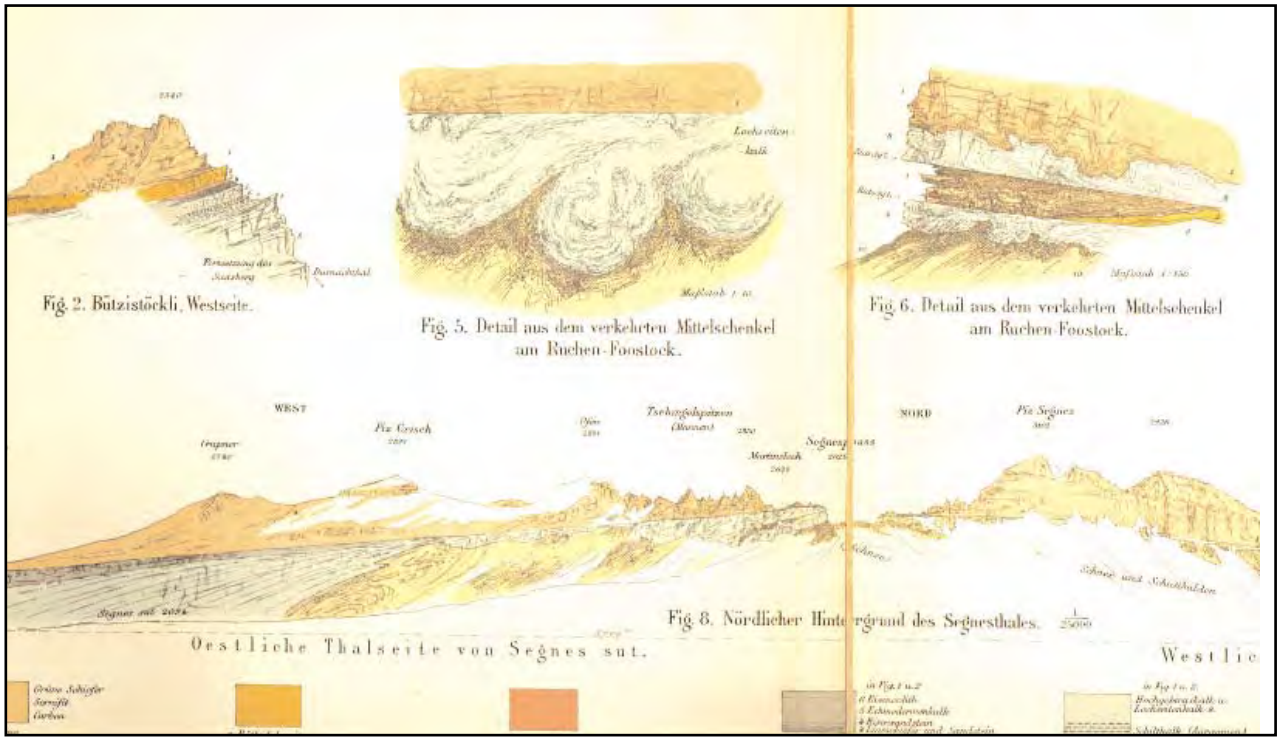

Fig. 7

Observations géologiques de Heim (1891) dans les Alpes glaronnaises. Reproduit de Heim (1891). De gauche à droite et de haut en bas: (1) Panorama du Bützistock, vue depuis l'ouest (2) Détail du contact du chevauchement de Glaris au Ruchen-Foostock, notez le contact très fortement lobé entre la Lochsitenkalk et le flysch dans le mur. (3) Détail du contactct du chevauchement de Glaris au Ruchen-Foostock, notez le niveau de flysch ou de Verrucano pris en sandwich entre deux niveaux de Lochsitenklalk. Les contacts inférieur et supérieur de la Lochsitenkalk sont lobés (4) Panorama du chevauchement de Glaris des deux côtés du Col du Segnas, vue depuis le sud.

ques chevauchements locaux dirigés vers le sud et vers le nord. Mais en 1893, Schardt réalise que les brèches de la Hornfluh d'âge jurassique reposent sur des flysch tertiaires, mettant ainsi en évidence la présence de grands chevauchements. Dans un grand élan novateur, ce concept fut étendu aux Préalpes entières et même au flanc nord des Alpes. Simultanément, de grands chevauchements étaient découverts dans le nord de l'Ecosse et en Scandinavie. La théorie des nappes était née et immédiatement appliquée au chevauchement de Glaris. Dans le troisième volume de Antlitz der Erde de Suess publié en 1901, la théorie des nappes est établie et Heim rejoint le rang de ses défenseurs. Ceci aura des conséquences drastiques sur les calculs de raccourcissement et donc sur les considérations tectoniques.

Etudes précédentes: Oberholzer, Schmid, Pfiffner et Cie

Tant d'études ont été menées sur le chevauchement de Glaris qu'il est impossible de toutes les citer. Ainsi, seuls les travaux contenant des informations cruciales au sujet rapporté dans le présent travail seront discutés ci-dessous.

Néanmoins il semble virtuellement impossible de ne pas mentionner la contribution de Jakob Oberholzer, un enseignant marié à une femme usante (Truempy 1991). Pour échapper à cette désagréable situation, il passa ses étés dans les Alpes glaronnaises et cartographia toute la région couvrant le chevauchement de Glaris à l'échelle 1:50'000. Dans son livre de référence, Geologie der Glarner Alpen, Oberholzer (1933) produit des panorama, des profils géologiques, des cartes et des descriptions lithologiques d'une rare richesse (Fig 3/8). Dans un premier temps, (Oberholzer 1908) se présentera comme un défenseur de la théorie du double pli suivant les vues de son men-

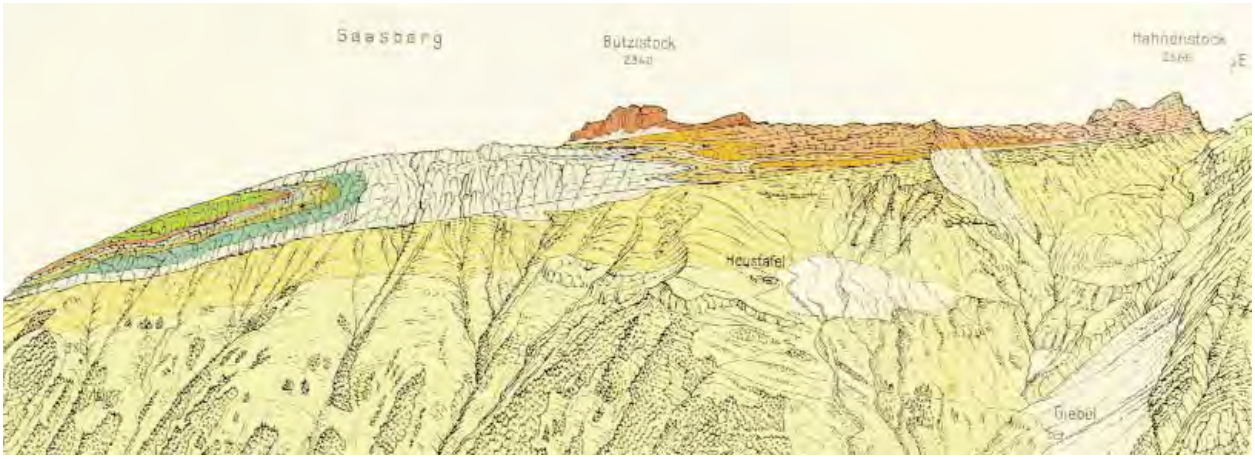

Fig. 8
Panorama du Bützistock, vue depuis le sud-ouest. Notez le changement latéral de Verrucano en carbonates mésozoïques dans le toit en direction de l' ouest. Reproduit de Oberholzer (1933).

tor Heim, mais dans sa contribution de 1933, il émet quelques réserves.

Une longue série de travaux portant sur la mécanique du chevauchement de Glaris commença à la fin des années soixante avec la contribution de Hsue (1969). Afin de tester l'hypothèse de Hubbert and Rubey (1959), qui les premiers attestèrent qu'une pression de fluide très élevée était nécessaire pour permettre le mouvement de grandes nappes de charriage, Hsü fit une analyse mathématique de la statique et de la cinétique du chevauchement de Glaris. Il conclut que les mouvements le long du chevauchement se firent en deux phases distinctes au moins. Lors d'un phase précoce, le mouvement principal était lié à un «fluage» de la Lochsitenkalk dans la zone de chevauchement associé à une pression de fluide égale à la pression lithostatique dans un régime de compression horizontale. Hsü considérait alors que la

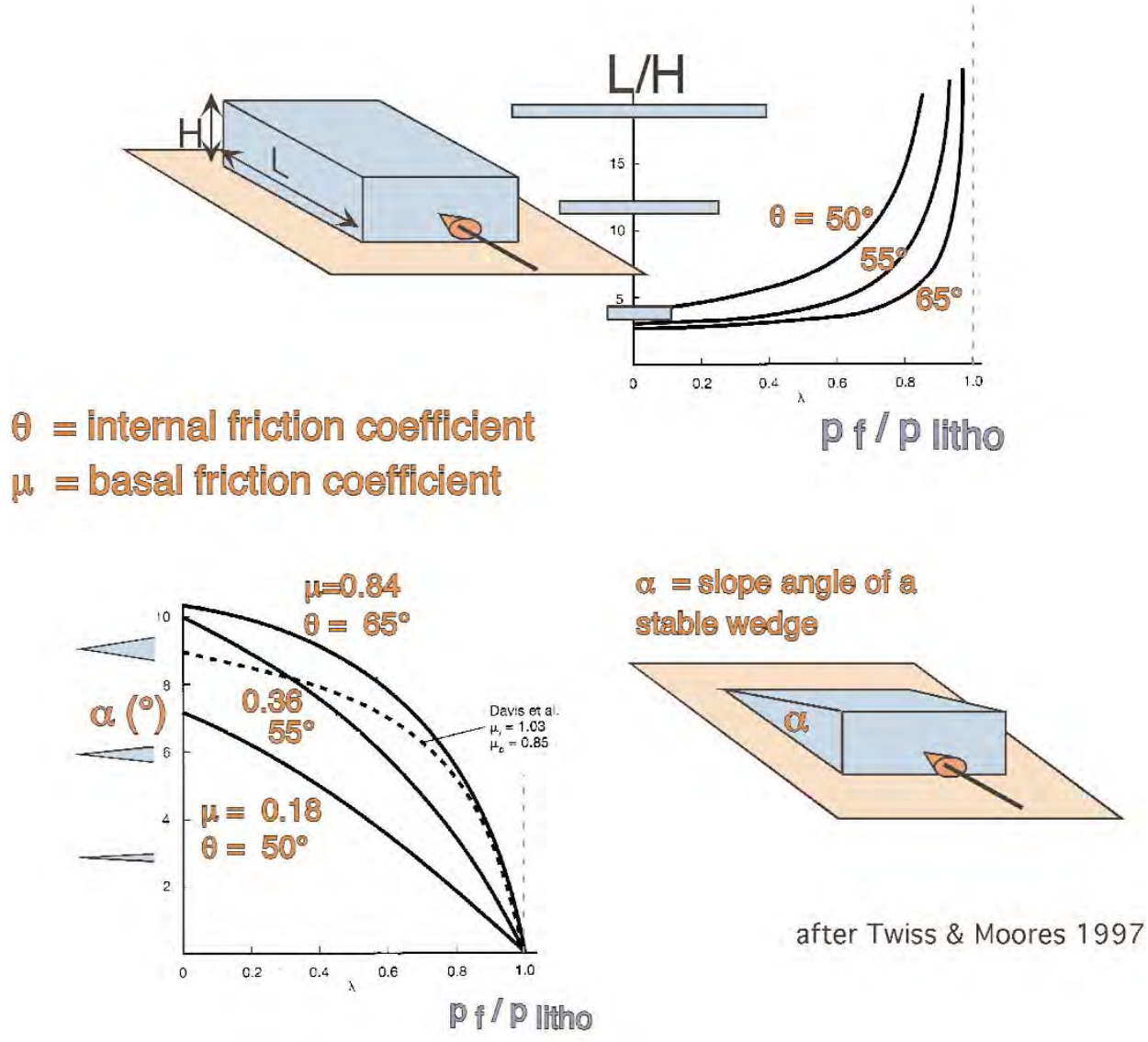

Fig. 9

Géométrie permise pour les nappes de charriage en fonction du rapport de la pression de pore à la pression de fluide l. Partie supérieure: rapport largeur(L)/hauteur(H) maximal possible pour une nappe en forme de parallélipipède rectangle, rapporté en fonction de l. Partie inférieure: angle d'équilibre de la pente (α) pour une nappe en forme de coin rapporté en fonction de l. Modifié d'après Twiss and Moores (1992)

totalité de la déformation liée au chevauchement était concentrée dans la Lochsitenaklk. La phase tardive de mouvement par glissement frictionnel produisait la «fault gouge» dans la Lochsitenkalk. Cette phase était liée à la remontée du Massif de l'Aar, la pression de fluide étant retombée à la normale afin d'éviter le glissement du chevauchement sous son propre poids dans sa partie nord. Cette dernière conclusion était basé sur l'idée, par ailleurs fausse, que la forme arquée du chevauchement de Glaris était une caractéristique existant lors de la deuxième phase de mouvement. Hsü calcula une vitesse de mouvement de 0.2 cm/année lors de la première phase de transfert.
Cette publication contient des idées intéressantes et novatrices, telle que la nécessité d'une pression de fluide élevée pour pemettre un quelconque mouvement le long d'une pente montante. Mais le modèle présenté est inutilement compliqué par l'hypothèse d'un mouvement tardif le long d'une pente descendante le long d'un chevauchement de Glaris déjà arqué.

Schmid (1975;1982) et Schmid et al. (1977; 1981) ont investi avec force et moyen les microstructures et textures dans la Lochsitenkalk afin de définir les mécanismes de déformation qui ont permis d'accommoder les 35 km de chevauchement vers le nord. Dans sa première contribution, Schmid (1975) conclut alors que «globalement, l'idée d'un niveau mylonitique extrêmement ductile localisé le long de l'interface entre deux blocs rigides et accommodant le mouvement différentiel à la base du bloc supérieur, est correcte.» Cette conclusion est fondée sur l'idée que la foliation mylonitique observée dans le Verrucano antidate le chevauchement et que les structures liées au transport le long du chevauchement sont quasi absentes dans le toit et dans le mur, la déformation liée au transport étant concentrée dans la Lochsitenkalk. Il calcula alors une vitesse de déformation de 10^{-10} sec^{-1}. La comparaison avec des échantillons de calcaire de Solnhofen, déformés expérimentalement et caractérisés par une taille de grain identique à la Lochsitenkalk, révèle que ces roches sont bien trop solides pour fluer à des vitesses aussi rapides. La conclusion inévitable est que le mécanisme de déformation active dans la nature et dans les expériences est différent (Schmid 1975).
Les prochains travaux de Schmid et al. (1977) portent sur les mécanismes de déformation actifs dans des calcaires déformés expérimentalement. Ils reconnaissent alors trois régimes de déformation par glissement, le troisième désignant le régime superplastique caractérisé par une forte dépendance envers la taille de grain, une prédominance du glissement aux joints de grain. Les textures résultant d'un tel mécanisme se définissent par une quasi absence de fabrique cristallographique et par des fabriques de forme très peu prononcées comparé aux deux autres régimes de glissement de dislocation. La vitesse de déformation augmente de manière marquée avec la diminution de la taille de grain pour un état de contrainte donnée. Au moment de cette étude, aucun exemple naturel de superplasticité n'était connu, mais Schmid et al. (1977) avouaient que «la mylonite calcaire à grains fins… du chevauchement de Glaris dans les Alpes suisses….est couramment étudiée de ce point de vue.»

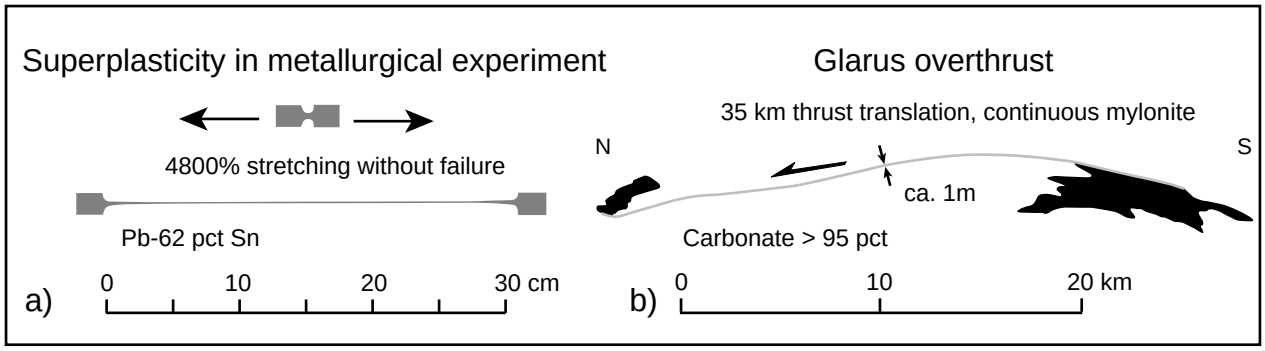

Fig. 10

La superplasticité a été proposée comme explication de l'extrême localisation de la déformation dans la Lochsitenkalk (Schmid et al. 1977). A) Un alliage de Plomb-62%Etain est déformé dans une expérience d'étirement en métallurgie (Langdon, 1982). B) Coupe géologique schématique du chevauchement de Glaris. Une mylonite d'épaisseur métrique relie les carbonates mésozoïques dans le toit et dans le mur sur une distance totale d'environ 30 km du nord au sud. Si elle était dessinée à l'échelle, la mylonite mesurerait moins de 2 microns d'épaisseur dans cette figure.

Dans leur contribution de 1981, Schmid et al. présentent une étude des orientations cristallographiques de la calcite déterminées au goniomètre à rayons X sur des échantillons de tectonites provenant du chevauchement de Glaris. La majorité des échantillons de Lochsitenkalk se caractérisent par une très faible texture cristallographique ce qui fut interprété par Schmid et al. (1981) comme une prédominance de la superplasticité par glissement aux joints de grains sur les autres mécanismes de déformation, la superplasticité étant favorisée par une taille de grain extrêmement petite (Fig. 10). Dans un échantillon, une forte orientation préférentielle des axes cristallographique fut détectée dans la matrice microcristalline. Schmid et al. (1981) expliquèrent cette observation par l'héritage d'une texture cristallographique que des gros grains avaient acquis par mâclage et qui par la suite recristallisèrent en une matrice à grains ultrafins. Ceci conduisit Schmid et al. (1981) à conclure qu' «un tel changement de mécanisme de déformation induit par la recristallisation dynamique aurait affaibli de manière dramatique ce niveau de décollement (Schmid 1975), ce qui expliquerait l'extrême concentration de la déformation dans ce niveau mylonitique très fin le long du chevauchement de Glaris.»

Par la suite, Schmid (1982) confirma et approffondit ses idées sur ces mécanismes de déformation. Il présenta des images de Lochsitenkalk illustrant le mécanisme de recristallisation dynamique par rotation de sous-grains, ce qui induit un changement de la taille de grain du matériel. Si la taille de grain initiale est modifiée, les mécanismes de déformation par glissement de dislocation sensible à la taille de grain (superplasticité) peuvent ou non prendre le dessus sur les autres mécanismes de déformation suivant la taille du matériel recristallisé et la limite entre les mécanimes de glissement suivant une loi de puissance (power-law creep) et la superplasticité (Fig. 11). Il conclut pourtant que «la recristallisation instantanée paraît peu probable dans la nature. L'évolution d'un agrégat de grains équiaxes par recristallisation conduit à une distribution bimodale de la taille de grain, certains domaines étant

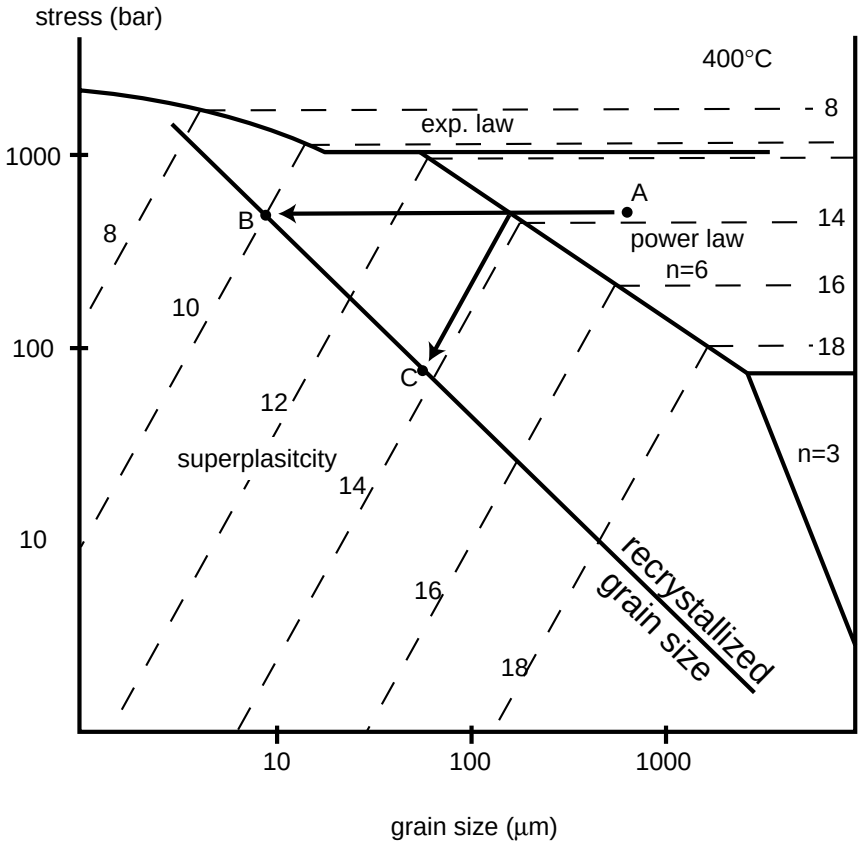

Fig. 11

Carte des régimes de déformation de la calcite à une température de 400°C présentée dans des coordonnées de contrainte différentielle versus taille de grain. Les contours des vitesses de déformations sont nommés d'après l'exposant négatif de la vitesse de déformation mesurée en s^{-1}. Dans le régime de la superplasticité, l'équation pour le régime de déformation dépendant de la taille de grain pour les calcaires de Solnhofen a été utilisé (Lange 1968). Les lois de fluage pour les régimes de glissement suivant une loi exponentielle ou de puissance sont tirées des données sur les marbres de Carrara (Rutter, 1974, Schmid et al., 1980). En surimpression est ajoutée la courbe nommée «recrystallised grain size». Un agrégat de calcite se déforme à une vitesse et sous des conditions de contrainte indiquées par le point A. La position de ce point montre que le matériel a une taille de grain plus grande que les sous-grains et les grains recristallisés dont on pense qu'ils doivent se former lorsque la déformation augmente. Le matériel se déformant par glissement de dislocation au point A va éventuellement recristalliser en une taille de grain le long de la courbe qui va amener l'agrégat à se trouver dans le champ de la superplasticité. Les chemins vers les points B et C indiquent des cas extrêmes possibles si la production d'une nouvelle taille de grain par recristallisaton était instantanée. Le cas B montre que sous des conditions aux limites de contrainte constante, une accélération notable de la vitesse de déformation aurait lieu en réponse à un changement de la taille de grain. Si au contraire la vitesse de déformation était gardée constante, une chute de la contrainte résulterait (cas C). Modifié d'apès Schmid (1982)

totalement recristallisés alors que la taille de grain originelle est préservée dans d'autres domaines. Ceci peut mener à la situation où la superplasticité et les mécanismes de glissement suivant une loi de puissance peuvent être actifs simultanément dans différents domaines de la roche». Une telle situation ne peut être décrite par un point unique dans la Fig. 11. Au début de la déformation, les domaines totalement recristallisés seront isolés et ne formeront qu'une faible partie du volume. Le fluage restera stable. «Avec l'augmentation du volume recristallisé, la vitesse de déformation globale va augmenter et /ou la contrainte diffférentielle va chuter par augmentation de la contri-

bution de la superplasticité à la déformation globale de la roche."

En conclusion, la recristallisation dynamique va induire un changement des microstructures qui à leur tour vont induire un changement des mécanismes de déformation qui vont conduire à la «fluidification» de la roche. La ressemblance entre les microstructures finales dans la Lochsitenkalk et celles des calcaires de Solnhofen déformés de manière superplastique est frappante. La texture cristallographique des domaines totalement recristallisés dans la mylonite est faible (Schmid et al. 1981). Ceci suggère une dérive des mécanismes de déformations vers la superplasticité. **Dès lors, la Lochsiten-mylonite sera classiquement considérée comme dérivant de calcaires helvétiques du toit ou du mur qui se sont déformés dans le régime de la superplasticité par glissement aux joints de grains.**

Pfiffner (1982) étudia les textures et microstructures de la Lochsitenkalk et des carbonates mésozoïques du mur sous-jacent à l'aide de la microscopie optique à transmission et du microscope électronique à transmission. Il nota une diminution de la fabrique de forme en s'approchant du chevauchement qu'il interpréta par une augmentation de la participation des glissements aux joints de grains dans les processus de déformation. Mais il fit une distinction claire entre la partie nord et la partie sud du chevauchement. Au nord, l'absence de texture cristallographique et de fabrique de forme indique une déformation dans le régime de la superplasticité. Dans la section sud, de la présence possible de fabrique de forme et de l'absence de texture cristallographique Pfiffner (1982) conclut que la superplasticité était restreinte à certaines domaines de la mylonite, alors que le reste de la Lochsitenkalk se déformait par des processus de glissement suivant une loi de puissance.

Dans la Lochsitenkalk, un événement tardif de mâclage (voir aussi Groshong et al. 1984) affecta jusqu'aux plus petits grains témoignant d'une contrainte différentielle élevée (Pfiffner 1982).

Cet événement tardif marqué par une haute contrainte différentielle fut aussi documenté par Briegel and Goetze (1978) qui mesurèrent des densités de dislocation dans des échantillons de Lochsitenkalk par microscopie électronique à transmission. Ils en déduisirent une contrainte d'environ 2 kbar. Sur la base de données expérimentales sur le fluage et la fracturation de calcaires à grains fins, ils conclurent alors que le dernier événement de déformation laissant son empreinte dans les microstructures prit place en dessous de 300°C dans une région où les propriétés mécaniques des roches sont indépendantes de la température, probablement lorsque le mouvement le long de la faille s'est gelé lors de l'exhumation (Briegel and Goetze 1978). Schmid (1982), au contraire, attribue cet événement à contrainte différentielle élevée aux prémices de la déformation dans un régime de glissement suivant une loi de puissance.

La structure à grande échelle des Alpes glaronnaises, parfaitement décrite et illustrée par Oberholzer (1933) a fait l'objet de nombreuses études ces derniers trente ans. Les études de Pfiffner (1977; 1978) ont porté sur les structures

du complexe infrahalvétique et ont conduit à la définiton des différentes phases de déformation (voir ci-dessus). Les prochains travaux de Pfiffner 1981; 1985; 1993) ont surtout été concentrés sur la géométrie et la chronologie des différents chevauchements et les déplacement et structures résultant des mouvements le long de ces failles dans l'Helvétique de Suisse orientale. Ceci a mené à la construction de coupes rétrodéformées, à des déductions sur la localisation des chevauchements dans les Alpes Helvétiques et apporta de nouveaux éléments sur les différents stages de déformation des Alpes. Le flysch tertiaire du complexe infrahelvétique a fait l'objet d'une cartographie structurale détaillée par Lihou et Mange Rajetzky (1996), qui ont confirmé le caractère hors-séquence du chevauchement de Glaris et documenté des mouvements décrochants dans l'Infrahelvétique synchrones du chevauchement de la nappe de Glaris.

Les travaux de Burkhard et Kerrich (1990) et Burkhard et al. (1992) sonnent le glas des vieilles écoles et marquent le début d'une série de travaux dont l'approche très différente de l'histoire de la déformation du chevauchement de Glaris va apporter de nouveaux éléments sur une affaire pourtant classée. Inspiré par un travail dans les Alpes helvétiques occidentales (Burkhard et Kerrich 1988), dans lequel des flux de fluides ont été documentés le long des chevauchements basaux par l'étude des isotopes de l'oxygène, Burkhard et Kerrich (1990) et Burkhard et al. (1992) déterminèrent les rapports isotopiques de l'oxygène et du strontium de la calcite dans la Lochsitenkalk en cinq sites le long du chevauchement, et dans un profil vertical à travers le chevauchement. Parallèlement, des analyses XRF des éléments majeurs et traces furent entreprises dans un profil vertical dans le Verrucano : si ce n'est un enrichissement en carbonate et en quartz

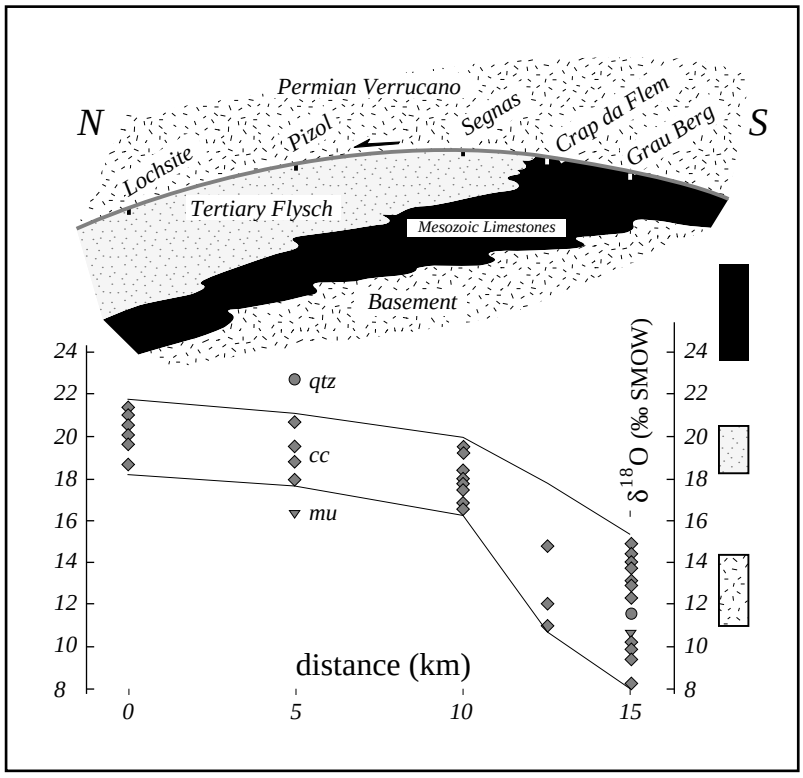

Fig. 12
Graphe des valeurs de $\delta^{18}O$ de la Lochsitenkalk reporté sur une coupe schématique N-S du chevauchement de Glaris. La gamme de composition isotopique de la roche totale de différents réservoirs est indiquée sur la droite de l'axe Y en utilisant les motifs correspondants. Modifié d'après Burkhard et Kerrich (1990)

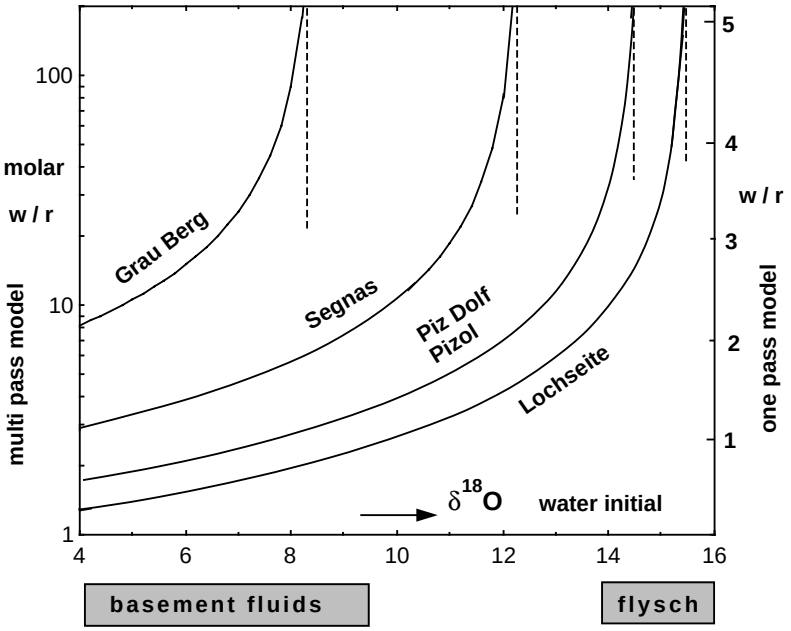

Fig. 13
Rapport molaire Eau(W)/Roche(R) calculés pour différents sites d'échantillonage de la mylonite calcaire le long du chevauchement de Glaris. Les rapports W/R (échelle logarithmique) sont rapportés en fonction de la composition initiale inconnue de l'eau à 300°C, d'où un Δ^{18}Occ-H_2O of 5‰ résulte. Un δ^{18}O de 25.4‰ est assumé pour le protolithe calcaire (Burkhard and Kerrich 1988). Les rapports W/R sont calculés selon les formules de Taylor pour les systèmes fermés (e.g. Ohmoto 1986). Ce modèle «multi-pass» est reporté sur la gauche alors que les W/R correspondant au modèle «single pass» sont reportés sur l'axe de droite. Modifié d'après Burkhard et al. (1992).

dans le Verrucano et quelques changements mineurs (dissolution de la chlorite et de l'albite), aucune anomalie géochimique associée au chevauchement de Glaris ne fut détectée. Les études isotopiques révélèrent des faits bien plus intéressants (Fig. 12). Le δ^{18}O de tous les échantillons de Lochsitenkalk était systématiquement abaissé suivant une augmentation du sud (δ^{18}O=10‰ SMOW) au nord (δ^{18}O=20‰ SMOW) par rapport au δ^{18}O des carbonates mésozoïques (25‰) considérés comme leur protolithes. Burkhard et Kerrich (1990) et Burkhard et al. (1992) interprétèrent ces observations par une advection vers le nord et le long du chevauchement de fluides appauvris en ^{18}O trouvant leur origine dans le socle des racines du chevauchement. Ils calculèrent des rappots Eau/Roche (W/R) d'après les modèles de Taylor (1977) (multi-pass and one-pass model) (Fig. 13).

Ces calculs furent très critiqués car le W/R varie sur un profil le long du chevauchement puisque la composition du fluide évolue lors de son advection vers le Nord par intercation avec les roches. Bowman et al. (1994), sur la base des données de Burkhard et Kerrich (1990) et Burkhard et al. (1992), proposèrent un mode de calcul des paramètres de flux beaucoup plus solide basé sur la théorie de transport (Baumgartner et Rumble 1988; Bickle et Baker 1990; Baker et Spiegelman 1995) pour la circulation de fluides documentée le long du chevauchement. Un flux intégré sur le temps de 2950-5900 m^3/m^2 et un nombre de Peclet de 10 ont ainsi été dérivés (Fig. 14). Malheureusement, des mathématiques trop solides cachèrent une analyse géologique trop faible. Cette nouvelle approche du chevauchement de Glaris fut l'occasion pour Burkhard et Kerrich (1990) et Burkhard et al. (1992) de reconsidérer le rôle des fluides dans les mécanismes de déformation ayant accommodé les 35 km de déplacement

vers le nord. Pour la première fois, il était proposé que la Lochsitenkalk pourrait en partie ou en totalité être formée de calcite secondaire précipitée à partir des fluides circulant le long du chevauchement (Burkhard and Kerrich 1990). Le rôle de la déformation fragile était clairement souligné et une alternance entre déformation ductile et déformation cassante lié à une variation cyclique de la pression de fluide était proposée (Burkhard et al. 1992). Malheureusement aucun argument sérieux n'était présenté pour supporter cette idée.

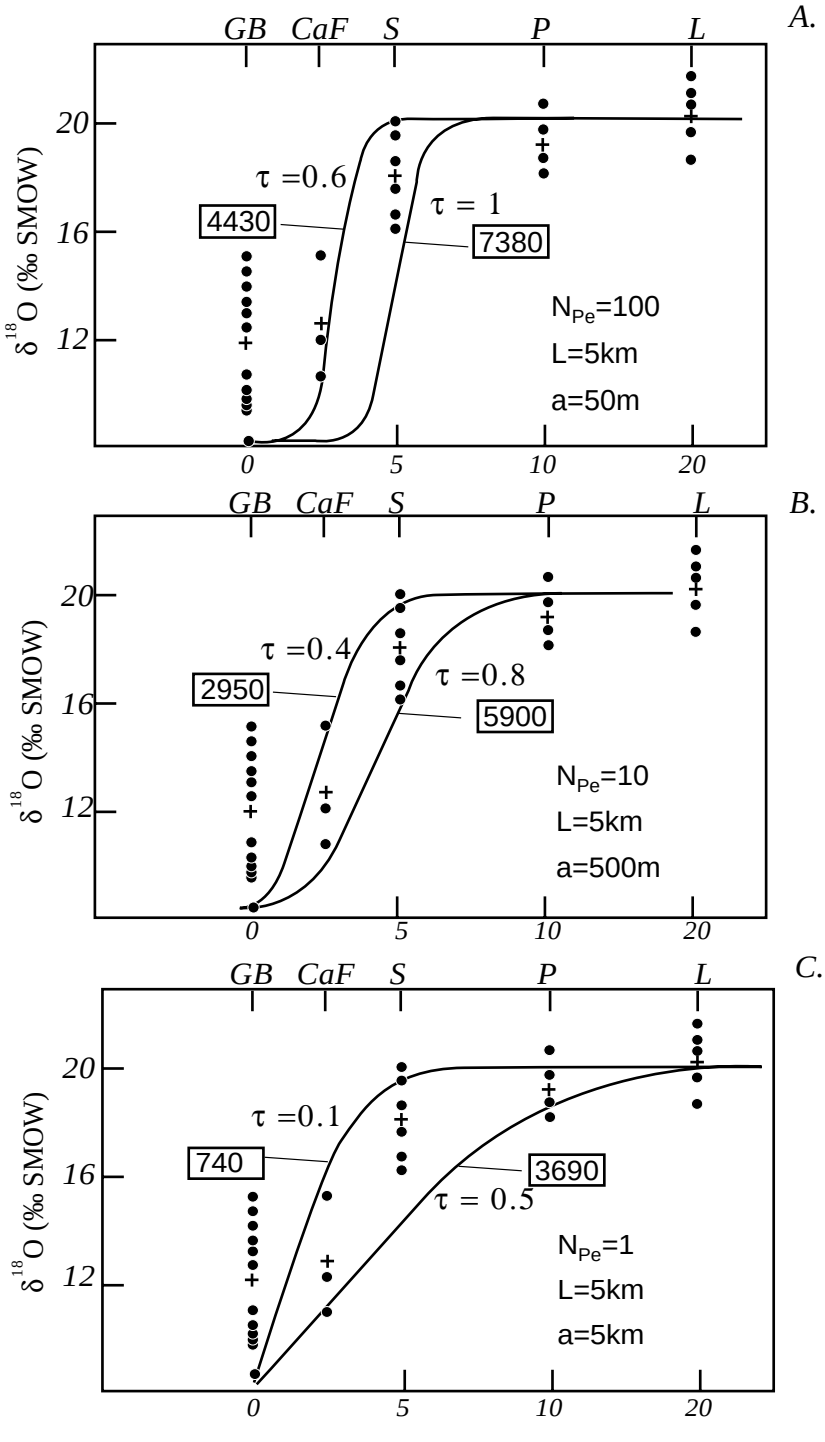

Fig. 14
Des fronts d'échange isotopiques modélisés avec une valeur de $\delta^{18}O$ de 4.5 pour mille pour le fluide qui s'infiltre et avec différentes valeurs de N_{Pe}, sont indiqués en surimpression sur les valeurs de $\delta^{18}O$ mesurées par Burkhard et Kerrich (1990) le long du chevauchement de Glaris. Les fronts se développant avec une valeur de N_{Pe} de 10, des valeurs de temps sans dimension (t) de 0.4 -.0.8 montrent les meilleures corrélations avec les données qui définissent le front isotopique de l'oxygène (défini par la moyenne maximal à Crap da Flem, et Segnas). Sont encore indiqués en surimpression les flux intégrés sur le temps (m^3/m^2) définis par le modèle de transport. Les abbréviations pour les sites d'échantillonage sont: GB= Grau Berg, CaF= Crap da Flem, S= Segnas, P= Pizol and L=Lochsite. L est une distance sans dimensions, a est le coefficient de dispersion. Modifié d'après Bowman et al. (1994)

But de cette étude

Depuis les travaux de Schmid (1975; 1982) et Schmid et al. (1977; 1981), la Lochsitenkalk était classiquement reconnue comme un exemple naturel de roche se déformant par glissement aux joints de grains dans le régime de la superplasticité. Burkhard et Kerrich (1990) et Burkhard et al. (1992) proposèrent l'alternance de déformation plastique et fragile, liée à une variation cyclique de la pression de fluide, pour accommoder les 35 km de déplacement vers le Nord le long du chevauchement de Glaris.

Burkhard et Kerrich (1990) et Burkhard et al. (1992) ont documenté une anomalie de la signature isotopique de l'oxygène le long d'un profil N-S du chevauchement de Glaris qu'ils interprétèrent comme un front d'échange isotopique lié à une circulation de fluides appauvris en ^{18}O trouvant leur source dans la zone de racine du chevauchement. Les données de Burkhard et Kerrich (1990) et Burkhard et al. (1992) furent utilisées par Bowman et al. (1994) pour calculer les paramètres de flux. Malheureusement ces simulations étaient basées sur un bien maigre jeu de données, et les variations isotopiques verticales à travers le chevauchement n'avaient pas été considérées.

Cette étude se propose de résoudre définitivement deux problèmes liés au chevauchement de la nappe de Glaris afin d'enterrer à tous jamais les spectres de la superplasticité et des rapports W/R. Premièrement, les mécanismes de déformation actifs dans la Lochsitenkalk pendant la phase de chevauchement ont été étudiés en analysant des échantillons de Lochsitenkalk au moyen de la microscopie optique à transmission, de la microscopie électronique à balayage et de la cathodoluminescence. L'analyse de microtextures et microstructures à l'échelle millimétrique a permis de mieux évaluer les rôles relatifs de la déformation ductile (superplasticité, déformation intracristalline par glissement de dislocations) et de la déformation cassante (fracturation hydraulique) dans la formation et l'évolution de la mylonite.

Deuxièmement, la systématique des isotopes de l'oxygène, du carbone et du strontium sera précisément définie: plus de 40 sites ont été choisis le long du chevauchement de Glaris pour une échantillonage précis de la Lochsitenkalk et de profils verticaux à travers le chevauchement. Les patrons de variations isotopiques nous ont permis de déterminer la géométrie des différents systèmes de circulation de fluides et de calculer des paramètres de flux, tels que, le flux intégré sur le temps, le nombre de Peclet et la distance de diffusion des systèmes de flux. Finalement, la véracité de ces déductions a été contrôlée en simulant la géométrie des systèmes de circulation à l'aide d'un programme de simulation par éléments finis, développé à l'Université Laval de Québec dans le but de mieux contraindre quels ont été les paramètres qui ont déterminé les chemins de circulation des fluides pendant le chevauchement de la nappe de Glaris.

Description et répartition du travail

Ce travail est le résultat d'une intense collaboration internationale et, pour des raisons déontologiques, il est de mon devoir d'informer le lecteur de ma contribution à ce travail par rapport à celle

des co-auteurs des différents articles qui constituent l'ossature de ce manuscrit.

Le chapitre II traite des mécanismes de déformation actifs dans la Lochsitenkalk lors du chevauchement. L'activité alternée de mécanismes de déformation cassants et plastiques dans la mylonite calcaire a été mise en évidence par l'étude de lames minces et ultra-minces, supportée par des observations d'échantillons de Lochsitenkalk au microscope électronique à balayage (MEB) et à la cathodoluminescence. A la fin de ce chapitre, des interprétations originales et provocantes du déplacement de la nappe de Glaris en terme de glissement sismique dans un régime globalement ductile sont proposées. Hormis les analyses par cathodoluminescence qui ont été conduites à l'Université de Berne en collaboration avec le Dr. K. Ramseyer, je peux me prévaloir d'avoir accompli toutes les préparations et analyses restantes à l'Université de Neuchâtel. Lors de la préparation des lames ultra-minces et des observations au MEB, l'assistance de l'équipe de l'ancien « Insitut de Métallurgie Structurale », nouveau « Comlab au CSEM » et en particulier du Dr. M. Dadras m'a été particulièrement bénéficiaire. Le premier jet de l'article fut mon œuvre, mais au vue des carrences d'anglais, les corrections d'el Professore Martin Burkhard étaient cruciales. L'article subit ensuite un sérieux processus de révisons avant d'être publié dans Terra Nova. Alors que la majorité de mes idées originelles furent sauvées lors de ce processus de révision, ce dernier fut pour moi un apprentissage des procédures de négociation et de diplomatie entre les différentes parties.

Les chapitres III et IV présentent deux interprétations possibles des données des isotopes du carbone, de l'oxygène et du strontium mesurées dans des profils détaillés à travers et le long du chevauchement de Glaris. Dans le chapitre III, les patrons isotopiques sont expliqués par un flux de fluides canalisé le long du chevauchement au sud et un flux de fluides vers le haut à travers le chevauchement du flysch dans le Verrucano au nord. Les rapports isotopiques du carbone, de l'oxygène et du strontium ont été mesurés sur plus de 30 sites le long du chevauchement dans la Lochsitenkalk et sur 10 profils verticaux à travers le chevauchement. J'ai assuré le travail de terrain durant les étés 1998 et 1999 occasionellement accompagnés d'amis et de Martin Burkhard lors de périples dangereux. Lors de l'été 1998, une visite commune de 3 jours a été organisée avec R. Abart et A. McCaig. Pour sa part, R. Abart a conduit sa propre campagne d'échantillonage à Grauberg et Lochsite en 98/99. Un total d'environ 800 échantillons de Lochsitenkalk, de Flysch, de Verrucano ou de carbonates du mur ont été analysés afin d'obtenir le $\delta^{18}O$ (SMOW) et le $\delta^{13}C$ (PDB) de la calcite. Ces analyses ont été conduites à l'Université de Graz (env. 75%, R. Abart) et à l'Université de Berne (25%, S. Burns) sur des lignes d'extraction automatisées. Mon activité était alors restreinte à la préparation de poudres de roche. De plus, environ 50 rapports $^{87}Sr/^{86}Sr$ ont été déterminés sur des morceaux de Lochsitenkalk à l'Université de Leeds. Lors d'un stage à l'Université de Leeds, j'ai préparé quelques 50 aliquots de poudre pour analyse au spectromètre de masse sous la direction des docteurs A. McCaig et B. Cliff. Une intense discussion sur

les données du strontium a conclu ce stage et est largement reflétée dans le chapitre III. Ce dernier fut élaboré avec R. Abart. Ma contribution a été de préparer les figures et d'écrire l'article, hormis la partie sur les mathématiques des modélisations de flux qui a été faite par R. Abart. Le premier jet a bénéficé des commentaires et corrections de R. Abart, M. Burkhard et A. McCaig. Néamoins, ce papier présente mes analyses et interprétations des données isotopiques et je crois pouvoir m'attribuer plus de 80% du travail.

Le chapitre IV présente une interprétation alternative des chemins de flux le long du chevauchement de Glaris. Un flux de fluides vers le bas du Verrucano dans les carbonates du mur au sud et un flux de fluides vers le haut du flysch dans le Verrucano sont proposés pour expliquer les profils verticaux des données isotopiques du carbone, de l'oxygène et du strontium de la calcite combinées aux rapports isotopiques de l'oxygène dans le quartz et aux données pétrologiques. Contrairement au chapitre III, seuls deux profils à travers le chevauchement sont considérés, respectivement à Grauberg et Lochsite. La majorité des échantillons requis par cette étude ont été collectés et préparés par R. Abart.
Ce chapitre est l'œuvre de R. Abart. Son interprétation par échange verticaux d'isotopes contraste fortement avec la mienne, c'est-à-dire un flux canalisé le long du chevauchement. Ainsi, ma contribution à ce chapitre se restreint à de l'information sur la géologie régionale, la participation à l'interprétation des tendances régionales, ce qui correspond à une part de 10% environ.

Dans le chapitre V, je présente des simulations numériques par éléments finis des circulations de fluides le long du chevauchement de Glaris qui permettent de déduire les paramètres responsables de la géométrie des systèmes de flux déduits des zonations isotopiques. Lors d'un stage à l'Université Laval de Québec (Canada), j'ai appris à utiliser le programme de simulation FRAC3D, développé par Therrien et Sudicky, sous la direction des professeurs Georges Beaudoin et René Therrien. Lors de mon séjour au Canada, j'ai eu l'occasion de conduire une bonne dizaine de simulations, et, à mon retour en Suisse, j'ai poursuivi ces simulations grâce au protocole Telnet. Les meilleures simulations sont présentées dans les annexes. Le but de ces modélisations était de reproduire au mieux la zonation des isotopes de l'oxygène dans la Lochsitenkalk le long du chevauchement de Glaris. Ceci m'a permis de démontrer que les chemins empruntés par les fluides sont principalement contrôlés par la configuration des sources et drains et par le « percement » de la limite lithostatique-hydrostatique par la nappe qui avance. L'article qui constitue le chapitre V est le résultat d'une intense collaboration entre Georges Beaudoin, Martin Burkhard, René Therrien et moi-même. Mon travail a été de conduire les simulations, de choisir les figures et les meilleurs simulations et finalement d'écrire cet article. Ce dernier a bénéficié des corrections très constructives de Georges Beaudoin, Martin Burkhard et René Therrien.

Dans le chapitre VI, les conclusions des chapitres II-V sont discutées et âprement critiquées d'un point de vue plus philosophique. Ces considéra-

tions générales soulignent les pours et les contres des conclusions des différents chapitres et, par exemple, présentent une discussion élargie du problème non résolu flux canalisé vs. flux vertical dans la partie sud du chevauchement (comparaison des chapitres III et IV). Ce chapitre apporte aussi de plus amples informations sur les contributions relatives de la déformation plastique et de la déformation fragile au déplacement total de la nappe de Glaris.

Finalement, les annexes servent de support aux observations présentées et discutées dans les différents chapitres. Quelques indications supplémentaires sont données dans les légendes des différentes annexes.

References

Bailey, E. B. (1935). Tectonic Essays, Mainly Alpine. Oxford, Oxford University Press.

Baker, J. and M. Spiegelman (1995). "Modelling an infiltration-driven geochemical front." Earth and Planetary Science Letters 136(3-4): 87-96.

Baumgartner, L. P. and D. I. Rumble (1988). "Transport of stable isotopes: I: development of a kinetic continuum theory for stable isotope transport." Contributions Mineralogy Petrology 98: 417-430.

Bertrand, M. (1884). "Rapport de structure des Alpes de Glaris et du bassin houiller du Nord." Bulletin de la Société géologique de France 3(12): 318-330.

Bickle, M. J. and J. Baker (1990). "Advective-diffusive transport of isotopic fronts; an example from Naxos, Greece." Earth and Planetary Science Letters 97(1-2): 78-93.

Bowman, J. R., S. D. Willett, et al. (1994). "Oxygen isotopic transport and exchange during fluid flow; one-dimensional models and applications." American Journal of Science 294(1): 1-55.

Briegel, U. and C. Goetze (1978). "Estimates of differential stress recorded in the dislocation structure of Lochseiten Limestone (Switzerland)." Tectonophysics 48(1-2): 61-76.

Burkhard, M. and R. Kerrich (1988). "Fluid regimes in the deformation of the Helvetic nappes, Switzerland, as inferred from stable isotope data." Contributions Mineralogy Petrology 99: 416-429.

Burkhard, M. and R. Kerrich (1990). "Fluid-rock interactions during thrusting of the Glarus nappe - evidence from geochemical and stable isotope data." Schweizerische Mineralogisch Petrographische Mitteilungen 70: 77-82.

Burkhard, M., R. Kerrich, et al. (1992). "Stable and Sr-isotope evidence for fluid advection during thrusting of the Glarus nappe (Swiss Alps)." Contributions Mineralogy Petrology 112: 293-311.

Escher, A. (1846). Gerbirgskunde. O. a. B. Heer, J. J., der Cantons Glarus, Bd 7, Gemälde der Schweiz. Huter/St-Gallen/Bern.

Escher, A. (1866). Sur la géologie du Canton de Glaris. 50e session, Neuchâtel.

Frey, F. (1965). Geologie der östlichen Claridenkette. Vjschr. der naturf. Ges. Zürich. 110: 280pp.

Frey, M. (1988). "Discontinuous inverse metamorphic zonation, Glarus Alps, Switzerland; evidence from illite "crystallinity" data." Schweizerische Mineralogische und Petrographische Mitteilungen = Bulletin Suisse de Mineralogie et Petrographie 68(2): 171-183.

Groshong, R. H., Jr., O. A. Pfiffner, et al. (1984). "Strain partitioning in the Helvetic thrust belt of eastern Switzerland from the leading edge to the internal zone." Journal of Structural Geology 6(1-2): 5-18.

Heim, A. (1878). Untersuchungen über den Mechanismus der Gebirgsbildung. Basel, Schwabe.

Heim, A. (1891). "Geologie de Hochalpen zwischen Reuss and Rhein." Beitraege zur Geologischen Karte der Schweiz = Matériaux pour la Carte Géologique de la Suisse = Materiali per la Carta Geologica della Svizzera 1/25: 1-503/1-76.

Heim, A. (1921). Geologie der Schweiz. Band 2: Die Schweizer Alpen 1. Hälfte. Leipzig, Tauchniz.

Hsue, K. J. (1969). "Kinetics of Glarus overthrust, Switzerland." Eos 50(4): 313.

Hubbert, M. K. and W. W. Rubey (1959). "Role of fluid pressure in mechanics of overthrust faulting." Geological Society of America Bulletin 70(2): 115-166.

Hunziker, J. C. (1987). Radiogenic isotopes in very low-grade metamorphism. Low Temperature Metamorphism. F. M. Glasgow, Blackie: 200-226.

Hunziker, J. C., M. Frey, et al. (1986). "The evolution of illite to muscovite; mineralogical and isotopic data from the Glarus Alps, Switzerland." Contributions to Mineralogy and Petrology 92(2): 157-180.

Lange, H. (1968). "Neue Ergebnisse ueber das Alter der Lochwaldschichten der helvetischen Zone in der Wertachenge (Allgaeu). Translated title: New data on the age of the Lochwald beds in the Helvetic zone of the Wertach gorge, Allgaeu." Neues Jahrb. Geol. Palaeontol., Monatsh. No. 173(incl. Engl. sum).

Lihou Joanne, C. and A. Mange Rajetzky Maria (1996). "Provenance of the Sardona Flysch, eastern Swiss Alps; example of high-resolution heavy mineral analysis applied to an ultrastable assemblage." Sedimentary Geology 105: 3-4.

Milnes, A. G. and O. A. Pfiffner (1977). "Structural development of the Infrahelvetic Complex, eastern Switzerland." Eclogae Geol. Helv. 70(1): 83-95.

Oberholzer, J. (1908). "Die Ueberfaltungsdecken auf der Westseite des Linthales." Eclogae Geologicae Helvetiae 10(4): 531-555.

Oberholzer, J. (1933). Geologie der Glarner Alpen. Beiträge Geologische Karte Schweiz, geologische Kommission. F28.

Pfiffner, O. A. (1977). "Tektonische Untersuchungen im Infrahelvetikum der Ostschweiz. Translated title: Tectonic studies of the Infrahelvetic Complex, eastern Switzerland." Zuerich, Univ., Geol. Inst Eidgenoess. Tech. Hochsch., Geol. Inst., Mitt 217(5911): 164.

Pfiffner, O. A. (1978). "Der Falten- und Kleindeckenbau im Infrahelvetikum der Ostschweiz. Translated title: The faults and small nappes in the Infrahelvetic Complex of East Switzerland." Eclogae Geol. Helv. 71(1): 61-84.

Pfiffner, O. A. (1981). Fold- and -thrust tectonics in the Helvetic Nappes (E. Switzerland). Thrust and Nappe Tectonics. R. Price. London, The Geological Society of London: 319-327.

Pfiffner, O. A. (1982). "Deformation mechanisms and flow regimes in limestones from the Helvetic Zone of the Swiss Alps." Journal-of-Structural-Geology 4(4): 429-442.

Pfiffner, O. A. (1985). "Displacements along thrust faults." Eclogae-Geologicae-Helvetiae 78(2): 313-333.

Pfiffner, O. A. (1993). "The structure of the Helvetic nappes and its relation to the mechanical stratigraphy." Journal of Structural Geology 15(3-5): 511-521.

Rothpletz, A. (1883). "Zum Gebirgsbau der Alpen beiderseits des Rheines." Ztschr. deutsch. geol.Ges. Jg 1883: 135-189.

Rothpletz, A. (1894). Geotektonische Probleme. Stuttgart, Schwiezerbart.

Rothpletz, A. (1898). Das Geotektonisch Problem der Glarner Alpen. Jena, Fischer.

Schardt, H. (1893). "Sur l'origine des Préalpes

Romandes." Eclogae Geologicae Helvetiae 4: 129-142.

Schmid, S. M. (1975). "The Glarus overthrust; field evidence and mechanical model." Eclogae Geol. Helv. 68(2): 247-280.

Schmid, S. M. (1982). "Laboratory experiments on rheology and deformation mechanisms in calcite rocks and their application to studies in the field." Mitt. Geol. Inst. ETH u. Universität Zürich n.F. 241: 106.

Schmid, S. M. (1982). Microfabric studies as Indicators of Deformation Mechanisms and Flow Laws Operative in Mountain Building. Mountain Building processes. K. J. Hsü. London, Academic Press: 95-110.

Schmid, S. M., J. M. Boland, et al. (1977). "Superplastic flow in finegrained limestone." Tectonophysics 43: 257-291.

Schmid, S. M., M. Casey, et al. (1981). "The microfabric of calcite tectonites from the Helvetic Nappes (Swiss Alps)." McClay, K R., Price, N. J. Thrust and nappe tectonics; International conference. Univ. London, Dep. Geol., London, United-Kingdom. Special-Publication-Geological-Society-of-London(9): 151-158.

Schmid, S. M., O. A. Pfiffner, et al. (1997). Integrated croos section and tectonic evolution of the Alps along the Eastern Traverse. Deep Structure of the Swiss Alps. O. A. Pfiffner, P. Lehner, P. Heitzmann, S. Mueller and S. A. Basel, Birkhäuser Verlag: 289-304.

Siddans, A. W. B. (1979). "Deformation, metamorphism and texture development in Permian mudstones of the Glarus Alps (eastern Switzerland)." Eclogae-Geol.-Helv 72(3): 601-621.

Staub, R. (1954). "Der Bau der Glarneralpen und seine prinzipielle Bedeutung fuer die Alpengeologie." 1(200).

Theobald, G. (1866). "Geologische Uebersicht der Rhätischen Alpen." Jahr Schwiez Alpenclub Jg 1866: 1-45.

Theobald, G. (1869). "Der Kistenpass und seine Umgebung." Jb natur. Ges. Graubünden, n. F. 14: 109-145.

Truempy, R. (1991). The Glarus nappes; a controversy of a century ago. Controversies in modern geology; Evolution of geological theories in sedimentology, Earth history and tectonics. D.-W. Mueller, J.-A. McKenzie and H. Weissert. Press. London, Acad: 385-404.

Twiss, R. J. and E. M. Moores (1992). Structural Geology. New York, W. H. Freeman And Company.

Chapter 2: Brittle-Ductile deformation in the Glarus thrust Lochseiten (LK) calc-mylonite

paper in press at Terra Nova

Nicolas P. Badertscher, Martin Burkhard

Institut de Géologie, 11 Rue Emile-Argand, case postale 2, 2007 Neuchâtel, Switzerland

nicolas.badertscher@unine.ch
martin.burkhard@unine.ch

phone 0041 32 718 2600
fax 0041 32 718 2601

Abstract

The Glarus thrust accommodated at least 30 km of northward displacement strongly localized within a meter thin layer of "Lochseiten" (LK) calc-mylonite. This layer displays veins in various states of plastic deformation and a wildly refolded foliated gouge texture. Lattice- and shape-preferred-orientations are observed within the fine grained, recrystallized matrix. These features indicate the alternate activity of brittle and ductile deformation mechanisms. In contrast to the classical view that grain boundary sliding (superplasticity) is the dominant deformation mechanism, we advocate fluids, derived from the footwall and expelled along the thrust, as responsible for hydrofracturing and cataclastic deformation. In periods between fracture events, deformation was ductile. In our new interpretation a substantial amount of the total thrust displacement was accommodated by numerous short-lived and strongly localized fracture events at the base of the Verrucano thrust sheet, rather than a permanently weak décollement lithology.

Introduction

Large overthrusts have been recognized since the end of the nineteenth century, but a mechanical paradox quickly appeared since the motion of large rock masses along low angle thrust faults seemed mechanically impossible, or restricted to distances smaller than about 10 km (e.g Hsü, 1969). Proposals to solve this problem include: 1) large strength contrasts between exceedingly weak rocks in the décollement horizon and much stronger ones within the thrust sheet, 2) propagation of incremental slip domains and 3) close to lithostatic fluid pressures within the décollement horizon (e.g. Schmid, 1975; Price, 1988; Henry and Le Pichon, 1991; Twiss and Moores, 1992).
Displacement along the Glarus thrust is at least 30 km (Pfiffner, 1985) (Fig. 2). This thrust is a very

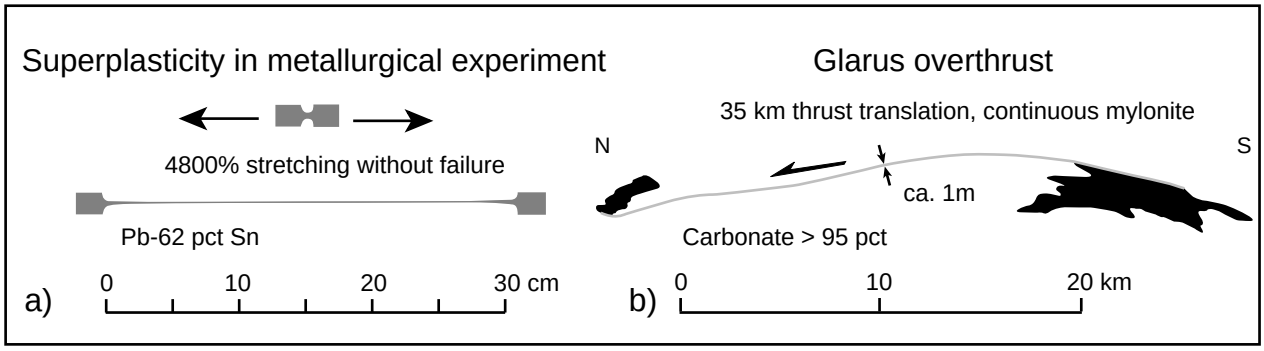

Fig. 1

Superplasticity has been proposed as an explanation for the extreme strain localization in the Lochseiten calc-mylonite (Schmid et al., 1977). a) Superplastically deformed Pb-62%Sn alloy in a metallurgical stretching experiment from Langdon (1982). b) schematic cross section of the Glarus thrust. A metre thick calc-mylonite connects Mesozoic carbonates in the foot- and hanging-wall over a total thrusting distance of about 30 km north-south, drawn to scale, the calc-mylonite would measure less than 2 µm thin in this figure!

well defined fault underlined by a thin layer of the famous "Lochseitenkalk" (LK)(Heim, 1921). Classically, the LK is interpreted to be smeared out Mesozoic carbonates from footwall and/or hangingwall (Schmid, 1975; Pfiffner, 1982). Superplastic flow has been proposed as the dominant deformation mechanism within the LK to explain the extremely high strains "without necking" (Fig. 1) and as a solution to the mechanical paradox of large overthrusts (Schmid et al., 1981; Schmid, 1982b). Earlier speculations about the mechanics of the Glarus thrust involved lithostatic fluid pressures (Hsü, 1969). Based on strongly altered stable isotope signatures within the LK and structural observations, Burkhard and Kerrich (1990) and Burkhard et al. (1992) proposed a veiny origin for most, if not all of the mylonite calcite.

In this paper we provide new structural and microstructural observations relevant to the discussion of the origin and structural evolution of the LK and the mechanics of this large overthrust.

Geological setting

Tectonic units at the front of the Alps in Eastern Switzerland (Fig. 2) are subdivided into a "Helvetic complex" above and an "Infra-Helvetic complex" below the Glarus thrust (Pfiffner, 1981; Pfiffner, 1993). The Helvetic Glarus nappe comprises Permian Verrucano overlain by a concordant Mesozoic series. The "Infrahelvetic" complex consists of a crystalline basement overlain by a sedimentary cover of Mesozoic carbonates and Tertiary Flysch and some South Helvetic and Penninic (Sardona) Flysch. The latter were emplaced onto the parautochthonous carbonates in early Oligocene times during the "Pizol phase" (Pfiffner, 1977). In a second, main deformation stage (Calanda phase), the whole Infrahelvetic complex was intensely folded and imbricated. Thrusting of the Glarus nappe (Ruchi phase) postdates these deformations (Pfiffner, 1977) in an out-of-sequence manner.

Metamorphism ranges from anchizone in the north to lower greenschist facies in the south

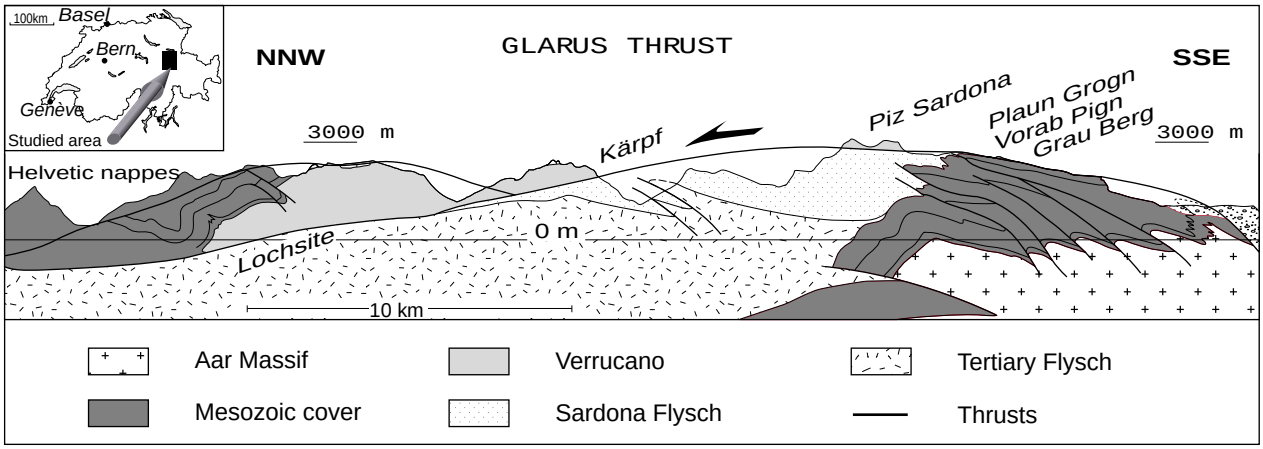

Fig. 2

Tectonic overview of the central, accessible portion of the Glarus overthrust (modified from Oberholzer, 1933). Some of the key localities mentioned in the text are indicated for their relative position in a NNW-SSE profile. North of the type locality "Lochsite" the thrust surface plunges below topography; it reemerges some 15 km further north.

(Frey, 1988; Rahn et al., 1995). The peak of this metamorphism post-dates the Calanda phase deformations (Groshong et al., 1984) estimated at 30-25 Ma. The "anchi-/epizone- boundary" is offset along the Glarus thrust by about 2 km (Groshong et al., 1984 Fig.3; Frey,1988) as the result of post-peak-metamorphic thrusting between 25 and 20 Ma (Hunziker et al., 1986).

Macroscopic observations at the Glarus thrust contact

The Glarus thrust is characterized by the presence of a continuous thin layer (20 cm to 5 m) of calcmylonite (LK) and a strongly asymmetric strain gradient away from the contact. Thrust related deformations are virtually absent two to five meters below the contact, whereas strong mylonitic foliations, subparallel to the main thrust, can be observed tens of meters above it and fading out gradually into the hangingwall. In this paper, attention is focused on structures within the LK; for a complete description of the structures in the footwall and hangingwall (Fig. 3) see (Schmid, 1975; Siddans, 1979; Burkhard et al., 1992; Lihou, 1996). Schmid (1975) and Burkhard et al. (1992) described the turbulent appearance of the LK due to the refolded alternation of white, pure calcite and black stylolitic layers. This banding locally defines sheath folds and very complex 3-D patterns (Fig. 5a left-hand side). Neither pervasive schistosity nor stretching lineation are observed within the classic LK (Schmid, 1975). The so-called "septum" is a conspicuous extremely thin (mm to cm) planar horizon cross-cutting all internal structures of the LK. It consists either of gouge or a very sharp shear zone and has been interpreted as being due to some modest, late motion of the Glarus nappe (Schmid, 1975).

The lower contact of the LK with the Flysch is strongly cuspate-lobate (Schmid, 1975) (Fig. 3). The upper contact with the Verrucano, as well as lower contacts with Mesozoic carbonates (in the South) are irregular too, but lobes and cusps have

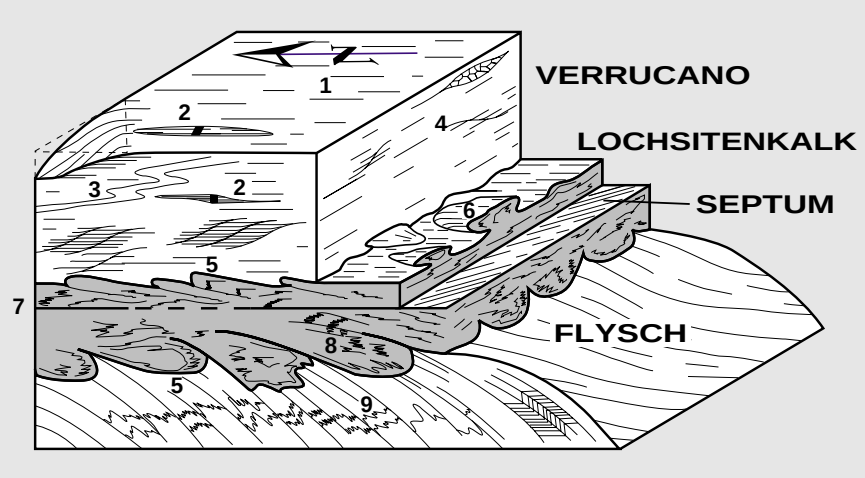

Fig. 3

Schematic overview of macroscopically observed structures within the LK and its contacts with Flysch in the footwall and Verrucano in the hangingwall (modified after Burkhard, 1992). In the Flysch a steeply dipping foliation (Calanda phase) can be totally transposed by a younger crenulation cleavage (9) within the last few meters below the contact (Ruchi phase). In the Verrucano a well-developed foliation, sub-parallel to the thrust, is increasingly mylonitic towards the contact. Stretching lineations in the hangingwall (1) have a very constant N-S direction (compare Siddans, 1979). Crenulations (3) within the Verrucano immediately above the contact have N-S oriented fold axes, parallel to the stretching lineation. Further up, however, crenulations are oriented E-W. Abundant C' shear bands (4) and asymmetric strain fringes (2) on pyrite grains consistently indicate thrusting towards the North.

Structures in the LK (see also text) include: 5-cuspate/lobate contacts, 6-sheath folds, 7-"septum", 8-internal banding: strongly folded, sheared and crumpled stylolites and former veins.

smaller amplitudes. The pattern of cusps and lobes seems to indicate a higher viscosity for the LK than for the Flysch or Verrucano. This observation, confirmed by the boudinage of LK in the Flysch, contrasts with the expected weak behaviour of the calc-mylonite (see Schmid, 1975).

In the South, where the footwall consists of Mesozoic carbonates, LK seems to be derived from the former and has a generally smoother appearance (Fig. 5b) with a locally pervasive foliation and well developed stretching lineation (see also Pfiffner, 1982).

In a few places, lenses of Verrucano are trapped within the LK. They can be interpreted either as slivers of tectonically emplaced Verrucano within the LK, or as "islands" of Verrucano isolated from their surrounding country-rock by the addition of massive calcite veins, affected by strong ductile overprinting and folding near the basal thrust contact. West of Risetenpass, the LK deviates significantly from its ordinary planar configuration, describing a North-vergent fold of metric amplitude with Flysch in the anticline core. This fold clearly demonstrates that ductile deformation continued after the formation of some planar LK (see also Schmid, 1975). In some places the LK - Verrucano contact exhibits macroscopic evidence of brecciation and cataclasis (e.g. at Ringelspitz and Pizol) (Fig. 5a right-hand side).

Microscopic observations

A) Thin section observations

At low magnification typical LK from the northern areas exhibits the chaotic structure of a foliated and folded cataclasite (Snoke et al. (1998), fig.16 compare with our Fig. 4B). The foliation is underlined by the alternation of dark stylolitic and light coloured layers. The light layers can often be identified as former veins variably fractured, folded and sheared (see also Burkhard et al., 1992). Several generations of veins can be distinguished. In the southern areas the structure is smoother and locally a true planar foliation is developed (Fig. 4A). However, former white veins parallel to this foliation can still be recognized. In both types of LK younger veins crosscut the general structure at high angles, even these latest veins are often fractured and sheared (Fig 4A).

B) Optical microscopy on ultra thin sections

Microstructures on the grain scale within the LK mylonite are observed in ultra thin sections (< 3 µm) where calcite appears in different shades of grey. Grain size ranges from > 100 µm to <1 µm. Coarse grains clearly belong to veins and are always heavily twinned (type III or IV according to Burkhard, 1993) (Fig. 6A-B). Intermediate size grains occur in isolation within a matrix of very fine grains (<5µm). Vein calcite grains display variable degrees of disruption and exhibit ample evidence for dynamic recrystallization (Fig 6A-B) in the form of subgrains, sutured grain boundaries and a mortar structure. Grain boundary migration (GBM) is clearly observed on thick twins (type IV according to Burkhard (1993)). Increasing deformation and associated recrystallization causes coarse and intermediate grains to be progressively replaced by very small "matrix" grains. In contrast to the strongly sutured grain boundaries of large and intermediate grains very fine grains have more regular, smoother grain boundaries, but bulging still documents GBM (Fig 6C-D). Even very small grains of less than 2 µm are occasionally twinned, as already pointed

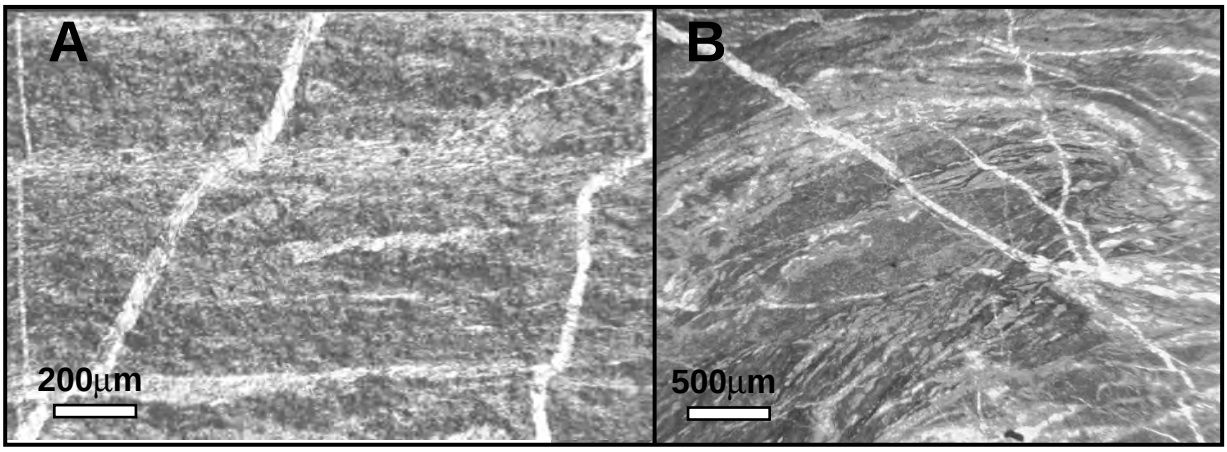

Fig. 4

Microphotographs of Lochseiten calc-mylonites. A) sample from Grau Berg (736.300/192.900), South. B) foliated gouge structure in a sample from Lochsite (725.860/206.400), North.

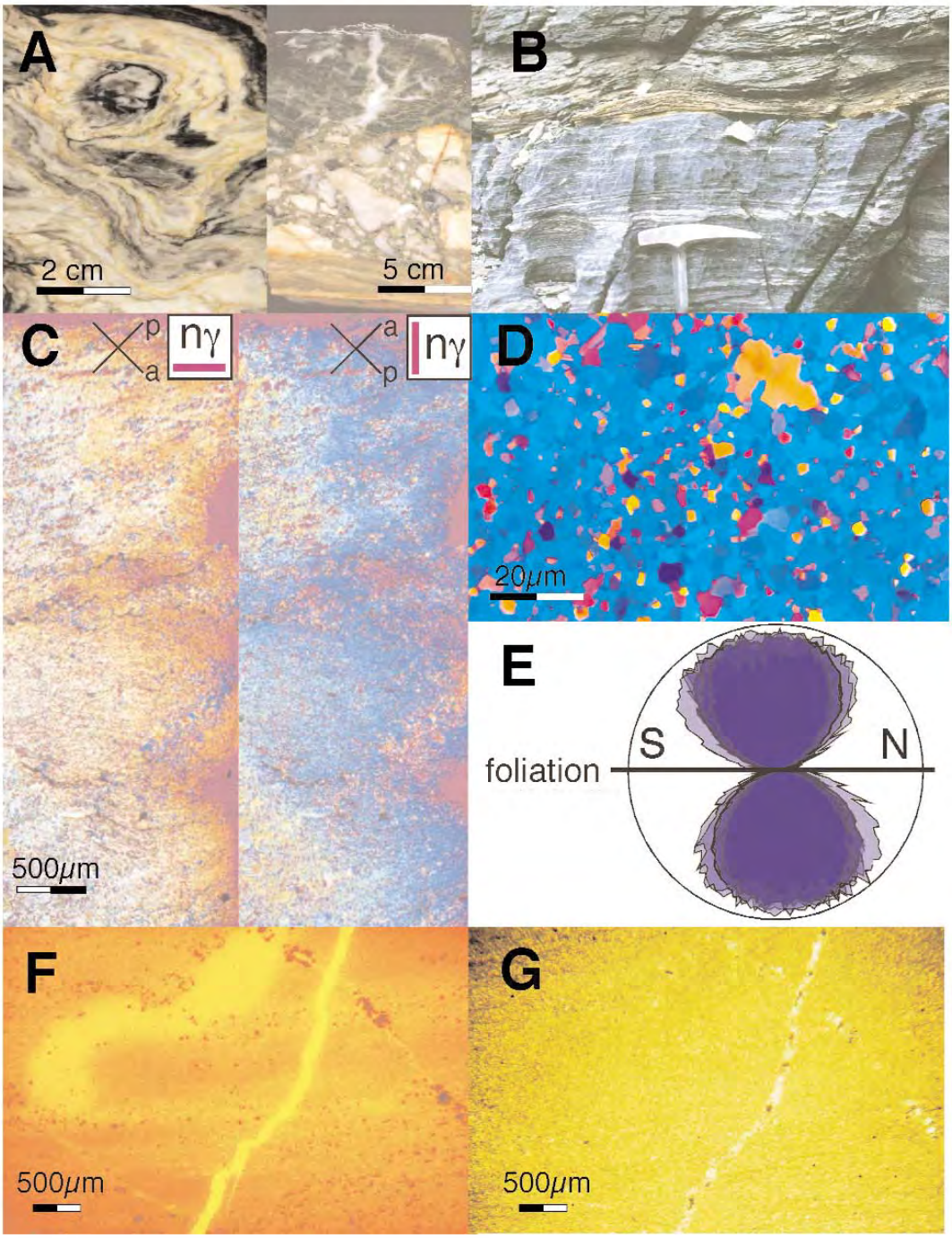

Fig. 5

Structural and micro-structural observations in LK mylonites.

A) Left hand side: complex structures observed in the LK from northern exposures include sheath folds, shear bands and "crumpling" of the alternation of white, pure calcite and black, stylolitic layers. Sample from Piz Sardona (738.150/197.600). Right hand side: Contact LK-Verrucano at Ringelspitz (745.200/195.800), the Verrucano is brecciated and cut by the septum consisting of a cataclasite (lower contact). B) Glarus thrust at Plaun Grond (730.3/192) with LK representative of southern localities. General banding in different colours is due to strongly deformed light coloured veins, dark stylolites and traces of secondary dolomite responsible for the orange/yellow alteration colour at the LK-Verrucano (green) contact. C) Ultrathin (<3mm) edges of a LK thin section from Kärpf (726.3/196.95) display strong lattice preferred orientation visualized through the use of a gypsum plate (530nm) and crossed polarizers. Note horizontal banding. D) Close up of the same sample as shown in C. Average grain size of matrix calcite is less than 3 µm; note fairly straight grain boundaries and the absence of a shape preferred orientation. The large ameboid orange grain possibly represents the relic of a former vein. E) Photometrically determined rose diagram illus-

trates the preferred orientation of calcite c-axes (projected onto the plane of observation) measured in six different spots with 200mm diameter along the ultrathin edge of the section shown in C. F) Cold cathodoluminescence reveals the presence of a old and sheared ghost vein in the calc-mylonite sample from the Grau Berg locality (South). Three successive generations of veins are easily distinguished in CL. Dark red grains along the second vein are quartz. G) Same thin section as F, seen in normal light displays a homogeneous fine-grained calcite matrix in the places where CL reveals the presence of ghost vein.

out by Schmid et al. (1981).

Matrix grains often show very strong Lattice Preferred Orientation (LPO), as visualized through the use of a gypsum plate (Fig. 5C-D) and documented by semi-quantitative, photometric analyses (Price, 1973) (Fig. 5E). Along the ultra-thin edges of thin sections, LPO's can be seen to be coherent on the scale of a few millimeters across domains with very fine-grained matrix and coarser grains. No Shape Preferred Orientations (SPO) could be detected in the very fine-grained matrix in the North, whereas weak SPO with mean axial ratios of up to 2 are developed in the South (Fig. 6C-D).

C) Cathodoluminescence on thin-sections

In cold cathodoluminescence (CL), calcite appears in various shades of orange and yellow due to minute substitutions of Ca^{2+} by Mn^{2+} and the presence of other trace elements (Barbin and Schvoerer, 1997). CL microscopy reveals the presence of an unexpected composite layering within

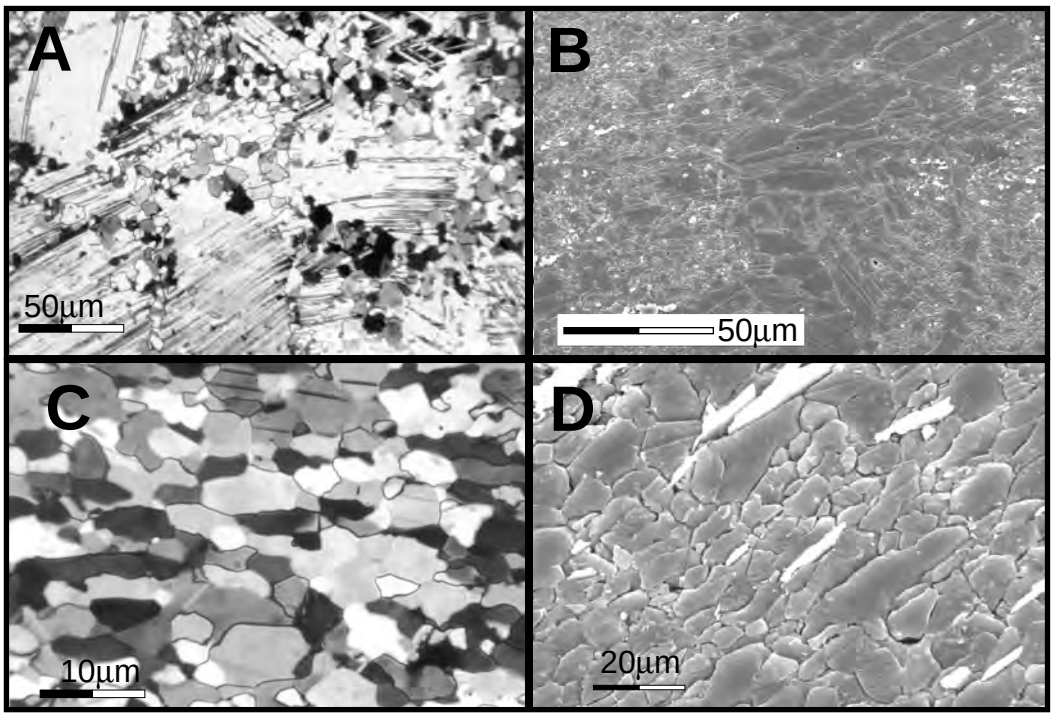

Fig. 6

A) Heavily twinned coarse calcite grains of veiny origin. Recrystallized "matrix" grains nucleate along twin- and grain-boundaries resulting in a mortar texture. Sample from Kärpf (726.250/197), thin section view, crossed polarizers.B) idem, SEM view. C) Shape preferred orientation in a LK sample from Vorab Pign (732.25/192.525), southern part of the Glarus thrust, thin section view, crossed polarizers. D) idem, SEM view.

optically homogeneous veins. Most interestingly, CL provides evidence for completely recrystallized "ghost" veins within the ultrafine-grained matrix (Fig. 5F, G). Optically non-detectable, such ghost veins apparently preserved some subtle geochemical vein signature despite intense folding and shearing and associated dynamic recrystallization. Diffuse boundaries (Fig. 5F, G) of such ghost veins are thought to be the result of chemical diffusion associated with GBM (Hay and Evans, 1987).

Discussion and conclusions

Based on experimental data and the absence of clear LPO's within LK mylonite samples, (Schmid et al., 1977; Schmid et al., 1981; Schmid, 1982a) proposed grain boundary sliding (superplastic flow) as the dominant deformation mechanism to account for the extreme strain localization observed at the base of the Glarus thrust. In this interpretation, the LK is considered as a very weak décollement layer on which the Glarus nappe was translated as a rigid block. Burkhard et al. (1992) provided stable isotope evidence for considerable fluid advection during thrusting and therefore speculated about the role of such fluids in deformation (compare Bowman et al., 1994). Meso- and microstructural observations document the alternating activity of brittle and crystal-plastic deformation processes and the omnipresence of dissolution-crystallization processes. These observations are difficult to reconcile with the idea of a single, dominant deformation mechanism such as the superplasticity proposed by Schmid et al. (1977, 1981) and Schmid (1982a). Brittle deformation features have been noted by earlier authors (Heim, 1921; Schmid et al., 1981; Pfiffner, 1982) but generally such observations were discarded as unimportant, late overprinting. However, there is no evidence for an evolution from plastic to brittle deformation with time. Foliated gouge textures and overprinted vein bands are more obvious in northern localities than in the South. This, however, can be interpreted in terms of a temperature gradient updip, rather than reflecting an evolution through time. Ductile deformation and dynamic recrystallization were merely more efficient in wiping out the evidence for brittle deformations further south, rather than being more important in terms of their contribution to total strain and thrust translation.

The absence of LPO's was a central argument used by Schmid et al. (1977) in favour of superplasticity. Our observations of the presence of strong LPO's seen in optical microscopy (Fig. 5C-E) contrast with the lack of LPO's in the XRD-samples analyzed by Schmid et al. (1981). It could be argued that our optical LPO's are a local phenomenon, inherited from LPO's due to twinning of some coarse vein grains that have totally recrystallized. However, according to Walker et al. (1990), grain boundary sliding in the fine-grained matrix, should not allow the preservation of strong LPO's. Alternatively, LPO's, when measured integrally on large (cm-size) slides by XRD techniques, may be "diluted" by the rotation of mm- to cm-size rock fragments which are apparent in the form of "chaotic" foliated gouge textures (Fig 4B, 5A).

The Glarus thrust roots at mid-crustal levels

(Pfiffner, 1985). Dewatering by compaction and prograde metamorphism in the footwall produce considerable amounts of fluids with a general tendency to escape upward - forelandward (Oliver, 1986; Marquer and Burkhard, 1992). The role of such fluids in deformation depends critically on the fluid production rate and permeability in the surrounding rock masses (Connolly and Thompson, 1989; Gueguen et al., 1991). We propose that an abrupt change in permeability between the footwall and hangingwall lead to fluid channelling at this particular thrust contact. In this scenario fluids produced in the footwall percolate continuously upward preferentially along the steeply inclined pre-existing (Calanda phase) foliation. The clay rich Verrucano thrust sheet, with actively forming subhorizontal foliation, represents a permeability barrier to this percolation. In analogy to the fault-valve scenario (Sibson, 1990), fluid pressures would increase below this contact up to the threshold for hydrofracturing associated with seismic slip (Sibson, 1990; Petit et al., 1999). Due to dilatency, fluid pressures would drop abruptly to values lower than within wall rock. Healing of the fracture network and formation of veins progressively seals the thrust fault, allowing fluid pressures to build up again. Between fracture events, ductile intracrystalline deformation and dynamic recrystallization result in the formation of a microcrystalline matrix within the LK and of LPO's within this matrix. Thrust faults do not have the ideal orientation for such fault-valve behaviour (Sibson, 1990; Nguyen et al., 1998). However, similar structural observations and interpretations have been reported from other thrusts in the Apennines (Coli and Sani, 1990), the McConnell thrust in the Canadian Rockies and the Hunter Valley thrust in the Appalachians (Kennedy and Logan, 1997; Kennedy et al., 1998) and the Gavarnie thrust in the Pyrenees (McCaig et al., 1995).

The paradox of the lobate-cuspate contact, which suggests a competent LK sandwiched in between less comptetent Verrucano and Flysch finds an elegant solution in the fault-valve / seismic failure scenario. Fracturing and calcite mineralizations along the base of the Verrucano thrust sheet are triggered by fluctuations in fluid pressure, because fluids are stored below this "permeability barrier". The planar septum horizons, cataclasites and veins reflect some of the latest brittle events. Background deformation of the entire thrust zone in the ductile regime is responsible for the repeated shearing and folding of older septums, veins and the LK-wall-rock contacts, as well as mylonitisation of the Verrucano and folding of the topmost meters of Flysch. The relative contributions of seismic and plastic deformation to the total thrust translation are difficult to evaluate. In our interpretation the thrust translation was mostly accommodated by numerous seismic slip events. In summary the Glarus nappe with its enigmatic LK, is a good candidate for a major thrust fault which owes its localization and apparent softening to transiently near lithostatic fluids pressures (Etheridge et al., 1984; Carter and Dworkin, 1990; Carter et al., 1990; Henry and Le Pichon, 1991), rather than to the presence of a permanently weak décollement lithology.

Acknowledgements

The authors would like to thank F. Gainon, N. Challandes and A. Aubry for their help with field work and sampling; K. Ramseyer for CL imagery. A. M. McCaig and R. Abart are thanked for stimulating discussions and active collaboration. We acknowledge thorough and constructive reviews by S.M. Schmid and B. den Brok. This study is supported by the Swiss National Science Foundation Grants N° 20-50535.97, 20-56920.99.

References

Barbin, V. and Schvoerer, M., 1997. Cathodoluminescence et géosciences. Earth Planet. Sci., 325, 157-169.

Bowman, J.R., Willett, S.D. and Cook, S.J., 1994. Oxygen isotopic transport and exchange during fluid flow, one-dimensional models and applications. Am. J. Sci., 294, 1-55.

Briegel, U. and Goetze, C., 1978. Estimates of differential stress recorded in the dislocation structure of Lochseiten Limestone (Switzerland). Tectonophysics, 48, 61-76.

Burkhard, M., 1993. Calcite twins, their geometry, appearance and significance as stress-strain markers and indicators of tectonic regime; a review. J. Struct. Geol., 15, 351-368.

Burkhard, M. and Kerrich, R., 1990. Fluid-rock interactions during thrusting of the Glarus Nappe; evidence from geochemical and stable isotope data. Schweiz. Min. Pet. Mitt. = Bull. Suisse Min. Pét., 70, 77-82.

Burkhard, M., Kerrich, R., Maas, R. and Fyfe, W.S., 1992. Stable and Sr-isotope evidence for fluid advection during thrusting of the Glarus nappe (Swiss Alps). Contr. Miner. Petrol., 112, 293-311.

Carter, K.E. and Dworkin, S.I., 1990. Channelized fluid flow trough shear zones during fluid-enhanced dynamic recrystallization, Northern Apennines, Italy. Geology, 18, 720-723.

Carter, N.L., Kronenberg, A.K., Ross, J.V. and Wiltschko, D.V., 1990. Control of fluids on deformation of rocks. In: Deformation mechanisms, Rheology and Tectonics (R.J. Knipe and E.H. Rutter, eds.), 54, pp. 1-13. Geological Society Special Publications, Leeds, United Kingdom.

Coli, M. and Sani, F., 1990. Vein distribution in a thrust zone: a case history from the Northern Apennines, Italy. In: Deformation mechanisms, Rheology and Tectonics (R.J. Knipe and E.H. Rutter, eds.), 54, pp. 475-482. Geological Society Special Publications, Leeds, United Kingdom.

Connolly, J.A.D. and Thompson, A.B., 1989. Fluid and enthalpy production during regional metamorphism. Contr. Miner. Petrol., 102, 347-366.

Etheridge, M.A., Wall, V.J., Cox, S.F. and Vernon, R.H., 1984. High fluid pressures during regional metamorphism and deformation; implications for mass transport and deformation mechanisms. J. Geophys. Res., 89, 4344-4358.

Frey, M., 1988. Discontinuous inverse metamorphic zonation, Glarus Alps, Switzerland; evidence from illite "crystallinity" data. Schweiz. Min. Pet. Mitt. = Bull. Suisse Min. Pét., 68, 171-183.

Groshong, R.H., Pfiffner, O.A. and Pringle, L.R., 1984. Strain partitioning in the Helvetic thrust belt of eastern Switzerland from the leading edge to the internal zone. J. Struct. Geol., 6, 5-18.

Gueguen, Y., David, C., Gavrilenko, P. and Torgersen, T.P., 1991. Percolation networks and fluid transport in the crust. In: Crustal-scale fluid transport; magnitude and mechanisms, 18, pp. 931-934, Snowbird, UT, United States.

Hay, R.S. and Evans, B., 1987. Chemically induced grain boundary migration in calcite; temperature dependence, phenomenology, and possible applications to geologic systems. Contr. Miner. Petrol., 97, 127-141.

Heim, A., 1921. Geologie der Schweiz. Band 2: Die Schweizer Alpen 1. Hälfte. Tauchniz, Leipzig.

Henry, P. and Le Pichon, X., 1991. Fluid flow along a decollement layer; a model applied to the 16 degrees N section of the Barbados accretionary wedge. J. Geophys. Res., B, 96, 6507-6528.

Hsü, K.J., 1969. A preliminary Anlysis of the Statics and Kinetics of the Glarus Overthrust. Eclogae geol. Helv., 62, 143-154.

Hubbert, M.K. and Rubey, W.W., 1959. Mechanics of fluid-filled porous solids and its application to overthrust faulting, role of fluid pressure in mechanics of overthrust faulting. Geol. Soc. Am. Bull., 70, 115-166.

Hunziker, J.C., Frey, M., Clauer, N., Dallmeyer, R.D., Friedrichsen, H., Flehmig, W., Hochstrasser, K., Roggwiler, P. and Schwander, H., 1986. The evolution of illite to muscovite; mineralogical and isotopic data from the Glarus Alps, Switzerland. Contr. Miner. Petrol., 92, 157-180.

Kennedy, L.A. and Logan, J.M., 1997. The role of veining and dissolution in the evolution of fine-grained mylonites; the McConnell Thrust, Alberta. J. Struct. Geol., 19, 785-797.

Kennedy, L.A., Logan, J.M., Chester, F.M.E., Engelder, T.E. and Shimamoto, T.E., 1998. Microstructures of cataclasites in a limestone-on-shale thrust fault; implications for low-temperature recrystallization of calcite. Rock deformation; the Logan volume. Tectonophysics, 295, 167-186.

Langdon, T.G., 1982. The mechanical properties of superplastic materials. Mettalurgical transactions, 13A, 689-701.

Lihou, J.C., 1996. Structure and deformational history of the Infrahelvetic Flysch units, Glarus Alps, eastern Switzerland. Eclogae geol. Helv., 89, 439-460.

Marquer, D. and Burkhard, M., 1992. Fluid circulation, progressive deformation and mass-transfer processes in the upper crust; the example of basement-cover relationships in the External Crystalline Massifs, Switzerland. J. Struct. Geol., 14, 1047-1057.

McCaig, A.M., Wayne, D.M., Marshall, J.D., Banks, D. and Henderson, I., 1995. Isotopic and fluid inclusion studies of fluid movement along the Gavarnie Thrust, central Pyrenees; reaction fronts in carbonate mylonites. Am. J. Sci., 295, 309-343.

Nguyen, P.T., Cox, S.F., Harris, L.B. and Powell, C.M., 1998. Fault-valve behaviour in optimally oriented shear zones; an example at the Revenge gold mine, Kambalda, Western Australia. J. Struct. Geol., 20, 1625-1640.

Oberholzer, J., 1933. Geologie der Glarner Alpen. Beiträge Geologische Karte Schweiz, F28.

Oliver, J., 1986. Fluids expelled tectonically from orogenic belts; their role in hydrocarbon migration and other geologic phenomena. Geology, 14, 99-102.

Petit, J.-P., Wibberley, C.A.J. and Ruiz, G., 1999. "Crack-seal" slip: a new fault-valve mechanism. J. Struct. Geol., 21, 1199-1207.

Pfiffner, O.A., 1977. Tektonische Untersuchungen im Infrahelvetikum der Ostschweiz. Translated title: Tectonic studies of the Infrahelvetic Complex, eastern Switzerland. Zuerich, Univ., Geol. Inst Eidgenoess. Tech. Hochsch., Geol. Inst., Mitt, 217, 164.

Pfiffner, O.A., 1981. Fold- and -thrust tectonics in the Helvetic nappes (E. Switzerland). In: Thrust and Nappe Tectonics (R. Price, ed.), pp. 319-327. The Geological Society of London, London.

Pfiffner, O.A., 1982. Deformation mechanisms and

flow regimes in limestones from the Helvetic Zone of the Swiss Alps. J. Struct. Geol., 4, 429-442.

Pfiffner, O.A., 1985. Displacements along thrust faults. Eclogae geol. Helv., 78, 313-333.

Pfiffner, O.A., 1993. The structure of the Helvetic nappes and its relation to the mechanical stratigraphy. J. Struct. Geol., 15, 511-521.

Price, G.P., 1973. The photometric method in microstructural analysis. Am. J. Sci., 273, 523-537.

Price, R.A., 1988. The mechanical paradox of large overthrusts. Geol. Soc. Am. Bull., 100, 1898-1908.

Rahn, M., Mullis, J., Erdelbrock, K. and Frey, M., 1995. Alpine metamorphism in the North Helvetic Flysch of the Glarus Alps, Switzerland. Eclogae geol. Helv., 88, 157-178.

Schmid, S.M., 1975. The Glarus overthrust; field evidence and mechanical model. Eclogae geol. Helv., 68, 247-280.

Schmid, S.M., Boland, J.M. and Paterson, M.S., 1977. Superplastic flow in finegrained limestone. Tectonophysics, 43, 257-291.

Schmid, S.M., Casey, M. and Starkey, J., 1981a. The microfabric of calcite tectonites from the Helvetic Nappes (Swiss Alps). In: Thrust and Nappe Tectonics (R. Price, ed.), pp. 151-158. The Geological Society of London, London.

Schmid, S.M., 1982a. Microfabric studies as Indicators of Deformation Mechanisms and Flow Laws Operative in Mountain Building. In: Mountain Building processes (K.J. Hsü, ed.) , pp. 95-110. Academic Press, London.

Sibson, R.H., 1990. Conditions for fault-valve behaviour. In: Deformation mechanisms, Rheology and Tectonics (R.J. Knipe and E.H. Rutter, eds.), 54, pp. 15-28. Geological Society Special Publications, Leeds, United Kingdom.

Siddans, A.W.B., 1979. Deformation, metamorphism and texture development in Permian mudstones of the Glarus Alps (eastern Switzerland). Eclogae geol. Helv., 72, 601-621.

Snoke, A.W., Tullis, J. and Todd, V.R., 1998. Fault-related Rocks: A Photographic Atlas. Princeton University Press.

Twiss, R.J. and Moores, E.M., 1992. The Mechanics of Large Overthrusts. In: Structural Geology (R.J. Twiss and E.M. Moores, eds.), , pp. 206-213. Freeman, New York.

Walker, A.N., Rutter, E.H. and Brodie, K.H., 1990. Experimental study of grain-size sensitive flow of synthetic, hot-pressed calcite rocks. In: Deformation mechanisms, Rheology and Tectonics (R.J. Knipe and E.H. Rutter, eds.), 54, pp. 259-284. Geological Society Special Publications, Leeds, United Kingdom.

Chapter 3: FLUID FLOW PATHWAYS ALONG THE GLARUS OVERTHRUST DERIVED FROM STABLE AND Sr-ISOTOPE PATTERNS

paper submitted to American Journal of Science

NICOLAS P. BADERTSCHER*, RAINER ABART**, MARTIN BURKHARD*

* Institut de Géologie, 11 Emile-Argand, 2007 Neuchâtel, Switzerland
** Institut für Mineralogie und Petrologie, Universitaetsplatz 2, 8010 Graz, Austria

ABSTRACT.

The Glarus thrust of the eastern Helvetic Alps has been proposed as a major pathway for metamorphic fluids expelled from the footwall during alpine deformation and prograde metamorphism. The stable isotope composition of calcite in a thin continuous calc-mylonite layer and gradients into the overlying Verrucano siltstones and underlying flysch or carbonate are analysed in detail. A regional scale map of the $\delta^{18}O$ composition of the calc-mylonite covering 25 km E-W by 15 km N-S is interpolated from 35 sampling sites. This map reveals a steep northward increase in $\delta^{18}O$ from 11 to 18‰ (SMOW), interpreted as an isotopic front within the southernmost 6km, and levelling out at ca. 20‰ further north. Vertical profiles across the sharp thrust contact show significantly different isotopic fronts in the south, where Verrucano is thrust upon marine carbonates and in northern sites, where it rests on Tertiary Flysch. Southern sites display steep continuous isotopic gradients over about one meter above the thrust, where both $\delta^{18}O$ and $\delta^{13}C$ decrease to background, Verrucano values of 10-11‰ ($\delta^{18}O$ SMOW) and -6‰ ($\delta^{13}C$ PDB) respectively. Footwall carbonates are significantly depleted from their original value of ca. 26‰ within a zone of less than 10 m below the thrust contact. The front geometry of $\delta^{13}C$ increasing from -2 to +2‰ downward within about 1 m is much steeper than the one defined by $\delta^{18}O$. Northern sites, in contrast, display distended isotopic alteration fronts upward into the Verrucano, where higher than background values in $\delta^{18}O$ and $\delta^{13}C$ are found up to 15 m and 6 m above the thrust contact, respectively. No isotopic alterations could be detected within the footwall Flysch up to the very thrust contact. The $^{87}Sr/^{86}Sr$ systematics have been observed on the cm to mm-scale in vertical profiles across the calc-mylonite in three southern sites. In each sample (slab), a topmost zone of slightly enriched, homogeneous $^{87}Sr/^{86}Sr$ values (0.709 to 0.712) is found within a zone of highly sheared and dynamically recrystallized yellow veins alternating with dark stylolite seams on the sub-milli-

metre scale. In two slabs, smooth vertical downward gradients to marine carbonate values (0.708) could be observed on the cm-scale.

Regional and local isotopic gradients are explained as exchange between the different rock reservoirs through the advection / diffusion / dispersion of fluids interacting in a regime of brittle/ductile deformation associated with > 30 km northward thrust translation. Different scenarii of fluid flow along and / or across the thrust plane are modelled using transport theory coupled with isotopic exchange reactions at an assumed temperature of 300°C. Considerable amounts of externally derived ^{18}O -depleted, basement derived fluids are required to explain the isotopic characteristics in the southern part of the thrust. A time integrated fluid flux (TIFF) of 4500-9100 m^3/m^2 is calculated for the channellized flow component along the thrust, far exceeding any cross-thrust component of downward fluid infiltration of 3.45-5.7 m^3/m^2. In northern sites, however, any potential thrust parallel fluid flow is obscured by a dominant compenent of upward, cross-thrust flow of fluids derived from compaction / dehydration of Flysch units in the immediate footwall. These calcite saturated fluids left their imprint in the hangingwall Verrucano in the form of a increasingly ^{13}C and ^{18}O depleted secondary calcite.

INTRODUCTION

Faults and shear zones are recognized to play a crucial role in the control of fluid flow in the upper and middle crust (Cox, 1987, Dipple and Ferry, 1992, Kerrich and others, 1984, McCaig, 1984). Thrust faults may channelise fluids (Fyfe and Kerrich, 1985, McCaig, 1989, Oliver, 1986, Yardley and Lloyd, 1995, Dipple and Ferry, 1992, Marquer and Burkhard, 1992) by enhancing permeability through the generation of micro-cracks during deformation at high fluid pressures (Cox and Etheridge, 1989, Etheridge and others, 1984, Etheridge, Wall, and Vernon, 1983, Knipe, McCaig, and Parnell, 1994, McCaig, Wickham, and Taylor, 1990, Oliver, 1996, Oliver, Valenta, and Wall, 1990). Fluid flow along thrusts has been the subject of many investigations in the last two decades and is well documented in many collision belts (Burkhard and Kerrich, 1988, Burkhard and others, 1992, Cathless, 1990, Crespo-Blanc and others, 1995, McCaig and others, 1995) as well as in accretionnary prisms (Sample, 1996, Silver and others, 2000), where flow along faults is argued to explain thermal and chemical anomalies.

Close to lithostatic fluid pressure also plays an important role in the development of low angle thrust faults (Hubbert and Rubey, 1959) by lowering normal stress. This process has been proposed as a solution to the mechanical paradox of large overthrusts (Badertscher and Burkhard, 2001, Hsu, 1969, Price, 1988).

Isotopes in general, and stable isotopes of oxygen in particular, are a very powerful tool to study fluid-rock interaction, because oxygen is a major component of rocks and common geofluids. Isotopes are sensitive tracers if fluids get into contact with rocks that are not in isotopic equilibrium with them. (Eppel and Abart, 1997, McCaig,

1997). Among others, such a situation is likely to occur when isotopically distinct rock reservoirs are juxtaposed at a structural boundary. The situation of the Glarus thrust is ideal in this respect. The three lithologies involved in the Glarus thrust system display very contrasting oxygen isotope compositions.

According to transport theory (e. g. Baumgartner and Rumble, 1988, Bickle and McKenzie, 1987), any original step-like isotope front in a rock system will be displaced by advective fluid transport as a sharp front in the direction of flow by a distance proportional to the total flux. If the scale of diffusion and hydrodynamic dispersion is large compared to advection, initially sharp fronts may be dramatically broadened (Baker and Spiegelman, 1995, Bickle and McKenzie, 1987). Distension of sharp fronts may also occur if the rate of fluid-rock reaction is slow compared to fluid infiltration velocities (Abart and Pozzorini, 2000, Abart and Sperb, 1997, Bowman, Willett, and Cook, 1994, Lassey and Blattner, 1988). Inversely, the shape of an observed isotope front constrains the direction of fluid flow, the time-integrated fluid fluxes, the mechanism of fluid transport and the original fluid compositions.

The Helvetic fold and thrust belt has been subject to isotopic investigations regarding the fluid regimes during deformation (Burkhard and Kerrich, 1988, Crespo-Blanc and others, 1995, Kirschner, Masson, and Sharp, 1999, Marquer and Burkhard, 1992). All these studies found evidence for large-scale fluid flow along some thrust contacts. In a previous study of the Glarus overthrust, Burkhard and others (1992) discovered a conspicuous S-N increasing trend in the $\delta^{18}O$ composition of the calc-mylonite along the thrust fault (Fig. 1). From cross-section balancing considerations it is clear that the Glarus thrust must extend backward to mid-crustal levels (Pfiffner, 1985). Burkhard and

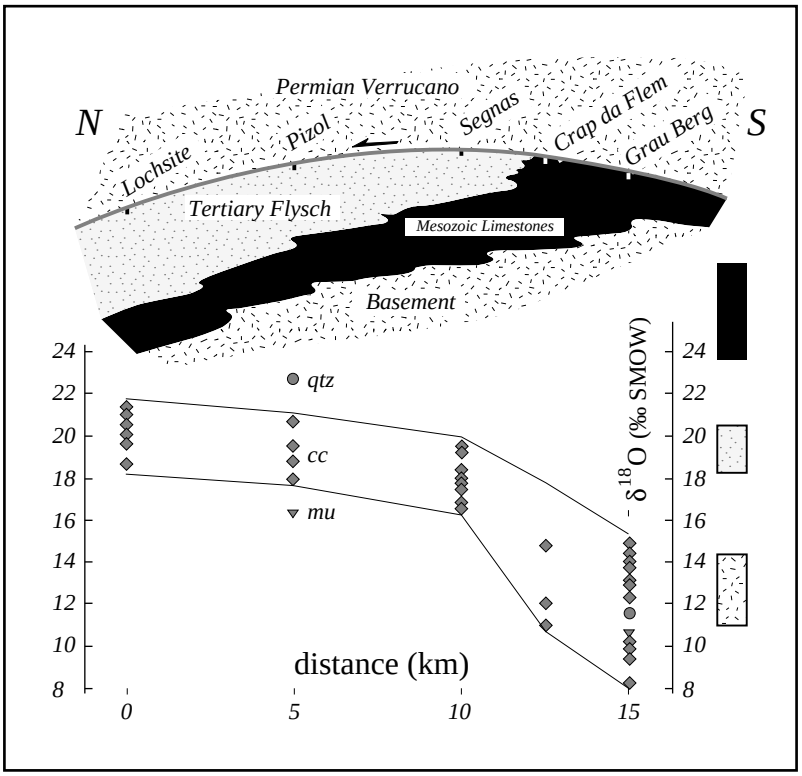

Fig. 1
Plot of calcite $\delta^{18}O$ values from the Lochsitenkalk mylonite on a schematic N-S cross section of the Glarus thrust. The range of whole rock isotopic composition for different potential fluid reservoirs are indicated to the right of the $\delta^{18}O$ scale using the corresponding shading (modified after Burkhard and Kerrich, 1990)

others (1992) and Bowman, Willett, and Cook (1994) interpreted the $\delta^{18}O$ trend as an isotope front due to the northward advection of ^{18}O depleted, externally derived fluids in a pre-existing carbonate along the thrust. Most likely these fluids were derived from devolatilisation reactions in the basement further south (Aar or Gotthard Massif, see Fig.2). In their contribution, Bowman, Willett, and Cook (1994) applied transport theory to model the $\delta^{18}O$ data of the Glarus thrust. They considered the Glarus thrust as a 1-D system along which ^{18}O depleted fluids flew northward, thereby displacing and broadening an initially sharp isotope front by advection and dispersion. The model of Bowman, Willett, and Cook (1994) suffers several weak points. First, they were obliged to use an unaltered initial $\delta^{18}O$ value of 20‰ for the pre-existing carbonate in order to get a reasonable fit with the data instead of the 25-26‰ value proposed by Burkhard and others (1992). Secondly, their model was built on a very limited data set from Lochsitenkalk mylonite only. Finally and most important, they have completely neglected the isotopic variations across the thrust, due to the limited data set available.

The aim of this paper is to define the flow pattern associated with the Glarus thrust by considering isotopic variations along and across the Glarus overthrust through extended sampling. We start with the establishment of a detailed isotopic characterisation of the calc-mylonite along the thrust on the km-scale. In addition, vertical profiles on the m-scale have been sampled in order to constrain the vertical flow components. $^{87}Sr/^{86}Sr$ provide information about the influence of "Basement" derived fluids. Together, these data define complex isotope fronts. Their shape and size is used to infer fluid flow parameters.

GEOLOGICAL SETTING

In the Eastern Helvetic Alps of Switzerland, tectonic units are subdivided into a "Helvetic complex" above and an "Infra-Helvetic complex" below the Glarus thrust (Pfiffner, 1981, Pfiffner, 1993) (Fig. 2a/b). The Helvetic Glarus nappe comprises Permian Verrucano that consists of a clastic series of predominantly siltstones and shales with some conglomeratic units and rare volcanoclastic horizons. This formation is overlain by a concordant Mesozoic series. The "Infrahelvetic" complex consists of a crystalline Basement overlain by a parautochthonous sedimentary cover of Mesozoic carbonates and Tertiary Flysch and some allochthonous South Helvetic and Penninic (Sardona) Flysch (Fig. 2b). The latter were emplaced onto the parautochthonous cover in early Oligocene times during the "Pizol phase" (Pfiffner, 1977). In a second, main deformation stage (Calanda phase), the whole Infrahelvetic complex was intensely folded and imbricated. Thrusting of the Glarus nappe (Ruchi phase) postdates these deformations (Pfiffner, 1977) in an out-of-sequence manner. Despite this out-of-sequence character, the Glarus overthust generally cuts up-section from South to North (Fig. 2B). In the southernmost exposures, Verrucano is thrust over parautochthonous Late Jurassic and Early Cretaceous limestone, whereas further north it overlies a more than kilometre thick sequence of Flysch, consisting of marly shales,

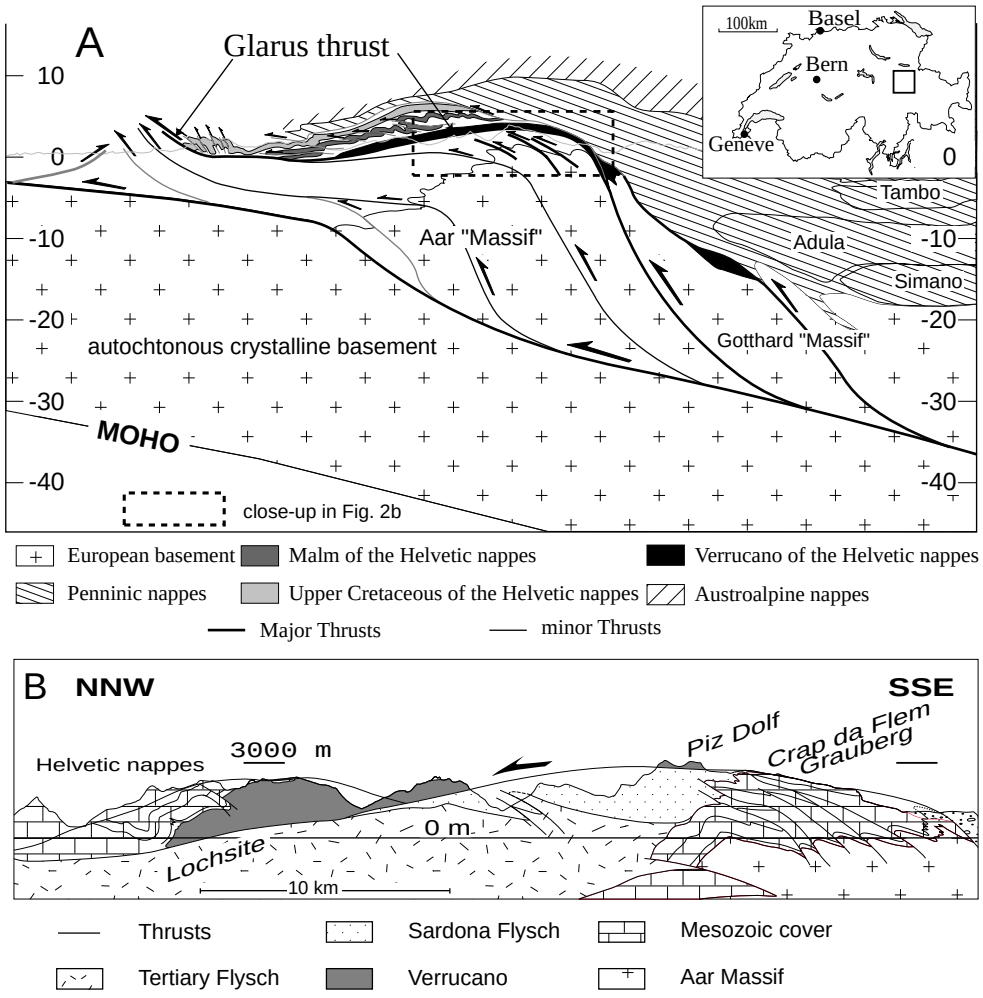

Fig. 2

(A) NNW-SSE crustal cross section through the eastern Alps of Switzerland (redrawn after cross section by Pfiffner, 1993, Schmid and others, 1997). The accessible part of the Glarus overthrust is indicated within the box.

(B) Cross section of the Glarus Alps in eastern Switzerland (according to Oberholzer, 1933). Some sampling sites are indicated.

sandstones and conglomerates (Fig. 2b). An intermediate thin layer (<1-5 m thick) of intensively deformed calc-mylonite, the so-called Lochsitenkalk (LK), accommodated a large part of the 35 km of thrust-translation towards the North (Schmid, 1975, Schmid, Boland, and Paterson, 1977).

Metamorphism ranges from anchizone in the North and in the footwall Flysch to lower greenschist facies in the South and in the Verrucano hangingwall (Frey, 1988, Rahn and others, 1995) as determined from illite crystallinity, mineral parageneses, vitrinite reflectance and fluid inclusions. The peak of this metamorphism post-dates the Calanda phase deformations (Groshong, Pfiffner, and Pringle, 1984) estimated at 30-25 Ma. The "anchi-/epizone- boundary" is offset along the Glarus thrust by about 2 km (Groshong, Pfiffner, and Pringle, 1984, Frey, 1988) as the result of post-peak-metamorphic thrusting between 25 and 20 Ma (Hunziker and others, 1986).

METHODOLOGY

Sampling strategy

The Glarus thrust is magnificently exposed over 15 km N-S by 21 km E-W. This configuration allowed for a detailed mapping of the 3D carbon and oxygen isotope pattern as a function of structural setting, metamorphic grade and lithological changes within the footwall. Regional trends are well constrained by more than 30 sampling sites chosen along the thrust (Fig. 3). The location of individual sites has been determined according to a regular grid of 5 km spacing. The final distribution is irregular, however, depending on outcrop conditions. At each site, we attempted to characterise the isotope composition ($\delta^{18}O$, $\delta^{13}C$) of calcite of the footwall, the calc-mylonite and the hangingwall. Special emphasis has been placed on the calc-mylonite, and up to 15 handspecimen have been obtained from this very thin horizon at each sampling location. In the case of favourable outcrop conditions, a complete vertical profile across the thrust has been sampled, typically starting 5 m below the thrust and ending some 10m above. Sample intervals were chosen in the decimetre range close to the thrust, metric further away. Detailed vertical profiles have been acquired for ten sites (Fig. 3). Syntectonic veins from within the hangingwall (Permian Verrucano) and the footwall (Tertiary Flysch or Mesozoic carbonates) have been sampled for a comparison of their stable isotope composition with the surrounding matrix.

Analytical techniques

For the determination of the $\delta^{18}O$ and $\delta^{13}C$ of calcite, 10-50 gr. of each pre-cleaned rock sample were crushed with a "jaw" crusher to obtain small chips (1 to 5 mm) of rock, then about 10 gr were ground again to a homogeneous powder with particle size <40 µm. A tungsten carbide drill bit with

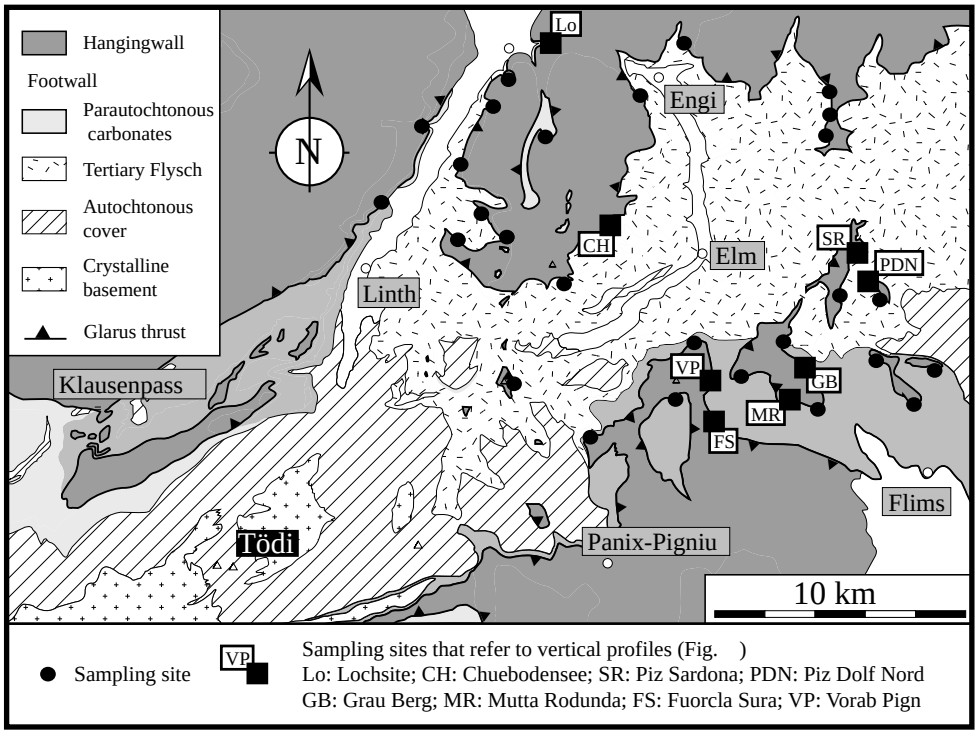

Fig. 3
(A) Simplified tectonic map of the Glarus Alps in eastern Switzerland (modified after Oberholzer, 1933). Sampling sites are indicated together with the sites that refer to Fig. 6/7/8 and 10.

a diameter of 3 mm was used for the sampling of veins and adjacent matrix. In the case of very small abundant veins, bulk rock (vein and matrix) and matrix were analysed separately, the matrix alone was obtained with the drill.

For the determination of $\delta^{18}O$ and $\delta^{13}C$ of calcite, bulk rock powders with an equivalent 0.1 to 0.3 milligrams carbonate content were loaded into individual glass vials. CO_2 was extracted by reaction with 102% H_3PO_4 at 70°C for four minutes on a Finnigan Kiel II device. The CO_2 was analysed on line with a Finnigan-MAT Deltaplus isotope ratio mass spectrometer. Reproducibility of replicate measurements was better than 0.1‰ (1σ) for both $\delta^{18}O$ and $\delta^{13}C$.

In addition to bulk rock samples, we analysed carbonate micro-samples from selected hand specimen. The micro-samples were taken with a dentist drill from polished rock surfaces.

Oxygen isotope analyses of silicates were done on a laser fluorination line of the design described by Sharp (1990). Samples of one to two milligrams were reacted in a BrF_5 atmosphere under a slightly defocussed 25 W CO_2 laser beam. The liberated oxygen was separated from excess reagent and reaction by-products cryogenically and by means of a 20 centimeter KBr column kept at 120°C. O_2 was collected on a molecular sieve at liquid nitrogen temperatures and finally expanded into the variable volumes of a Finnigan Deltaplus isotope ratio mass spectrometer. UWG-2 garnet (Valley an others., 1995) was used as an internal standard. Reproducibility of replicate measurements was better than 0.15‰ (1σ) Oxygen isotope compositions are given in the conventional δ - notation relative to V-SMOW.

Ratios of $^{87}Sr/^{86}Sr$ were determined at the School of Earth Sciences, University of Leeds. Three selected pre-cleaned slabs of calc-mylonite from three different sites on an N-S projection were used for these analyses. 44 aliquots were obtained using a diamond-tipped dental drill. Sample size varied from 2 to 3 mg with a spatial resolution of 1.6 mm and a hole depth of 50 µm. In order to obtain data for pure calcite, aliquots were initially treated with 2.5M HCl at room-temperature in screw-top Savillex capsules. Sr was isolated using standard ion exchange technique. For mass spectrometry, Sr was loaded using H_3PO_4 on a single Ta filament. It was then analysed on a fully automated VG-54E multi-collector mass spectrometer. All Sr data were fractionation corrected to $^{88}Sr/^{86}Sr = 0.1194$ and $^{87}Sr/^{86}Sr$ was normalized to NBS – 987 = 0.71022. Because of the young age of thrust activity (30-20 Ma) (Hunziker and others, 1986), age corrections of the data for radiogenic Sr are negligible (Burkhard and others, 1992). The total estimated error is ±0.00003.

The mineralogical composition of Permian Verrucano samples taken at 100 m above the thrust was obtained by a combination of XRF for major elements and XRD to identify the different mineral phases present in each sample. About 10 gr of rock powder were used for the XRF analyses and transformed in glassy pastilles with Li-borate that have been analysed on a Philips PW 2400 spectrometer at the Mineralogical and Petrography Institute of the University of Fribourg (Switzerland).

XRD analyses of the whole rock were carried out at the Geological Institute of the University of

Neuchâtel. 800 mg of the powder were pressed (20 bars) in a powder holder covered with a blotting paper and analysed by XRD. Semi-quantitative mineralogical rock composition was determined by XRD (SCINTAG XRD 2000 Diffractometer) based on methods described by Ferrero (1965), Ferrero (1966), Klug and Alexander (1974), Kübler, (1983) and Rolli, (1990).

A normative mineralogical composition was calculated based on the elemental composition obtained by XRF and on the semi-quantitative XRD determination of the following minerals: apatite, titanite, albite, calcite, dolomite, muscovite, Fe-Mg chlorite and quartz.

RESULTS

I. Large scale calcite oxygen isotope variations in the calc-mylonite

For each sampling site, a mean $\delta^{18}O$ and $\delta^{13}C$ value has been calculated from up to 15 individual samples. In order to document the large-scale oxygen isotope variations, maps of $\delta^{18}O$ have been constructed by plotting the mean $\delta^{18}O$ value for each sampling site against its geographical coordinates (Fig. 4). Interpolation between the different sites has been obtained by kriging. $\delta^{18}O$ values, from 22‰ down to 10‰, are invariably lowered with respect to the supposed marine carbonate protolith value of 25‰ (Burkhard and others, 1992). Two regional trends can be identified on the $\delta^{18}O$ surface (Fig. 4). The values increase from 11‰ in the southeastern exposures to 20‰ further north. A flattening out at about 20‰ is observed North of the Carbonate-Flysch boundary in the footwall. These trends can also be identified on Fig. 5. A striking S-N gradient in the southern part and the flattening out of the values in the North are observed. Despite these obvious regional trends, the calc-mylonite oxygen isotope composition is far from homogeneous. Heterogeneities are large in the South, where they reach 8‰ in individual sites, while in northern sites variations never exceed 3‰.

A region with slightly higher values of up to 22‰

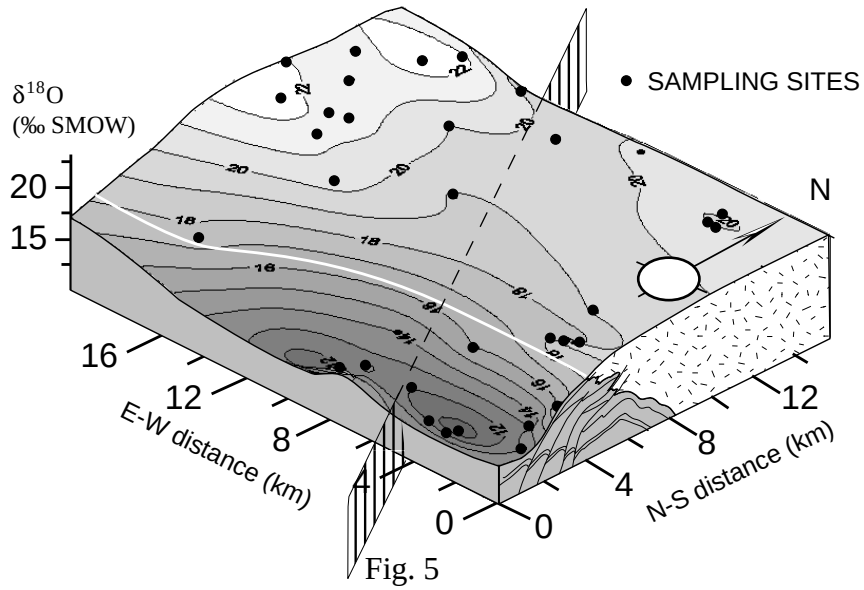

Fig. 5

Fig. 4
Regional variations in the mean $\delta^{18}O$ value measured in the Lochsiten calc-mylonite. Horizontal axes are geographic coordinates in km N-S and E-W. Vertical axis is $\delta^{18}O$ (‰-SMOW). Interpolation between sampling sites has been obtained by kriging. The white line represents the carbonate-Flysch boundary in the footwall of the thrust. A cross section of the footwall is indicated on the eastern vertical face of the plot.

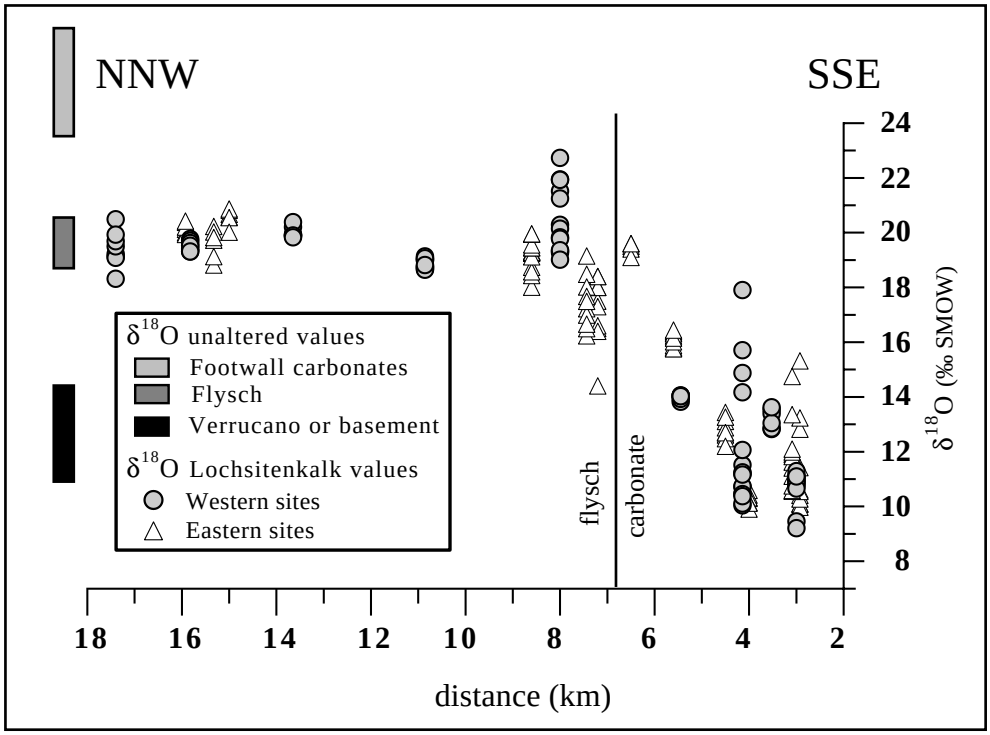

Fig. 5

(A) Plot of calcite $\delta^{18}O$ values of the Lochsitenkalk-mylonite projected onto a NNW-SSE cross section of the Glarus thrust. The range of whole rock isotope composition of the different rock reservoirs is indicated to the right of the $\delta^{18}O$ scale. Two groups of data are distinguished, those from sites situated on the western part of the studied area and those situated in the eastern part (Fig. 3) in order to avoid the comparison of sites that are more than 10 km apart from each other. The carbonate-Flysch boundary in the footwall is also indicated.

is found in the Northwest (Fig. 4), where the hangingwall consists of Mesozoic carbonates.

II. Calcite oxygen- and carbon isotope variations across the thrust

Two groups of profiles have been distinguished, those situated South or North of the carbonate-Flysch boundary in the footwall. Vertical $\delta^{18}O$ profiles of southern sites (Fig. 6) display very steep gradients in the first 0.5 to 1 m above the thrust contact. Calcites of the mylonitized Verrucano hangingwall are unaltered compared to their original $\delta^{18}O$ value of 10-13‰ at distances of more than 1m above the thrust. Altered values up to 14‰ close to the thrust are documented. In the footwall carbonates, depleted $\delta^{18}O$ values (14-22‰), compared to their expected marine signature of 25‰, are found up to 7 m below the thrust contact. They describe a smooth gradient from the contact down into the footwall. Calc-mylonite samples range from 10 to 16‰.

Carbon isotope compositions of calcite range from 2.3‰ to -5‰ ($\delta^{13}C$ PDB). A very sharp gradient of $\delta^{13}C$ is documented at the thrust contact (Fig. 6). Values of calcite in the mylonitized hangingwall show a conspicuous trend of decreasing values from around -2‰ close to the thrust to -5‰ at 50 cm to 1 m and higher above the thrust. The width of this alteration zone corresponds quite well to the one observed in $\delta^{18}O$. Uniform marine carbonate $\delta^{13}C$ values (1.3-2.6‰) are found in the footwall limestones, right up to the

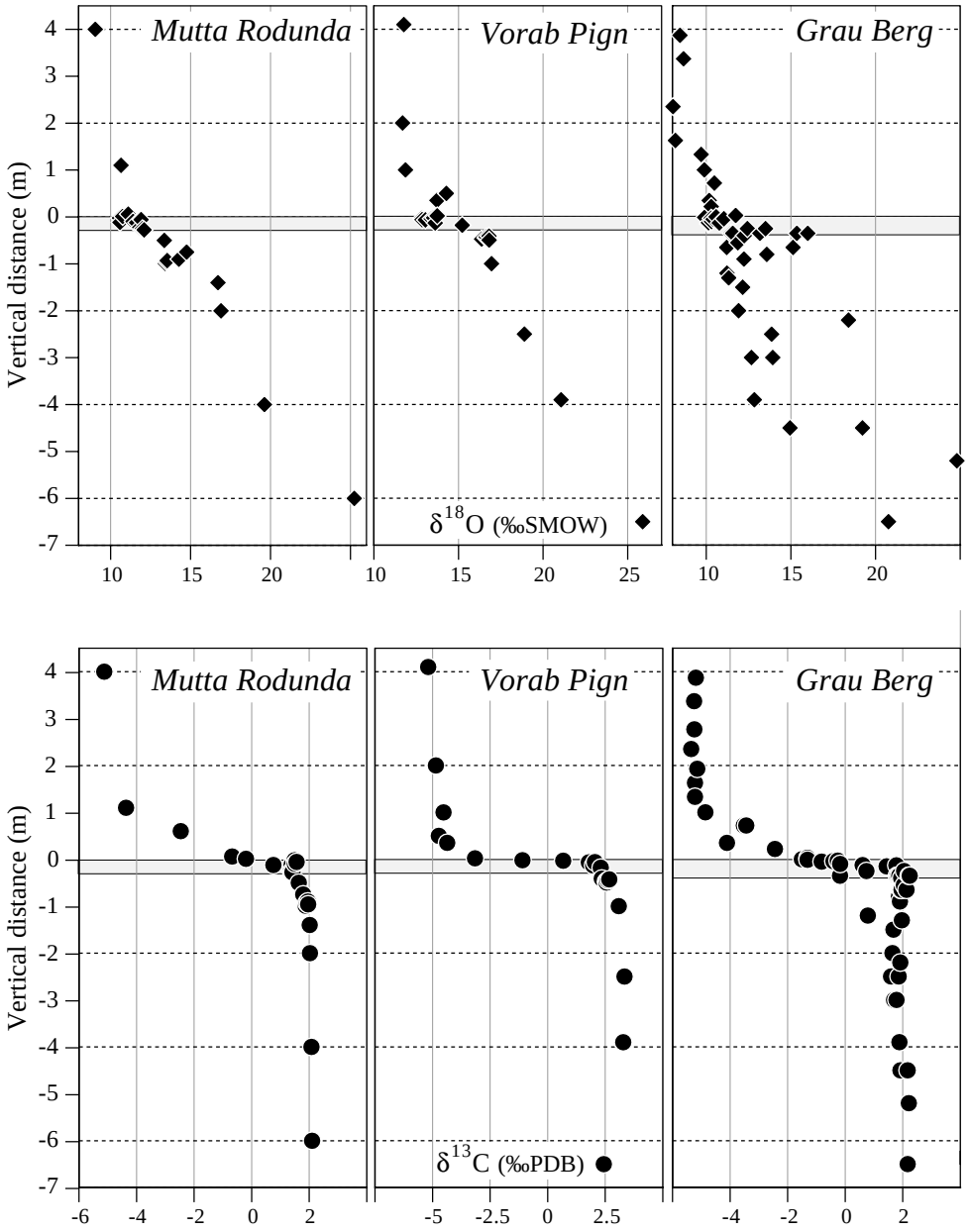

Fig. 6
$\delta^{18}O$ and $\delta^{13}C$ values of calcite vs. vertical distance across the Glarus thrust from three localities in the southern part of the study area (Fig. 3). The grey shaded area represents the Lochsiten calc-mylonite at the thrust contact. The hangingwall consists of Permian Verrucano siltstones, the footwall of Mesozoic carbonates.

thrust contact, in contrast with a $\delta^{18}O$ alteration zone of several meters wide. Calc-mylonite samples are variably ^{13}C depleted with $\delta^{13}C$ ranging from 2.4‰ to -4‰.

Vertical $\delta^{18}O$ profiles in Verrucano of northern sites (Fig. 7) are characterized by a broad nearly linear trend from values around 17-19‰ close to the thrust to 10-12‰ at 4 m or higher above the thrust. The distance from the thrust contact to the position where Verrucano background ^{18}O composition occurs seems to increase from South to North, from Piz Dolf to Lochsite, where the $\delta^{18}O$ value is still 17‰ 20 m above the thrust.

In the footwall Flysch, $\delta^{18}O$ values of calcite of 19-20‰ are quite homogeneous independent of the distance below the thrust contact. Calc-mylo-

nite samples are invariably depleted in ^{18}O relative to their presumed marine Helvetic carbonate protolith (25‰). A clustering of values between 18.5‰ and 20‰ appears in the calc-mylonite of northern sites. This contrasts with much higher scatter observed in the south (Fig. 7). Carbon isotope composition of calcite has a total range of 2.3‰ to -6‰ ($\delta^{13}C$), nearly identical to that of the southern profiles (Fig. 6). $\delta^{13}C$ values of calcite in the mylonitized hangingwall show a marked trend of decreasing values from around -2‰ close to the thrust to -6‰ at about 6 m above the thrust. In the footwall Flysch, the $\delta^{13}C$ values of calcite are quite homogeneous. No trend with respect to distance from the thrust contact could be detected. $\delta^{13}C$ values in the footwall Flysch range

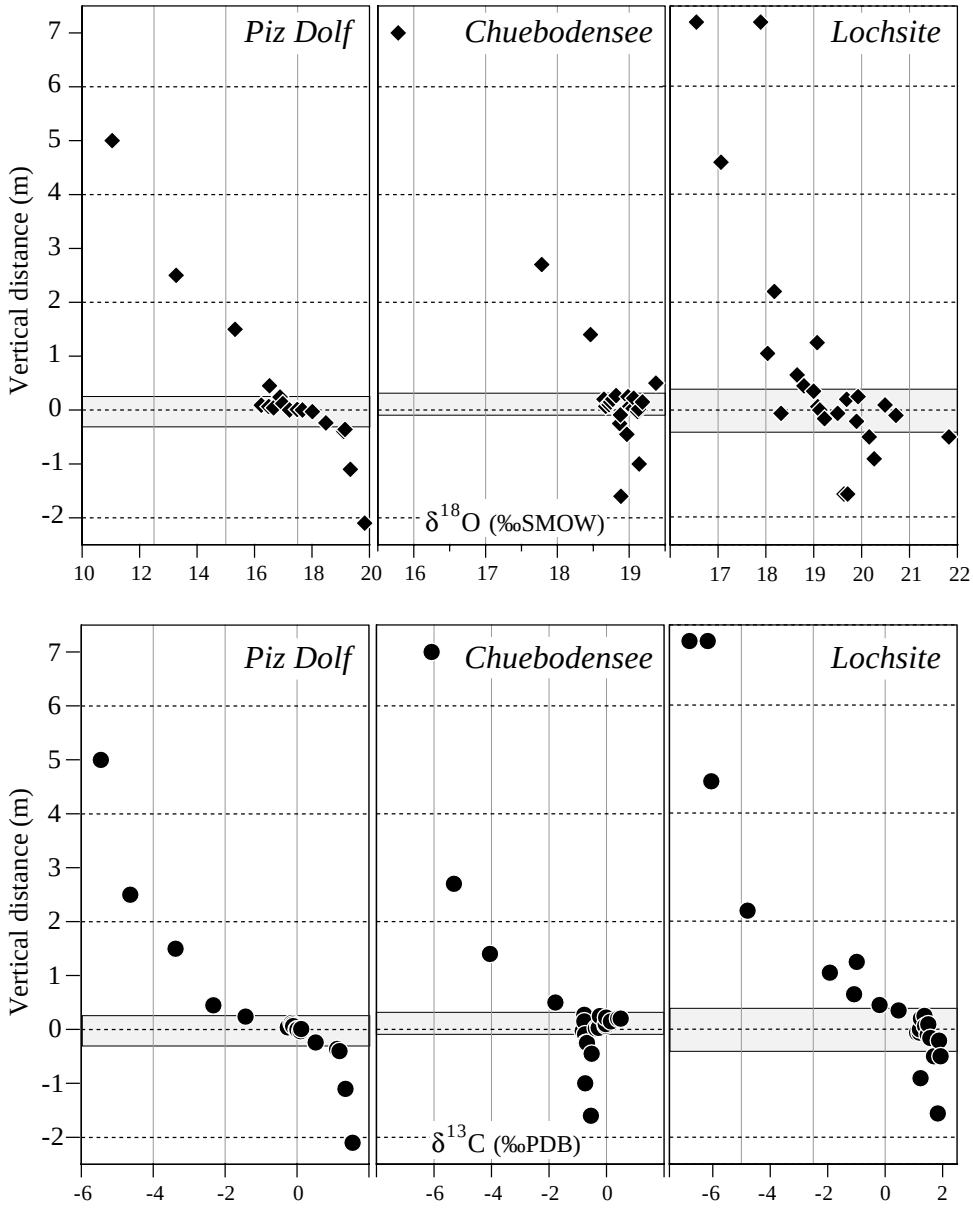

Fig. 7

$\delta^{18}O$ and $\delta^{13}C$ values of calcite vs. vertical distance across the Glarus thrust from three localities in the northern part of the study area (Fig. 3). The grey shaded area represents the Lochsiten calc-mylonite at the thrust contact. The hangingwall consists of Permian Verrucano siltstones, the footwall of Tertiary Flysch. The 0 reference on the vertical scale corresponds to the septum, a planar horizon that cross-cut all internal structures of the calc-mylonite.

from -0.5‰ (in Chuebodensee) to 2‰ (in Lochsite). Within the calc-mylonite, the $\delta^{13}C$ values show little variation and are similar to those of the footwall. In the northern sites, $\delta^{13}C$ and $\delta^{18}O$ vertical profiles display the same features. A smooth gradient prevails in the hangingwall, whereas the $\delta^{13}C$ and $\delta^{18}O$ values are homogeneous in the footwall, independent of the distance to the thrust contact. This correlation of $\delta^{13}C$ and $\delta^{18}O$ vertical profiles in the North strongly contrasts with the southern sites where the $\delta^{13}C$ and $\delta^{18}O$ vertical profiles are completely different.

III. "Background" oxygen isotope composition of the Verrucano.

To constrain potential large-scale $\delta^{18}O$ variations within the Verrucano hangingwall, 6 whole-rock samples from 5 sites along a S-N profile were examined. The "normative" mineralogical composition and the $\delta^{18}O$ of calcite and of the bulk rock have been determined. No regional trend in $\delta^{18}O$ could be detected (Fig. 8). $\delta^{18}O$ values are fairly homogeneous, about 13‰ for calcite and about 12‰ for the bulk rock. One exception is present at Kärpf, with a mean $\delta^{18}O$ value of 15.5‰ for calcite and about 14.5‰ for the bulk rock. In addition, the $\delta^{18}O$ of quartz in equilibrium with the whole rock was calculated for each sample, based on the normative mineralogy, an assumed temperature of 300°C and standard isotopic fractionation factors (Clayton, Goldsmith, and Mayeda, 1989, O'Neil, Clayton, and Mayeda, 1969)(Fig. 8). Mineralogically, a systematic trend of increasing quartz and muscovite content towards the North at the expense of

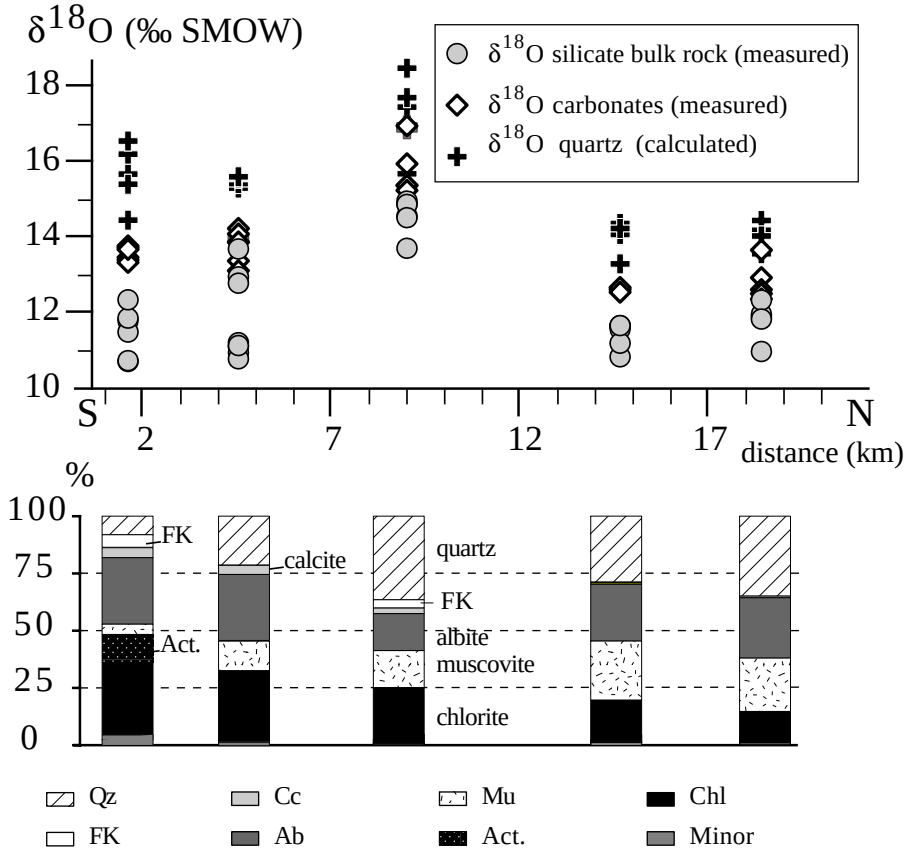

Fig. 8
A) $\delta^{18}O$ values of calcite, bulk rock and calculated quartz in equilibrium with Verrucano samples from five sites situated 100m above the thrust versus N-S distance along the Glarus thrust (upper part). B) Mineralogical composition of the Verrucano samples as calculated by an adapted norm based on XRF and XRD data.

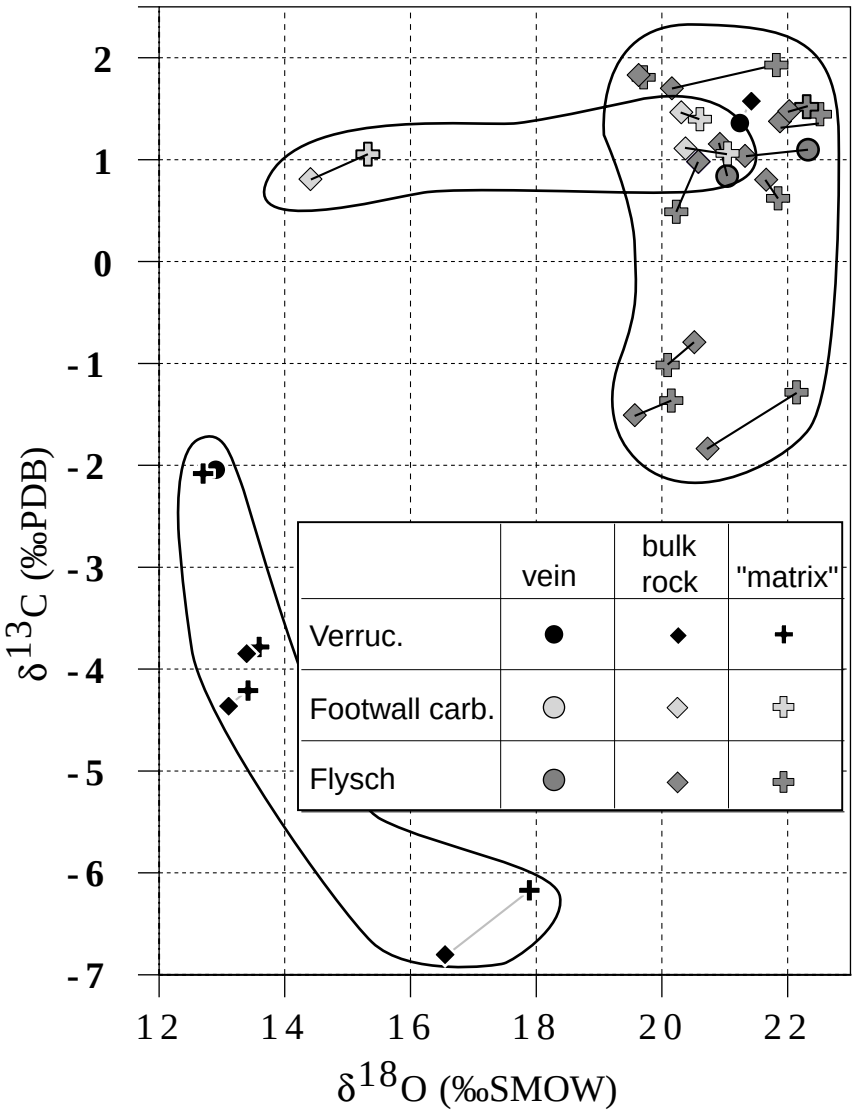

Fig. 9
Comparison of calcite veins and their immediate wall-rock matrix, represented in $\delta^{18}O$ vs. $\delta^{13}C$. Verrucano, footwall carbonates and Flysch samples from different sites along the Glarus thrust are distinguished by different symbols. A clear clustering appears for the Flysch calcites, whereas footwall carbonates and Verrucano calcites display large degrees of heterogeneity.

chlorite is documented. This trend is reflected in the calculated $\delta^{18}O$ composition of quartz, decreasing slightly from 16‰±1 to 15‰±1. However, with one out of the 5 sampling sites being an outlier (17‰±1), this trend is hardly significant.

IV. $\delta^{18}O$ and $\delta^{13}C$ co-variation of calcite from footwall and hangingwall veins and matrix

In samples of footwall and hangingwall with macroscopic veins, no large differences in $\delta^{18}O$ and $\delta^{13}C$ values of calcite can be documented between vein and matrix (Fig. 9). Veins invariably have $\delta^{18}O$ and $\delta^{13}C$ values close to their matrix or bulk rock. The largest differences observed between vein and wall rock are 2‰ for $\delta^{18}O$ and 0.5‰ for $\delta^{13}C$. While Flysch samples are clustered, between 20 and 22‰ in $\delta^{18}O$, Verrucano and footwall carbonate samples have a large spread of values. Calcites from the mylonitized Verrucano show large variations both in $\delta^{18}O$ (12-21‰) and $\delta^{13}C$ (-6 to 1.5‰). The highest values are strongly enriched compared to unaltered original Verrucano values (12‰ in $\delta^{18}O$ and -6‰ in $\delta^{13}C$). Calcites from footwall carbonates display a large range of depleted values in $\delta^{18}O$ (15-21%) but are relatively homogeneous in $\delta^{13}C$.

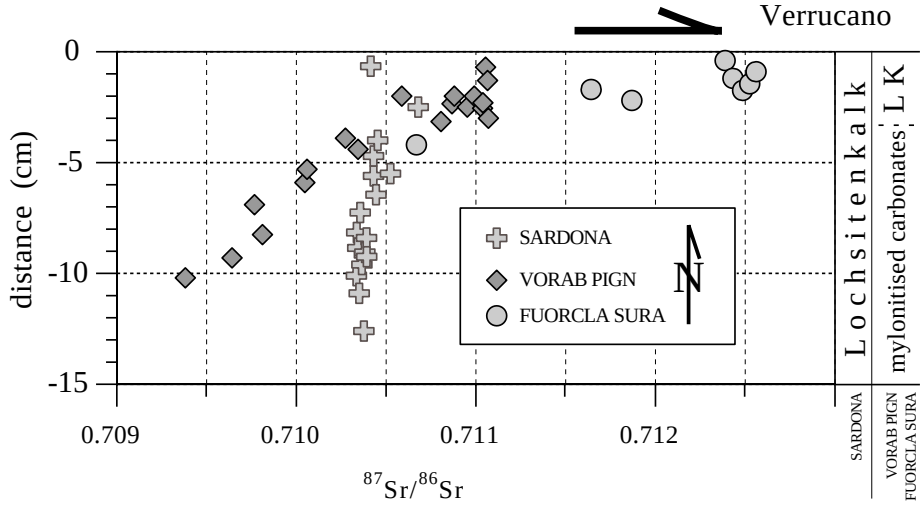

Fig. 10
$^{87}Sr/^{86}Sr$ values of calc-mylonite calcite vs. vertical distance across the Glarus thrust (Fig. 3). The footwall consists of mylonitized carbonates in Furocla Sura and Vorab Pign, of Flysch in Sardona. Note the different thickness of the Lochsiten calc-mylonite between Sardona and the two other localities.

V. $^{87}Sr/^{86}Sr$ of the calc-mylonite

$^{87}Sr/^{86}Sr$ has been analysed on three slabs of calc-mylonite from three different southern sites: Fuorcla Sura, Vorab Pign and Sardona from South to North (Fig. 3). The top of each slab corresponds to the calc-mylonite Verrucano contact (Fig. 10). Vertical $^{87}Sr/^{86}Sr$ profiles are characterized by a zone of homogeneous values at the top with a thickness of less than 4 cm in Fuorcla Sura and Vorab Pign and of at least 13 cm in Sardona (Fig. 10). The mean $^{87}Sr/^{86}Sr$ value in this zone decreases from Furocla Sura (0.7125) to Vorab Pign (0.7110) and to Sardona (0.7104). Petrographically, this zone of homogeneous $^{87}Sr/^{86}Sr$ values corresponds to a sub-mm-sized alternation of white/yellow layers and dark stylolitic seams. The light layers are easily recognized as deformed veins. This zone corresponds to the true calc-mylonite known as Lochsitenkalk. In the two slabs from Fuorcla Sura and Vorab Pign, $^{87}Sr/^{86}Sr$ values follow a decreasing trend towards a typical marine carbonate signature of 0.708. Petrographically, these trends have been identified within grey mylonitized footwall carbonates with very little veiny material. At Sardona, no decreasing trend was observed. Veiny Lochsitenkalk mylonite is 2 meter thick here and no mylonitized Mesozoic carbonate have been identified. Moreover, the alternation of white/yellow layers and dark stylolitic seams is intensively folded and disrupted.

DISCUSSION

I. *Regional $\delta^{18}O$ trends of the calc-mylonite*

The non linear regional trend of increasing $\delta^{18}O$ values of the calc-mylonite from 11‰ in the southernmost exposures to 17-19‰ somewhere south of the lithologic boundary between Cretaceous limestones and Tetriary Flysh in the footwall of the thrust (Fig. 4/5) may be interpreted as an oxygen isotope front (Bowman, Willett, and Cook, 1994, Burkhard and others, 1992). A possible scenario that may explain the observed pattern is migration of ^{18}O depleted, externally-derived fluids in a pre-existing limestone or calc-mylonite along the thrust. The oxygen isotope signature of the presumed marine helvetic carbonate protolith of the calc-mylonite would be 25‰

(Burkhard and others, 1992) (compare Bowman, Willett, and Cook, 1994). A $\delta^{18}O$ of 6‰ of the infiltrating fluid is inferred from the observation of $\delta^{18}O$ values as low as 11.5‰ in the southernmost exposures of the calc-mylonite and an oxygen isotope fractionation of 5.5‰ as given for the system H_2O-calcite at 300° by O'Neil, Clayton, and Mayeda (1969). Such fluids can be derived either from the overlying Verrucano during prograde metamorphism or from the Infrahelvetic Basement during metamorphism in the root zone of the thrust, but we favour the latter solution. The Verrucano alternative is rejected because it is less obvious why and how an N-S front should have developed within the domain where the footwall consists of carbonates, as there would not be any localized fluid inlet. In this case, the same amount of isotopic alteration would have resulted in the calc-mylonite along a N-S profile, no regional trend would exist. Further North, where the footwall is represented by Flysch, the calc-mylonite interacted with both these basement-derived fluids and fluids coming from the Flysch (see below).

As predicted by transport theory (e.g. Baumgartner and Rumble, 1988, Bickle and McKenzie, 1987), an original step-like isotopic front will be displaced by advectve fluid transport as a sharp front in the direction of flow by a distance proportional to the total flux. Coupled advective and diffusive/dispersive transport will result in displacement and broadening of the front. Dispersion is the process of mixing that is due to the heterogeneity of velocities caused by tortuosity in the porous medium.

Assuming equilibrium exchange, the position of the front with respect to the supposed fluid inlet bears information on the time integrated fluid flux (TIFF) along the thrust. The shape of the front, in particular its distension with regard to a supposed initially sharp front, contains information on the amount of diffusive/dispersive contributions to material transport. In advective diffusive/dispersive transport, an initially sharp front is broadened symmetrically around the advectively displaced position of the initial front. The diffusive/dispersive broadening of an initially sharp front between two different fluid reservoirs is governed by (Crank, 1975, equation 2.14):

$$R(x,t) = R_f + 0.5(R_f - R_r) * \mathrm{erfc}\frac{x+\omega}{2\sqrt{u}} \qquad (1)$$

Where Rf is the composition in equilibrium with the infiltrating fluid, Rr is the composition in equilibirum with the protolith, u = D*t and u^{-2} is referred to the characteristic length of disper-

Distension of sharp fronts may also occur if the rate of fluid-rock reaction is slow compared to fluid infiltration velocities (Abart and Pozzorini, 2000, Abart and Sperb, 1997, Bowman, Willett, and Cook, 1994, Lassey and Blattner, 1988). The Damköhler number N_D defined as:

$$N_D = \frac{k_k \phi L}{q} \qquad \text{(Bowman, Willett, and Cook, 1994)}$$

where q is the volumetric fluid flux, L is a scaling distance, ϕ is the porosity and k_k is the reverse rate of isotopic exchange. q/ϕ is known as the mean interstitial particle velocity υ . N_D relates the rates of advective transport and mineral-fluid exchange. High Damköhler numbers stands for scenarios with relatively rapid isotopic exchange rates, i. e. close to local equilibrium exchange.

sion/diffusion, t is time and D is the effective dispersion/diffusion coefficient. The parameter ω, ω = υ*t, gives the advective displacement of the front with respect to its original position, where υ is the mean interstitial particle velocity.

The parameters u and ω may be obtained from fitting the function R(x,t) to the observed data south of the carbonate-Flysch boundary in the footwall (Fig. 11). This procedure yields a D*t of 2.3 and 0.38 km^2 for the western and eastern cross section, respectively, and advective front displacements ω of 5.9 and 3 km for the western and eastern cross sections, respectively (Fig. 11).

There is no rigorous way to extract either time t, D or ν from this result. However, if either one is specified, the others are fixed by the front geo-

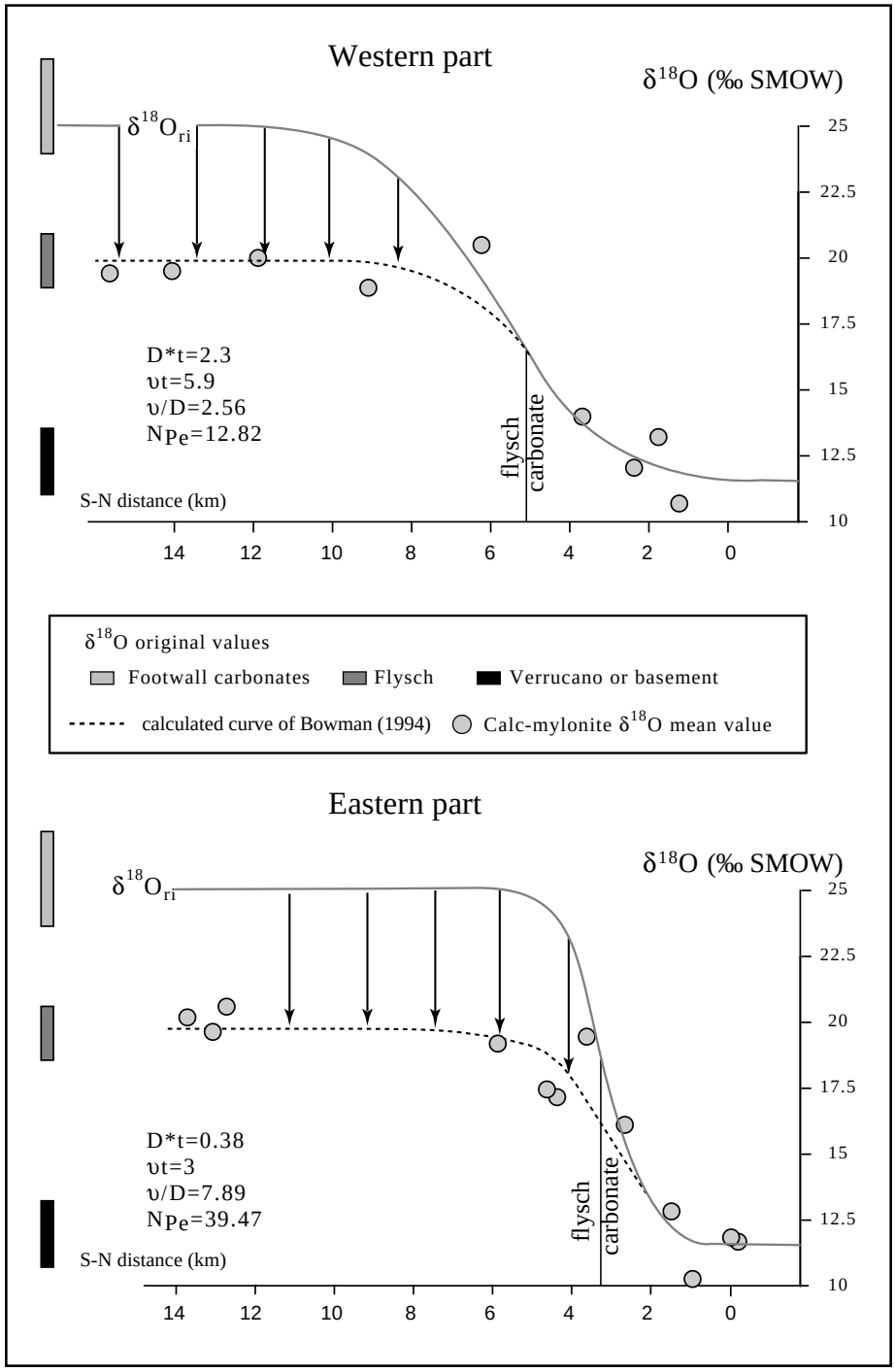

Fig. 11
Calculated curves for calcite $\delta^{18}O$ composition against N-S distance predicted by transport theory applied to the infiltration of a fluid with an $\delta^{18}O$ of 6‰ into a pre-existing carbonate with an original $\delta^{18}O$ of 25‰. These curves are represented together with the data point of mean $\delta^{18}O$ of the calc-mylonite at each site. Only those sites where footwall is represented by carbonates were considered to fit the curves with the data. A western and an eastern cross-section have been distinguished to avoid comparison of sites that are more than 10 km apart. N_{Pe}, the Peclet number, expresses the relative contribution of advective to diffusive/dispersive transport mechanisms. t is time and D is the effective oxygen dispersion/diffusion coefficient. D*t is referred to as the characteristic length of dispersion/diffusion. u*t, gives the advective displacement of the front with respect to its original position, where u is the mean interstitial particle velocity.

t (years)	t (s)	D (m^2/s)	υ_{west} (m/s)	υ_{east} (m/s)
10^5	$3.15E^{12}$	$7.3E^{-7}$	$1.4E^{-9}$	$1.9E^{-9}$
10^6	$3.15E^{13}$	$7.3E^{-8}$	$1.4E^{-10}$	$1.9E^{-10}$
10^7	$3.15E^{14}$	$7.3E^{-9}$	$1.4E^{-11}$	$1.9E^{-11}$

Table 1
Fluid flow parameters deduced from fitting curves with $\delta^{18}O$ data of calc-mylonite along two N-S profiles. The calculation is based on transport theory. t is time, D is the dispersive/diffusive coefficient and υ is the mean interstitial particle velocity for the channelized flow system that occured in the souterhn part of the Glarus overthrust. A western and eastern cross-section have been distinguished to avoid comparison of sites that are more than 10 km far from each other

metry. If oxygen dispersivities/diffusivities are calculated for geologically meaningful time scales, then effective oxygen dispersivity/diffusivities on the order of 10^{-9} to 10^{-7} m^2/s are obtained (see Table 1). It must be underlined that these are effective dispersivities/diffusivities. The effective dispersion/diffusion coefficient of a species in the pore fluid of a porous medium, D, is related to the diffusivity of the same species in the free fluid, Do, by:

$D = \tau \times \phi \times D_0$ (Abart and Pozzorini, 2000) (2)

Where τ is the tortuosity and ϕ is the porosity of the porous medium. The diffusivity of the H_2O species in water is about $5E^{-8}$ m^2/s at 300°C (experimental data compiled by Frank et al. 1996). The porosity in geologic materials may vary considerably, whereas tortuosity may only vary between <1 and 0.1.

If ϕ were 10^{-2} and τ were 0.1, an effective dispersivity/diffusivity of $5E^{-11}$ m^2/s , and if ϕ were 10^{-3} and τ were 0.1, an effective dispersivity/diffusivity of $5E^{-12}$ m^2/s would be calculated from the experimental data.

This is at least two orders of magnitude slower than the phenomenological oxygen diffusivities/dispersivities obtained for geologically relevant time scales from the geometry of the $\delta^{18}O$ front along the Glarus thrust. Hydrodynamic dispersion in the course of flow along the thrust may be responsible for the enhancement of oxygen diffusion/dispersion.

If the distance of displacement of the front ω (υ*t) is known, the total flux can be calculated. In the case of the Glarus thrust, the initial position of the front is uncertain, because the root zone of the thrust is not exposed and the geometry of the different lithological units and potential fluid sources in the root zone are not known. One may, however, obtain a minimum estimate of the time-integrated fluid flux (TIFF), if the northernmost conceivable position of the fluid inlet is considered. Bowman et al. (1994) placed the fluid inlet at Grauberg (cf. Fig 11). We shift the position of the fluid inlet further south to a position where the

mean $\delta^{18}O$ values of all model fronts coincide with the presumed fluid buffered composition of the calc-mylonite to within 0.1 per mil.

The inferred front displacement, ω (υ*t), is 5.9 and 3 km for the western and eastern cross-sections respectively. The time integrated fluid flux is related to front displacement by:

$$TIFF = \omega x Kd \qquad (3)$$

Where Kd, known as the solid/fluid partition coefficient, expresses the partitioning of oxygen between equivalent volumes of rock and pore fluid. Kd is given by:

$$Kd = \frac{nO_{rock} \bullet V_{fluid}}{nO_{fluid} \bullet Vr_{ock}} \qquad (4)$$

where n_{Orock} and n_{Ofluid} give the number of moles of oxygen per mole of rock and fluid, respectively, and V_{fluid} and V_{rock} refer to the molar volumes of fluid and rock. Considering the calc-mylonite as pure calcite and the fluid as pure water at 300°C and 3 to 4.5 kbar results in V_{rock} = 37 cm^3/mol and V_{fluid} = 19 cm^3/mol, and Kd = 1.5. This yields TIFF of 4500 m^3/m^2 and 9100 m^3/m^2 (compare Bowman, Willett, and Cook, 1994) for the eastern and western cross sections, respectively. From a comparison of the characteristic length of diffusion (D*t) and the displacement ω (υ*t) of the front with respect to its presumed initial position, the relative contributions of advection and diffusion/dispersion may be estimated ($N_{Pe}=\upsilon L/D$)[2]. The ratios for the eastern and western cross-sections are 7.89 and 2.56. If this is multiplied with an arbitrarily defined scaling length L=5 km (compare Bowman, Willett, and Cook, 1994), Pecklet numbers N_{Pe}[(1)] of 39.47 and 12.82 result for the eastern and western profiles, respectively (Fig. 11) and indicate a very important role of dispersion/diffusion (compare Bowman, Willett, and Cook, 1994).

It must be stated that the above model is strictly one-dimensional and therefore doesn't consider the influence of footwall or hangingwall on the isotopic signature of the calc-mylonite. The isotopic alteration of the uppermost five meters of the footwall carbonates and the lowermost 1 meter of the hangingwall Verrucano indicates that, in the scenario where northward flow is channelized along the thrust, the infiltrating fluid also exchanged its oxygen with the isotopically comparatively heavy footwall as well as, to a lesser extent, with the isotopically relatively light hangingwall. This scenario may be envisioned as a loss of tracer into the country rocks of a fluid conduit. As exchange with the relatively heavy footwall carbonates was significantly more pronounced than exchange with the hangingwall Verrucano, the net effect of such transversal tracer loss would be an increase of the retardation of the oxygen front

(1)The Pecklet number (N_{Pe}) is defined as:

$$N_{Pe} = \frac{qL}{\phi D}$$ e.g. (Bowman, Willett, and Cook, 1994)

where D is the dispersion/diffusion coefficient. The Pecklet number expresses the relative contribution of advective to diffusive/dispersive transport mechanisms (Abart and Pozzorini, 2000, Bowman, Willett, and Cook, 1994). High Pecklet numbers (∞) stands for advection-dominated transport.

with respect to the strictly one dimensional scenario. The inferences made from the 1-D model must, therefore, be considered as minimum estimates of both integrated fluxes and characteristic length scales of diffusion.

Towards the North, the O-isotope front measured within the calc-mylonite deviates significantly from an ideal symmetric shape predicted by transport theory for flow along the thrust in a pre-existing carbonate with an initial $\delta^{18}O$ marine signature of 25‰ (Fig. 11). The front rapidly flattens at about 20‰. In the interpretation of Bowman, Willett, and Cook (1994), this segment corresponds to the downstream part of the isotope front where no alteration of the pre-existing carbonate has occurred. This anomaly is best explained as an influence of the underlying Flysch (see Fig. 4), however. Northward, the calc-mylonite O-isotope composition rapidly converges toward the Flysch oxygen isotope composition rather than toward a marine mesozoic carbonate signature (Fig. 11). We think that most of the calc-mylonite in the northern part has formed by precipitation of veins from fluids expelled from the underlying Flysch (see below). This interpretation also explains the weak dispersion of $\delta^{18}O$ values in the North, where most of the calcite is of secondary origin. In the southern part, the marked heterogeneity reflects contrasting calcite $\delta^{18}O$ signatures resulting from a mixture of variably altered marine carbonates and secondary calcite precipitated from an external ^{18}O-depleted fluid (see Bowman, Willett, and Cook, 1994).

In the northwestern part of the studied area, the thrust contact consists of Mesozoic marine carbonates in the hangingwall and Flysch in the footwall. Calcite $\delta^{18}O$ values in the calc-mylonite reach 22‰. There, the calc-mylonite consists certainly partly of highly sheared carbonates that have interacted with ^{18}O depleted fluids coming

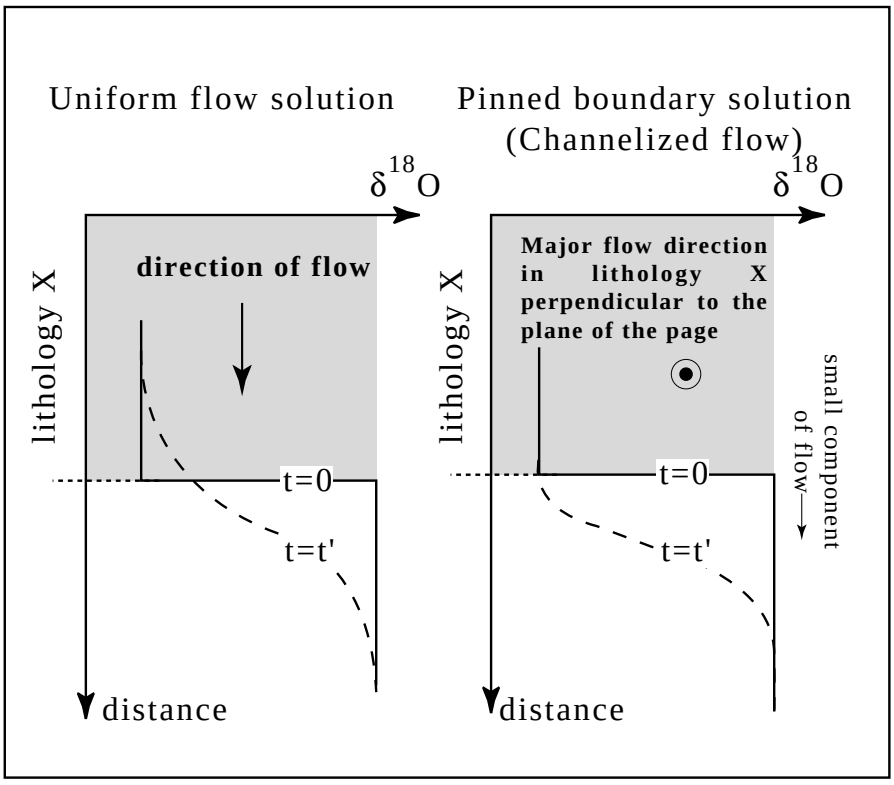

Fig. 12
Diagrammatic illustration of transport isotope step for different boundary conditions. On the left, the uniform flow advection displaces step and diffusion/dispersion smoothes this step. On the right, the pinned boundary solution indicates that copious flow in the lithology X, mainly parallel to layering, maintains the isotopic composition at the boundary at a constant value. Both diffusion/dispersion and a smaller component of flow transport this isotopic composition into the lower layer (modified after Bickle and Baker, 1990)

from the Flysch below.

II. Calcite $\delta^{18}O$ and $\delta^{13}C$ vertical profiles across the thrust

The isotopically contrasting footwall and hangingwall lithologies may be regarded as two distinct carbon and oxygen reservoirs, which exchange material by diffusive/dispersive and advective transport. In the South, where the main flow component most likely was thrust parallel, consideration of the vertical isotope variation within the framework of 1-D models in the direction perpendicular to the thrust may be employed to investigate cross thrust transport components. The trend of increasing $\delta^{18}O$ values from 11-15‰ at the thrust contact to 24‰ 7 m below (Fig.

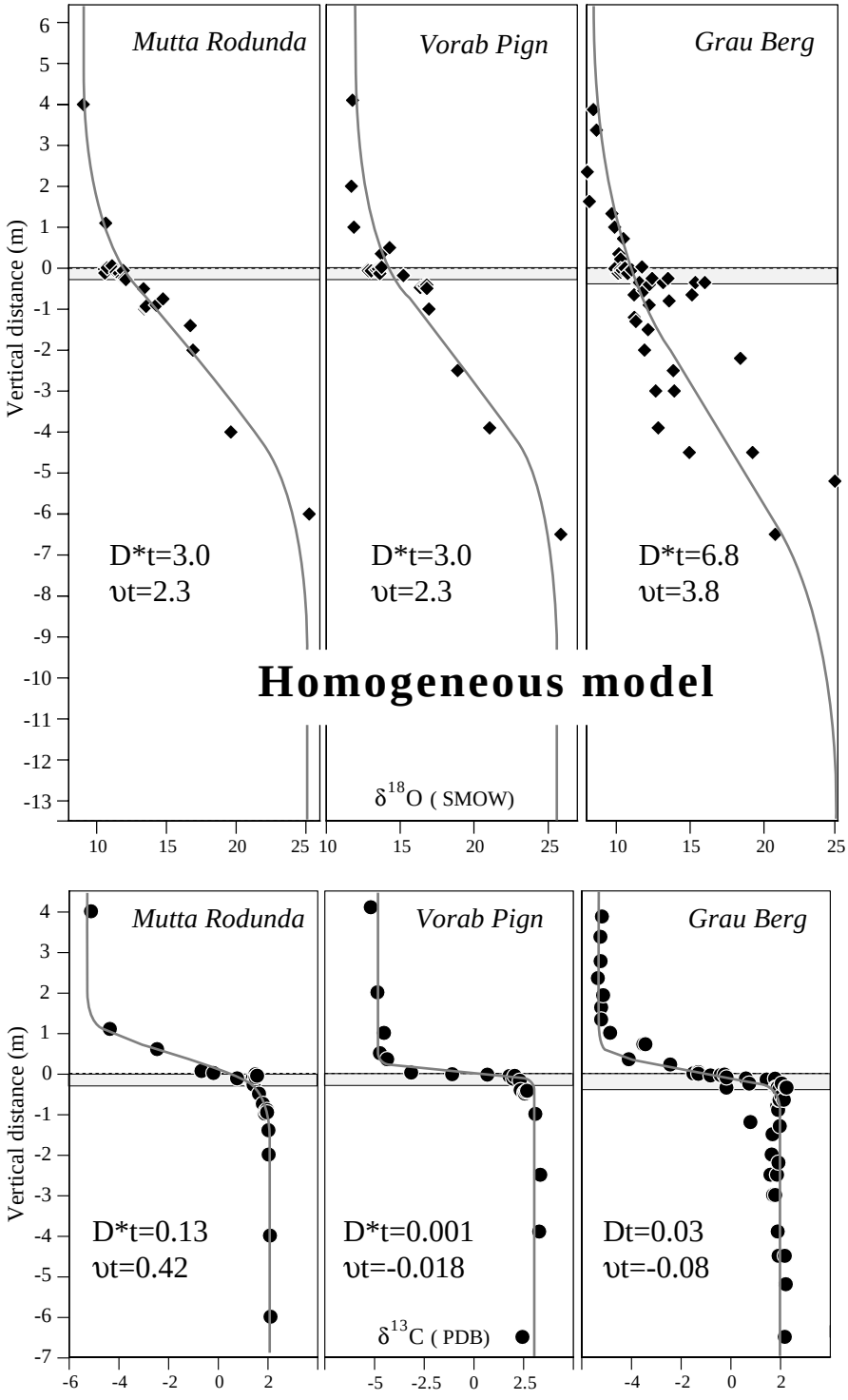

Fig. 13
Calculated curves for calcite $\delta^{18}O$ (upper part) and $\delta^{13}C$ (lower part) composition against vertical distance predicted by homogeneous flow model of Bickle and Baker (1990) are represented together with the $\delta^{18}O$ and $\delta^{13}C$ data from three sites of the southern part of the Glarus overthrust. t is time and D is the effective oxygen dispersion/diffusion coefficient. D*t is referred to as the characteristic length of dispersion/diffusion. u*t, gives the advective displacement of the front with respect to its original position

6) is interpreted as an isotope front that developed by isotopic exchange of the footwall carbonates with a relatively ^{18}O depleted reservoir. From the Verrucano/calc-mylonite contact down to the footwall, the calcite $\delta^{13}C$ values describe a very sharp increasing trend (Fig. 6). This exchange front is significantly retarded with respect to the oxygen isotope front. In the hangingwall, very sharp $\delta^{18}O$ and $\delta^{13}C$ gradients are described (Fig. 6). Only the first 50-100 cm display $\delta^{18}O$ and $\delta^{13}C$ values resulting from the interaction between the Verrucano and a relatively ^{18}O and ^{13}C enriched fluid.

One possibility to model the exchanges that occurred by combined dispersive/diffusive-advective transport at the thrust contact is to regard the transport parameters, i. e. fluid flow velocity and effective oxygen diffusivity as constants across the thrust (homogeneous flow model, according to Bickle and Baker, 1990)(Fig. 12, left). In this case the isotope composition is given by equation (1).

The corresponding model curves fitted to our data are shown in Fig. 13. The characteristic diffusion lengths are 3, 3, and 6.8 m^2 for the Mutta Rodunda, Vorab Pign, and Grauberg localities. The corresponding advective front displacements are 2.3, 2.3, and 3.8 meters downwards from the thrust. Considering the footwall carbonates as pure calcite and the fluid as pure water at 300°C and 3 to 4.5 kbar results in Kd = 1.5 (see above). This yields TIFF of 3.45, 3.45 and 5.7 m^3/m^2 for Mutta Rodunda, Vorab Pign and Grauberg respectively for the downwards infiltration of fluids into the footwall. This is three orders of magnitude lower than the calculated TIFF of flow along the thrust. The characteristic diffusion length and advective front displacements obtained for carbon is significantly smaller (see Fig. 13). The strong retardation of the carbon, with respect to the oxygen fronts testifies to a very low carbon to oxygen ratio in the fluid on the order of 1/1000 to 1/100.

Considering the relatively minute isotopic effects in the hangingwall and the pronounced alteration halo below the thrust, one may, alternatively, regard the hangingwall as an infinite reservoir that buffers the oxygen and carbon isotope compositions at the thrust contact (pinned boundary model according to Bickle and Baker, 1990)(Fig. 12, right). If downward transport is then regarded as a diffusive/dispersive process, the isotope composition is given by (Crank , 1975, eq. 2.45)

$$R(x,t) = R_r - (R_f - R_r) * \mathrm{erfc}\frac{x}{2\sqrt{u}} \qquad (5)$$

The corresponding model curves fitted to our data are shown in Fig. 14. In this model, the entire transport is attributed to diffusion/dispersion. Accordingly, the inferred diffusion length of 3.2, 3.2, and 8.3 respectively, are larger than in the homogenous flow model. As in the previous model, the strong retardation of the carbon, with respect to the oxygen fronts testifies to low C/O ratios in the pore fluid. On fig. 15A, the calcites of the footwall carbonates describe an L-shaped pattern that testify to interaction with ^{18}O, ^{13}C depleted fluid ($\delta^{18}O$=6-8‰ and $\delta^{13}C$= -7‰) that had a very low XCO_2 (see Bickle and McKenzie, 1987). These fluids come either from the overlying Verrucano or from the Basement further South. Oxygen diffusivities derived from the characteristic diffusion length and retarded flow

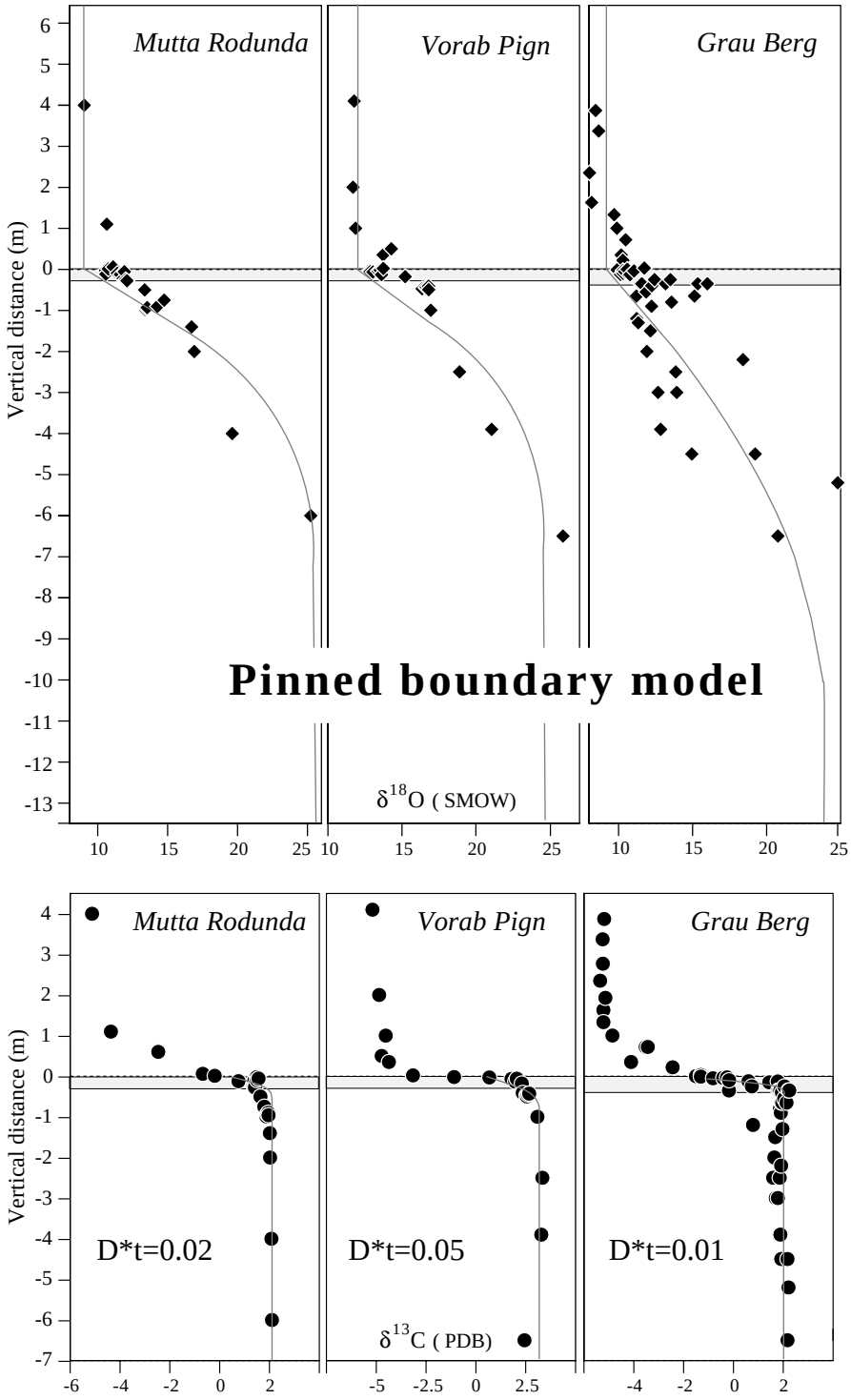

Fig. 14
Calculated curves for calcite $\delta^{18}O$ (upper part) and $\delta^{13}C$ (lower part) composition against vertical distance predicted by pinned boundary flow model of Bickle and Baker (1990) are represented together with the $\delta^{18}O$ and $\delta^{13}C$ data from three sites of the southern part of the Glarus overthrust. t is time and D is the effective oxygen dispersion/diffusion coefficient. D*t is referred to as the characteristic length of dispersion/diffusion.

velocities for geologically relevant time scales are given in Table 2. These are well within the range of oxygen diffusivities that would be predicted for porous rocks from experimental data on the self-diffusion of H_2O in water.

In summary, modelling indicates that cross thrust transport is several orders of magnitude slower than thrust parallel transport inferred from the S-N oxygen isotope front as attested by the differences in TIFF. It is, however, significant and it is preferably in the downward direction so that the oxygen, and to a lesser extent, the carbon isotope signature of the hangingwall Verrucano or Basement-derived fluids are imprinted on the

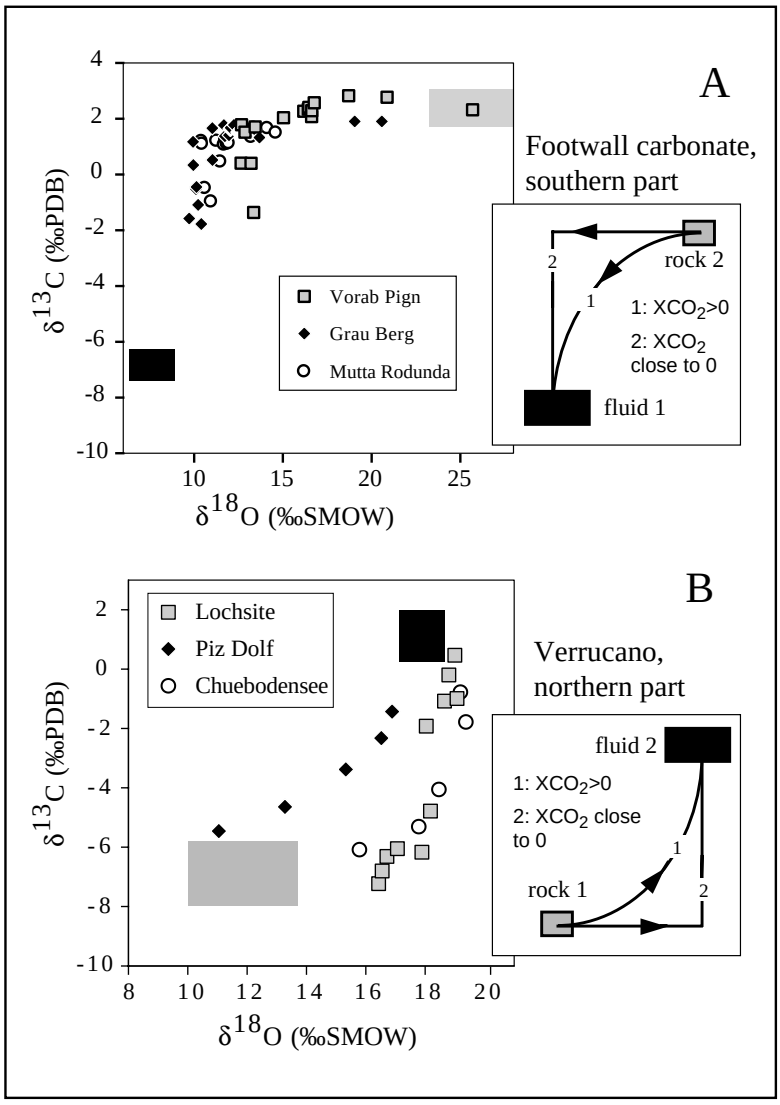

Fig. 15

(A) Isotopic composition of footwall carbonate calcite from different sites along the Glarus thrust in $\delta^{18}O$ vs. $\delta^{13}C$. Helvetic marine carbonate compositions are indicated by grey box (according to Burkhard and Kerrich, 1988). The compositions of the suspected fluid with which the carbonates interacted is indicated by a black box. The suggested exchange trend between the carbonates and a depleted external metamorphic fluid is indicated on the lower right. The exact trend depends on XCO_2. With XCO_2 close to 0 it has a typical L shape, if XCO_2 increases the curve becomes smoother.

(B) Isotopic composition of Verrucano calcites from different sites along the Glarus thrust in $\delta^{18}O$ versus $\delta^{13}C$. Verrucano unaltered compositions are indicated by grey box (according to Burkhard and others, 1992b). The compositions of the suspected fluid with which the Verrucano interacted is indicated by a black box. The suggested exchange trend between the Verrucano and an enriched fluid is indicated on the lower right. The exact trend depends on XCO_2. With XCO_2 close to 0 it has a typical L shape, if XCO_2 increases the curve becomes smoother.

uppermost few meters of the footwall.

Hydrodynamic dispersion on either side of the thrust contact is the most plausible explanation for the observed alteration in the hangingwall. Fluids flowing along the thrust penetrate in the footwall and hangingwall by hydrodynamic dispersion (Fig. 17). If a fluid has travelled through the footwall and has been enriched in ^{18}O and ^{13}C before infiltrating the hangingwall, a slight enrichment of the Verrucano will result. Details of these processes are discussed in Abart and Badertscher (2001).

In the northern area, decreasing trends of calcite $\delta^{18}O$ and $\delta^{13}C$ values have been identified from the thrust up to the hangingwall (Fig. 7), whereas footwall and calc-mylonite are indistinguishable in $\delta^{18}O$ and $\delta^{13}C$. No sign of infiltration of fluids can be detected in the footwall. These observations are best explained by Flysch-derived fluids infiltrating upward into the Verrucano. The calc-mylonite itself is explained as a secondary calcite mineralisation along this lithological/tectonic boundary. The gradient in the Verrucano can be interpreted in terms of a coupled advective and

t (years)	t (s)	D (m^2/s)	υ (m/s)
10^5	$3.15E^{12}$	1 to $4E^{-12}$	0.7 to 1.2 E^{-10}
10^6	$3.15E^{13}$	1 to $4E^{-13}$	0.7 to 1.2 E^{-11}
10^7	$3.15E^{14}$	1 to $4E^{-14}$	0.7 to 1.2 E^{-12}

Table 2

Fluid flow parameters deduced from fitting curves with $\delta^{18}O$ data of calc-mylonite in three vertical profiles of the southern part of the Glarus overthrust. The calculation is based on transport theory. t is time, D is the dispersive/diffusive coefficient and υ is the mean interstitial particle velocity for the downward infiltration system that occurred in the southern part of the Glarus overthrust.

diffusive/dispersive infiltration (or advection and kinetically-controlled exchange) of ^{18}O and ^{13}C enriched Flysch-derived fluids. A scenario, where the footwall is regarded as an infinite reservoir that buffers the oxygen and carbon isotope compositions at the thrust contact (pinned boundary model according to Bickle and Baker, 1990)(Fig. 12, right), can be modelled if upwards transport is regarded as a diffusive/dispersive process. The isotope composition is given by equation (5).

The corresponding model curves fitted to our data are shown in Fig. 16. The inferred diffusion lengths of 2.99 (Piz Dolf), 6.4 (Chuebodensee), and 9.1 (Lochsite), respectively, for oxygen and 1.8, 1.6, 1.97, respectively, for carbon increase from South to North. In other words, the upwards transport component increases northwards.

Another alternative is that fluids equilibrated with the Flysch and saturated in calcite escaped upward into the hangingwall and progressively precipitated increasingly ^{18}O and ^{13}C-depleted veins due to Rayleigh distillation (e. g. Abart and Pozzorini, 2000), because ^{18}O and ^{13}C first precipitate in veins compared to ^{16}O and ^{12}C.

The relatively weak retardation of the carbon, with respect to the oxygen fronts may testify to relatively high C/O ratios in the pore fluid. When looking at Fig. 15B, we could infer a XCO_2=0.3 in Chuebodensee and Lochsite and a XCO_2=0.4 in Piz Dolf (see Baumgartner and Rumble, 1988). Such a high XCO_2 is compatible with a formation of the calc-mylonite by the precipitation of calcite veins. In the North, fluids with high XCO_2 and with $\delta^{18}O$ and $\delta^{13}C$ equilibrated with the Flysch are ponded below the Verrucano, where they precipitate calcite in veins, before infiltrating the Verrucano.

III. Large scale variations in the Verrucano.

The increase of calcite $\delta^{18}O$ values in the Verrucano 10 meters above the thrust from 10-12‰ in the South to 17‰ in the North could potentially be interpreted as a N-S isotope front. The whole Verrucano with original calcite $\delta^{18}O$ of 17‰ could have been infiltrated by an ^{18}O depleted fluid coming from further south and $\delta^{18}O$ of 12‰ would represent the upstream segment of an isotope front where rock is equilibra-

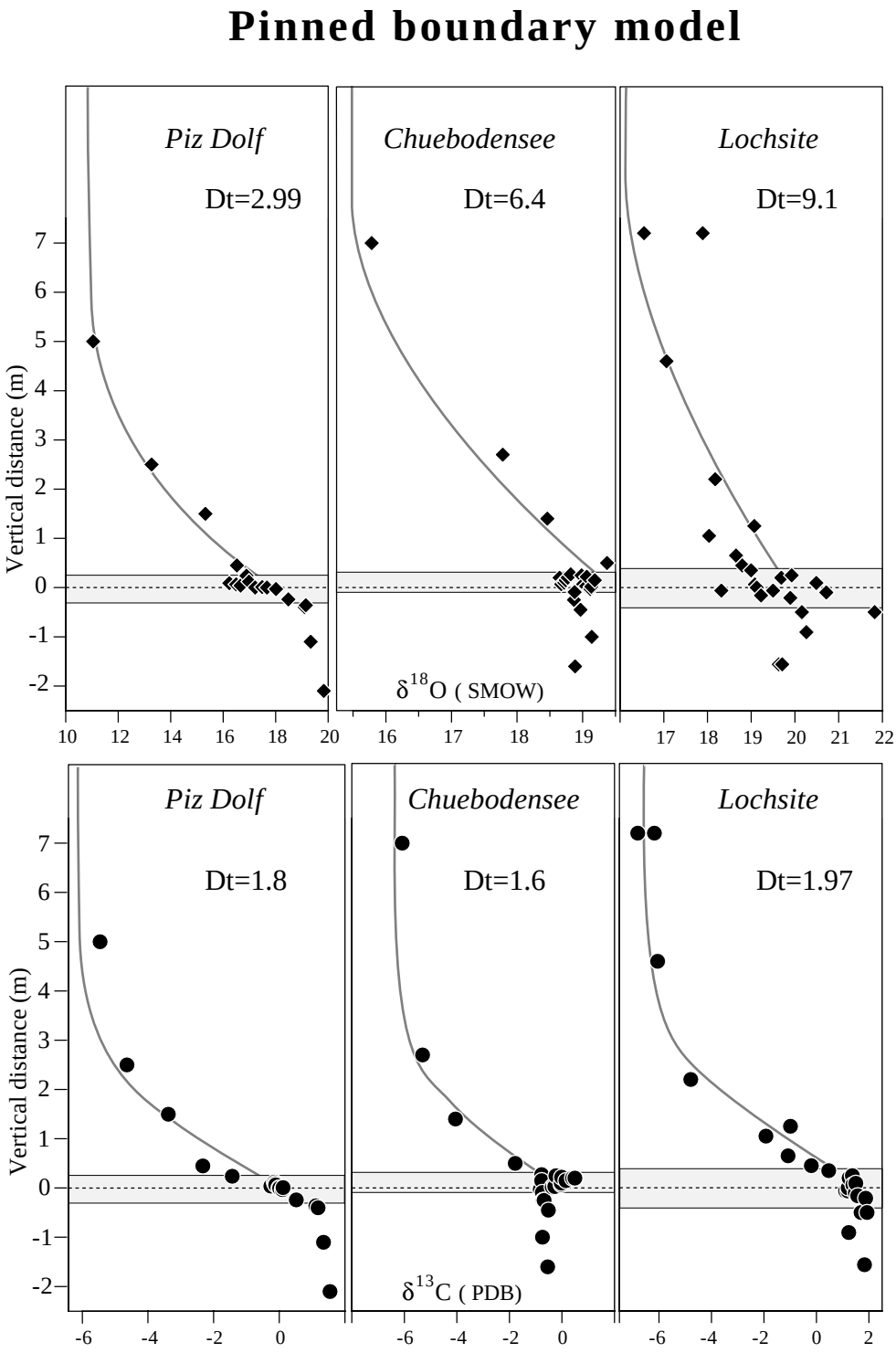

Fig. 16
Calculated curves for calcite $\delta^{18}O$ (upper part) and $\delta^{13}C$ (lower part) composition against vertical distance predicted by pinned boundary flow model of Bickle and Baker (1990) are represented together with the $\delta^{18}O$ and $\delta^{13}C$ data from three sites of the northern part of the Glarus overthrust. t is time and D is the effective oxygen dispersion /diffusion coefficient. D*t is referred to as the characteristic length of dispersion/diffusion.

ted with the fluid. Yet, 100 m above the thrust, no trend can be identified in the $\delta^{18}O$ values of calcite and bulk rock (Fig. 8). This clearly documents that this increasing trend is due to the northwards increasing amount of infiltration of ^{18}O enriched fluids from the footwall. This may be due to the thicker sequence of Flysch or to a more permeable Verrucano as it loses phyllosilicates (Fig. 8).

IV. $\delta^{18}O$ and $\delta^{13}C$ vein matrix relations

The generally small differences in calcite $\delta^{18}O$ and $\delta^{13}C$ values between veins and their matrix (Fig. 9) could be interpreted as closed system behaviour (see Burkhard and Kerrich, 1988). Some veins from within the Verrucano and footwall carbonates, display large deviations from their unaltered host-rock $\delta^{18}O$-$\delta^{13}C$ values ($\delta^{18}O$=10-12‰, $\delta^{13}C$ =-6‰ and $\delta^{18}O$=25‰ and $\delta^{13}C$ =-2-3‰, respectively). This gives clear indications for the infiltration of external fluids. These fluids were quickly rock-buffered as they travelled through these two lithologies and then precipitated veins with an isotopic signature in equilibrium with the direct wall rock. In the Flysch the clustering of $\delta^{18}O$ and $\delta^{13}C$ around an unaltered value supports the fact that no infiltration of externally derived fluids has taken place.

V. $^{87}Sr/^{86}Sr$ of the calc-mylonite

On the three rock slabs, the part with homogeneous $^{87}Sr/^{86}Sr$ values (Fig. 10) consists mainly of deformed, recrystallized and disrupted veins. The homogeneity of the values is therefore attributed to the precipitation of veins from an external fluid. The thickness of the homogeneous zone depends on the quantity of precipitated veins. In Fuorcla Sura and Vorab Pign, this fluid most probably originated either from the overlying Verrucano or it is externally derived (Basement further South, Fig. 2). We prefer the second solution, as it explains the decrease in mean $^{87}Sr/^{86}Sr$ values from South to North as ^{87}Sr is progressively removed from the fluid by fluid-rock interaction with low ^{87}Sr footwall carbonates. In Sardona the $^{87}Sr/^{86}Sr$ signature could result from the mixing of fluids coming from the underlying Flysch and of fluids channelized along the thrust. In Fuorcla Sura and Vorab Pign, the vertical gradients within grey mylonitized footwall carbonates with very little veiny material are interpreted as isotope fronts due to the infiltration of ^{87}Sr enriched fluids into the footwall carbonates that interacted with inherited marine calcites. The retardation of the $^{87}Sr/^{86}Sr$ front compared to that of $\delta^{18}O$ could provide additional data to constrain transport mechanisms and TIFF involved in this flow event. This is treated in detail in Abart and Badertscher (2001). In Sardona, the absence of any systematic trend on a slab with more than 15 cm width can be attributed to two factors: I) the dewatering underlying Flysch produces considerable amounts of calcite-saturated fluids that can precipitate veins with an identical $^{87}Sr/^{86}Sr$ signature II) the calc-mylonite displays a very chaotic texture. Mechanical mixing of calcite could strongly contribute to the homogenisation of the $^{87}Sr/^{86}Sr$ values.

VI. Insights into the origin and formation of Lochsiten calc-mylonite

The bulk flow pattern that results form the isotopic 3D picture constrains the origin and the formation of the Lochsiten calc-mylonite. In the northern area, where Flysch in the footwall produces large amounts of calcite-saturated fluids, the 1-5 m thick calc-mylonite appears as a pile of folded and disrupted veins separated by rare stylolites. On their way upward, the fluids are ponded below the apparently less permeable Verrucano. This

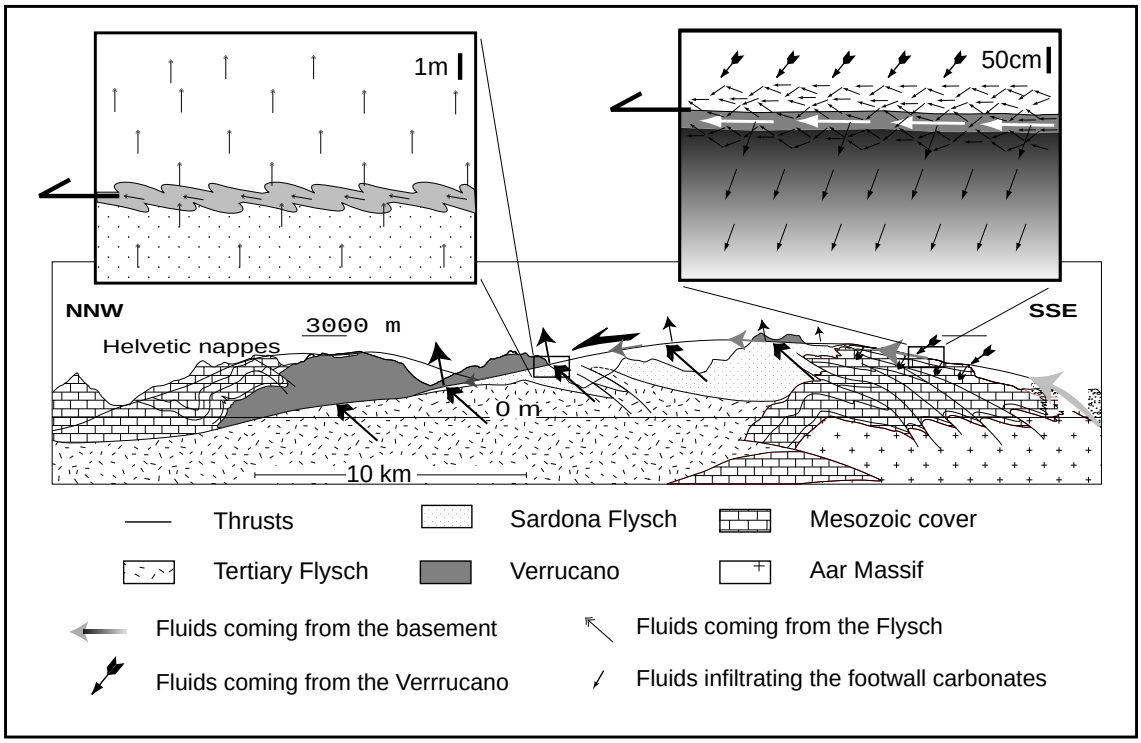

Fig. 17

Cross section of the Glarus Alps in eastern Switzerland (according to Oberholzer, 1933) on which are indicated the different flow systems (arrows). Two close-up views are given to show the details of the fluid flow patterns at the thrust contact. The size of arrows is proportional to the suspected flux of a particular flow system.

leads to the increase in fluid pressure and the treshold for hydrofracturation was repeatedly attained. After fracturing, calcite precipitated within the fractures. This also helped thrust translation by provoking seismic motion and lowering normal stress. In the southern area, these effects are reduced because the fluid supply from the footwall is much less efficient. The "true" Lochsitenkalk mylonite with apparent veins is only 5-15 cm thick. It is restricted to the zone of channelized fluid flow along the thrust.

CONCLUSIONS

In the Glarus area, fluid flow pathways have been derived from the stable and Sr-isotope systematics (Fig. 17). Two regions of different flow regimes, separated by the carbonate-Flysch boundary in the footwall, have been documented. South of the carbonate-Flysch boundary, fluids originating in the Infrahelvetic Basement (dehydration reactions products or old evolved formation brines) in the root zone of the thrust, were channelized along the thrust in a partly pre-existing carbonate with a general northward direction of flow (Burkhard and others, 1992)(compare McCaig and others, 1995). These fluids, characterized by an $\delta^{18}O$ of 4-7‰ have been transported by a coupled advective and dispersive/diffusive process and lead to a pronounced large-scale oxygen isotope front in the calc-mylonite. A Peclet number N_{Pe} of 12.82 to 39.47 for this flow system documents a very dispervsive/diffusive transport

mechanism. The characteristic length of dispersion/diffusion of 0.36 to 2.3 km cannot be accounted for by molecular diffusion alone and hence hydrodynamic dispersion is inferred to have played a major role during this flow event (compare Bowman, Willett, and Cook, 1994). Calcite veins precipitating from these fluids at the top of the calc-mylonite are strongly sheared leading to the characteristic "foliated gouge" aspect of the Lochsitenkalk-mylonite. Due to transversal hydrodynamic dispersion, these channelized fluids are also responsible for an ^{18}O and ^{13}C enrichment in the lowermost 50-100 cm of the hangingwall. In the footwall carbonates, $\delta^{18}O$, $\delta^{13}C$ and $^{87}Sr/^{86}Sr$ gradients are recognized as isotopic fronts due to the downward infiltration of fluids with $\delta^{18}O$ of about 7‰, $\delta^{13}C$ of –5‰, $^{87}Sr/^{86}Sr$ >0.715 and a XCO_2«0.1. These fluids came, either from the overlying Verrucano or may be regarded as lateral seepage of the channelized northwards migrating fluids. In either case, a downward directed TIFF of 3.45 to 5.7 m^3/m^2 is obtained. This indicates that the cross thrust infiltration is much weaker than the channelized flow component, for which a TIFF of 4500-9100 m^3/m^2 is calculated.

In the northern areas, the calcite $\delta^{18}O$ values of the calc-mylonite are strongly clustered around 20‰. This cannot be simply interpreted as the downstream segment of channelized flow along a pre-existing carbonate as there is a systematic deviation between the observed $\delta^{18}O$ values and the $\delta^{18}O$ value of 26‰ predicted from transport theory (Bowman, Willett, and Cook, 1994). An important upward fluid flow component has been documented on the vertical profiles. Calcite saturated fluids equilibrated with the dewatering Flysch escaped upward and forelandward (Marquer and Burkhard, 1992, Oliver, 1986) and infiltrated the Verrucano. At the thrust contact these fluids precipitated calcite with constant $\delta^{18}O$ and $\delta^{13}C$ signatures leading to a vein-dominated calc-mylonite. Further up, these fluids continued to precipitate increasingly depleted calcite as ^{13}C was preferentially precipitated in veins. These fluids are characterized by an XCO_2=0.3-0.4 and by an $\delta^{18}O$ of about 15‰. In the North, the presence of channelized flow along the thrust cannot be ruled out, but, at least, it is not necessary to explain the observed isotope patterns. The fact that calcite of the calc-mylonite is precipitated from an identical fluid explains the homogeneity of calcite $\delta^{18}O$ values in the North and the constant deviation from a $\delta^{18}O$ value of 26‰ predicted by transport theory applied to a 1D fluid flow in a pre-existing carbonate (Fig. 11). The calc-mylonite can therefore not be treated as a pre-existing carbonate in which fluids coming from the South are channelized (Burkhard and others, 1992). Other flow systems exist and apart from that the Lochsitenkalk is at least in part formed by precipitation of veins. Fluid flow upwards into the hangingwall and downward into the footwall have clearly been identified. In these cases, the fluids are quickly rock-buffered, and hence no great disequilibrium between veins and matrix could be created.

Finally, the role of fluids has been to lower normal stress and then to help thrust translation (Badertscher and Burkhard, 2001, Hsü, 1969, Hubbert and Rubey, 1959).

REFERENCES

Abart, R., and Pozzorini, D., 2000, Implications of kinetically controlled mineral-fluid exchange on the geometry of stable-isotope fronts: European Journal of Mineralogy, v. 12, p. 1069-1082.

Abart, R., and Sperb, R., 1997, Grain-scale stable isotope disequilibrium during fluid-rock interaction; 1, Series approximations for advective-dispersive transport and first-order kinetic mineral-fluid exchange: American Journal of Science, v. 297, p. 679-706.

Abart, R., Badertscher, N., Burkhard, M. and Povoden, E., 2001, Oxygen, carbon and strontium isotope systematics in two profiles across the Glarus Thrust: Implications for fluid flow: submitted to Contributions to Minralogy and Petrology

Badertscher, N. P., and Burkhard, M., 2001, Brittle-Ductile deformations in the Glarus thrust Lochsitenkalk (LK) mylonite: In press at Terra Nova.

Baker, J., and Spiegelman, M., 1995, Modelling an infiltration-driven geochemical front: Earth and Planetary Science Letters, v. 136, p. 87-96.

Baumgartner, L. P., and Rumble, D., 1988, Transport of stable isotopes; 1, Development of a kinetic continuum theory for stable isotope transport: Contributions to Mineralogy and Petrology, v. 98, p. 417-430.

Bickle, M. J., and Baker, J., 1990, Advective-diffusive transport of isotopic fronts; an example from Naxos, Greece: Earth and Planetary Science Letters, v. 97, p. 78-93.

Bickle, M. J., and McKenzie, D., 1987, The transport of heat and matter by fluids during metamorphism: Contributions to Mineralogy and Petrology, v. 95, p. 384-392.

Bowman, J. R., Willett, S. D., and Cook, S. J., 1994, Oxygen isotopic transport and exchange during fluid flow; one-dimensional models and applications: American Journal of Science, v. 294, p. 1-55.

Burkhard, M., and Kerrich, R., 1988, Fluid regimes in the deformation of the Helvetic Nappes, Switzerland, as inferred from stable isotope data: Contributions to Mineralogy and Petrology, v. 99, p. 416-429.

Burkhard, M., and Kerrich, R., 1990, Fluid-rock interactions during thrusting of the Glarus Nappe; evidence from geochemical and stable isotope data: Schweizerische Mineralogische und Petrographische Mitteilungen = Bulletin Suisse de Minéralogie et Pétrographie, v. 70, p. 77-82.

Burkhard, M., Kerrich, R., Maas, R., and Fyfe, W. S., 1992, Stable and Sr-isotope evidence for fluid advection during thrusting of the Glarus nappe (Swiss Alps): Contributions to Mineralogy and Petrology, v. 112, p. 293-311.

Cathless, L. M., III, 1990, Scales and effects of fluid flow in the upper crust: Science, v. 248, p. 323-329.

Clayton, R. N., Goldsmith, J. R., and Mayeda, T. K., 1989, Oxygen isotope fractionation in quartz, albite, anorthite and calcite: Geochimica et Cosmochimica Acta, v. 53, p. 725-733.

Cox, S. F., 1987, Antitaxial crack-seal vein microstructures and their relationship to displacement paths: Journal of Structural Geology, v. 9, p. 779-787.

Cox, S. F., and Etheridge, M. A., 1989, Coupled grain-scale dilatancy and mass transfer during deformation at high fluid pressures; examples from Mount Lyell, Tasmania: Journal of Structural Geology, v. 11, p. 147-162.

Crespo-Blanc, A., Masson, H., Sharp, Z., Cosca, M., and Hunziker, J., 1995, A stable and (super 40) Ar/ (super 39) Ar isotope study of a major thrust in the Helvetic nappes (Swiss Alps); evidence for fluid flow and constraints on nappe kinematics: Geological Society of America Bulletin, v. 107, p. 1129-1144.

Dipple, G. M., and Ferry, J. M., 1992, Metasomatism

and fluid flow in ductile fault zones: Contributions to Mineralogy and Petrology, v. 112, p. 149-164.

Eppel, H., and Abart, R., 1997, Grain-scale stable isotope disequilibrium during fluid-rock interaction; 2, An example from the Penninic-Austroalpine tectonic contact in eastern Switzerland: American Journal of Science, v. 297, p. 707-728.

Etheridge, M. A., Wall, V. J., Cox, S. F., and Vernon, R. H., 1984, High fluid pressures during regional metamorphism and deformation; implications for mass transport and deformation mechanisms: Journal of Geophysical Research, v. 89, p. 4344-4358.

Etheridge, M. A., Wall, V. J., and Vernon, R. H., 1983, The role of the fluid phase during regional metamorphism and deformation: Journal of Metamorphic Geology, v. 1, p. 205-226.

Ferrero, J., 1965, Dosage des principaux minéraux des roches par diffraction de Rayons X: Rapport C.F.P. (Bordeaux), inédit.

Ferrero, J., 1966, Nouvelle méthode empirique pour le dosage des minéraux par diffraction R.X.: Rapport C.F.P. (Bordeaux), inédit.

Frey, M., 1988, Discontinuous inverse metamorphic zonation, Glarus Alps, Switzerland; evidence from illite "crystallinity" data: Schweizerische Mineralogische und Petrographische Mitteilungen = Bulletin Suisse de Mineralogie et Petrographie, v. 68, p. 171-183.

Fyfe, W. S., and Kerrich, R., 1985, Fluids and thrusting: Chemical Geology, v. 49, p. 353-362.

Groshong, R. H., Jr., Pfiffner, O. A., and Pringle, L. R., 1984, Strain partitioning in the Helvetic thrust belt of eastern Switzerland from the leading edge to the internal zone: Journal of Structural Geology, v. 6, p. 5-18.

Hsu, K. J., 1969, Role of cohesive strength in the mechanics of overthrust faulting and of landsliding: Geol. Soc. America Bull, v. 80, p. 927-952.

Hsü, K. J., 1969, A preliminary Anlysis of the Statics and Kinetics of the Glarus Overthrust: Eclogae geologica Helvetiae, v. 62, p. 143-154.

Hubbert, M. K., and Rubey, W. W., 1959, Role of fluid pressure in mechanics of overthrust faulting: Geological Society of America Bulletin, v. 70, p. 115-166.

Hunziker, J. C., Frey, M., Clauer, N., Dallmeyer, R. D., Friedrichsen, H., Flehmig, W., Hochstrasser, K., Roggwiler, P., and Schwander, H., 1986, The evolution of illite to muscovite; mineralogical and isotopic data from the Glarus Alps, Switzerland: Contributions to Mineralogy and Petrology, v. 92, p. 157-180.

Kerrich, R., La Tour, T. E., Willmore, L., Kirby, S. H. e., and Scholz, C. H. e., 1984, Fluid participation in deep fault zones; evidence from geological, geochemical, and (super 18) O/ (super 16) O relations

Chemical effects of water on the strength and deformation of crustal rocks: Chemical effects of water on the strength and deformation of crustal rocks, v. 89, p. 4331-4343.

Kirschner, D. L., Masson, H., and Sharp, Z. D., 1999, Fluid migration through thrust faults in the Helvetic nappes (Western Swiss Alps): Contributions to Mineralogy and Petrology, v. 136, p. 169-183.

Klug, H. P., and Alexander, L., 1974, X-ray Diffraction Procedures for Polycrystalline and Amorphous Materials: New York.

Knipe, R. J., McCaig, A. M., and Parnell, J. e., 1994, Microstructural and microchemical consequences of fluid flow in deforming rocks, in Parnell, J. e., editor, Geofluids; origin, migration and evolution of fluids in sedimentary basinsGeological Society Special Publications, Geological Society Special Publications, p. 99-111.

Kübler, B., 1983, Dosage quantitatif des minéraux majeurs des roches sédimentaires par Diffractzion X.: Cahier de l'Institut de Géologie de Neuchâtel, v. Série AX

N°1.1 & 1.2.

Lassey, K. R., and Blattner, P., 1988, Kinetically controlled oxygen isotope exchange between fluid and rock in one-dimensional advective flow: Geochimica et Cosmochimica Acta, v. 52, p. 2169-2175.

Marquer, D., and Burkhard, M., 1992, Fluid circulation, progressive deformation and mass-transfer processes in the upper crust; the example of basement-cover relationships in the External Crystalline Massifs, Switzerland: Journal of Structural Geology, v. 14, p. 1047-1057.

McCaig, A. M., 1984, Fluid-rock interaction in some shear zones from the Pyrenees: Journal of Metamorphic Geology, v. 2, p. 129-141.

McCaig, A. M., 1989, Geology; fluid flow through fault zones: Nature (London), v. 340, p. 600.

McCaig, A. M., 1997, The geochemistry of volatile fluid flow in shear zones, in Holness, M. B., editor, Deformation-enhanced Fluid Transport inthe Earth's Crust and Mantle: London, Chapman & Hall, p. 227-266.

McCaig, A. M., Wayne, D. M., Marshall, J. D., Banks, D., and Henderson, I., 1995, Isotopic and fluid inclusion studies of fluid movement along the Gavarnie Thrust, central Pyrenees; reaction fronts in carbonate mylonites: American Journal of Science, v. 295, p. 309-343.

McCaig, A. M., Wickham, S. M., and Taylor, H. P., Jr., 1990, Deep fluid circulation in Alpine shear zones, Pyrenees, France; field and oxygen isotope studies: Contributions to Mineralogy and Petrology, v. 106, p. 41-60.

O'Neil, J. R., Clayton, R. N., and Mayeda, T. K., 1969, Oxygen isotope fractionation in divalent metal carbonates: The Journal of Chemical Physics, v. 51, p. 5547-5558.

Oberholzer, J., 1933, Geologie der Glarner Alpen, Beiträge Geologische Karte Schweiz, geologische Kommission.

Oliver, J., 1986, Fluids expelled tectonically from orogenic belts; their role in hydrocarbon migration and other geologic phenomena: Geology (Boulder), v. 14, p. 99-102.

Oliver, N. H. S., 1996, Review and classification of structural controls on fluid flow during regional metamorphism: Journal of Metamorphic Geology, v. 14, p. 477-492.

Oliver, N. H. S., Valenta, R. K., and Wall, V. J., 1990, The effect of heterogeneous stress and strain on metamorphic fluid flow, Mary Kathleen, Australia, and a model for large-scale fluid circulation: Journal of Metamorphic Geology, v. 8, p. 311-331.

Pfiffner, O. A., 1977, Tektonische Untersuchungen im Infrahelvetikum der Ostschweiz. Translated title: Tectonic studies of the Infrahelvetic Complex, eastern Switzerland: Zuerich, Univ., Geol. Inst Eidgenoess. Tech. Hochsch., Geol. Inst., Mitt, v. 217, p. 164.

Pfiffner, O. A., 1981, Fold- and -thrust tectonics in the Helvetic Nappes (E. Switzerland), in Price, R., editor, Thrust and Nappe Tectonics: London, The Geological Society of London, p. 319-327.

Pfiffner, O. A., 1985, Displacements along thrust faults: Eclogae-Geologicae-Helvetiae, v. 78, p. 313-333.

Pfiffner, O. A., 1993, The structure of the Helvetic nappes and its relation to the mechanical stratigraphy: Journal of Structural Geology, v. 15, p. 511-521.

Price, R. A., 1988, The mechanical paradox of large overthrusts: Geological Society of America Bulletin, v. 100, p. 1898-1908.

Rahn, M., Mullis, J., Erdelbrock, K., and Frey, M., 1995, Alpine metamorphism in the North Helvetic flysch of the Glarus Alps, Switzerland: Eclogae Geologicae Helvetiae, v. 88, p. 157-178.

Rolli, M., 1990, Dosage semi-quantitatif RX sur Scintag.: Cahiers de l'Institu de Géologie de Neuchâtel, Suisse, v. Série ADX, 1-49.

Sample, J. C., 1996, Isotopic evidence from authigenic carbonates for rapid upward fluid flow in accretionary wedges: Geology (Boulder), v. 24, p. 897-900.

Schmid, S. M., 1975, The Glarus overthrust; field evidence and mechanical model: Eclogae Geol. Helv., v. 68, p. 247-280.

Schmid, S. M., Boland, J. M., and Paterson, M. S., 1977, Superplastic flow in finegrained limestone: Tectonophysics, v. 43, p. 257-291.

Schmid, S. M., Pfiffner, O. A., Schönborn, G., Frotzheim, N., and Kissling, E., 1997, Integrated croos section and tectonic evolution of the Alps along the Eastern Traverse, in Pfiffner, O. A., Lehner, P., Heitzmann, P., Mueller, S., and A., S., editors, Deep Structure of the Swiss Alps: Basel, Birkhäuser Verlag, p. 289-304.

Silver, E., Kastner, M., Fisher, A., Morris, J., McIntosh, K., and Saffer, D., 2000, Fluid flow paths in the Middle America Trench and Costa Rica margin: Geology, v. 28, p. 679-682.

Yardley, B. W. D., and Lloyd, G. E., 1995, Why metasomatic fronts are really metasomatic sides: Geology (Boulder), v. 23, p. 53-56.

Oxygen, carbon and strontium isotope systematics in two profiles across the Glarus Thrust: implications for fluid flow

R. ABART, N. BADERTSCHER*, M. BURKHARD*, E. POVODEN

Institut of Mineralogy and Petrology,, Karl-Franzens-Universität Graz, A-8010 Graz, Austria Tel.: ++43-316-380 5541, Fax: ++43-316-380 9865, e-mail: rainer.abart@kfunigraz.ac.at

* Institut de Géologie, CH-2007 Neuchatel, Switzerland

Abstract

The Glarus thrust is a prominent tectonic feature in the eastern Helvetic Alps. It has been recognized as a potential major pathway for syn-tectonic crustal scale fluid flow. The oxygen, carbon and strontium isotope patterns obtained from two vertical profiles across the thrust indicate fundamentally different flow regimes in the southern section of the thrust, where the footwall is represented by Mesozoic limestones, and in the northern section, where the footwall is represented by Tertiary flysch. At the Grauberg locality in the south the observed isotope patterns give evidence of a net mass transport component from the hangingwall Verrucano to the footwall limestone with a maximum time integrated volumetric fluid flux of 6.1 m^3/m^2. In the south the hydration of the lowermost 10 to 20 meters of the hangingwall Verrucano requires introduction of an aqueous fluid by sub-horizontal flow along the thrust with a minimum time integrated flux of 240 m^3/m^2. At the Lochseite locality in the north, the isotope patterns indicate a vertical mass transport component from the footwall flysch to the hanging wall Verrucano with a time integrated fluid flux of 2.6 m^3/m^2. In the north, the fluids were probably derived from compaction and dehydration of the footwall flysch during thrusting. The ascending fluids were ponded below the Verrucano and "lubricated" the thrust. Short term pressure drops associated with seismic motion along the thrust led to the precipitation of calcite in veins at the thrust surface contributing material to the Lochseiten calc-mylonite, a thin calc-mylonite layer at the thrust contact. Although cross thrust fluid flow may have been two to three orders of magnitude smaller than flow along the thrust, it had a major impact on the isotopic composition of the Lochseiten calc-mylonite. In particular, it buffered the oxygen isotope composition of the calc-mylonite towards the relatively ^{18}O depleted composition of the hangingwall Verrucano in the south and towards the relatively ^{18}O enriched compositions of the footwall flysch in the north. By this mechanism a regional south to north ^{18}O

enrichment trend was simulated within the Lochseiten calc-mylonite.

Introduction

Tectonic structures such as thrusts and faults are potential pathways for fluid flow (e.g. Fyfe et al., 1978; Fyfe and Kerrich, 1985; Oliver, 1986; McCaig, 1989), Faults and shear zones may channelize fluid flow due to permeability enhancement during deformation (e.g. Etheridge et al. 1984; Cox, et al. 1986; Sibson, 1986). The stable isotopes of oxygen and carbon as well as strontium isotopes are particularly useful tracers for fluid flow (e.g. Nabelek, 1991). In this context isotopic fronts are of special interest (e.g. Bickle and McKenzie, 1987, Baumgartner and Rumble, 1988). Initially sharp fronts that may exist at lithologic contacts may be degraded by diffusive/dispersive[1] processes in the pore fluid and displaced by fluid advection[2]. The geometry of an isotopic front reflects the extent, the mechanisms and the relative rates of the processes involved in mass transport and mineral-fluid exchange (e.g. Abart and Pozzorini, 2000).

The Glarus thrust is a very well defined major thrust-fault structure in the eastern Helvetic Alps. A schematic cross section of the thrust is given in figure 1a. Permian siltstones and shales of the Verrucano formation were thrust over Mesozoic limestones in the south and Tertiary Flysch in the north during Early Miocene times. The thrust surface is characterized by the presence of a thin ($<$ 1 to 5 meters thick) continuous layer of calc-mylonite, which will be referred to here as the "Lochseiten calc-mylonite" (the "Lochseiten limestone" of Heim, 1921)[3] . Burkhard and Kerrich (1990) and more recently Badertscher et al. (2001) documented a regional south to north trend of ^{18}O enrichment in the Lochseiten calc-mylonite (see figure 1b). This trend was interpreted by Burkhard et al. (1992)

[1] In this context the term "dispersion" refers to the combined effects of molecular diffusion and hydrodynamic dispersion.

[2] Material transport by solid-state diffusion is several orders of magnitude slower than fluid-bound transport and will be disregarded in this paper

[3] In this communication the term "Lochseiten calc-mylonite" is only used for calc-mylonite with abundant macroscopically distinguishable veins. Grey calc-mylonites, which were unambiguously derived from the footwall limestones in the southern section of the thrust, are not included in this definition.

and Bowman et al. (1994) as an oxygen isotope front produced by northward migration of ^{18}O depleted fluids along the thrust. Based on the oxygen isotope compositions of the Lochseiten calc-mylonite and using a strictly one-dimensional model Bowman et al. (1994) derived time integrated volumetric fluid fluxes on the order of 5000 m^2/m^3 for flow along the thrust and characterized the transport mechanisms for the inferred crustal scale flow system. The latter authors did not take into account possible interactions of the Lochseiten calc-mylonite with the footwall and hangingwall lithologies. Such interactions are, however, likely, since the vertical extent of the Lochseiten calc-mylonite is vanishingly small compared to its horizontal extent. At the thrust contacts, lithologies with strongly contrasting isotopic compositions were juxtaposed and are separated only by the thin Lochseiten calc-mylonite layer. As, in this geological context, the isotope composition of the calc-mylonite may well have been influenced by material transport in the direction perpendicular to the thrust as well as by fluid migration along the thrust, we here investigate such cross thrust transport components. We present petrographic as well as oxygen, carbon and strontium isotope data from two vertical profiles at the Grauberg and the Lochseite localities, respectively. These are among the southernmost (Grauberg) and northernmost (Lochseite) exposures of the thrust. In particular, we investigate the possible influence of cross thrust isotopic exchange on the isotopic composition of the Lochseiten calc-mylonite. This information is crucial for the interpretation of regional south to north oxygen isotope trends reported from the Lochseiten calc-mylonite by Burkhard and Kerrich (1990) and by Badertscher et al. (2001).

Geologic setting

Regional geology

The Glarus thrust is a major tectonic feature in the Helvetic Alps of eastern Switzerland (see figure 1a). It separates the Helvetic nappes in the hangingwall of the thrust from the Infrahelvetic units in the footwall. The Helvetic nappes are a series of thin skinned décollement nappes comprised of Permian to Eocene sediments. The Infrahelvetic units comprise a crystalline basement with its parautochthonous Mesozoic to Tertiary sedimentary cover and also include allochthonous slices of south-Helvetic (Blattengrat) and Penninic (Sardona) flysch. The latter units have been emplaced on the parautochthonous units (N-Helvetic flysch) during an Oligocene deformation phase, referred to as the "Pizol" phase (Pfiffner, 1977). The whole Infrahelvetic complex was penetratively folded during the Upper Oligocene "Calanda" phase. The thrusting event, referred to as the "Ruchi" phase occurred during the Early Miocene (Milnes and Pfiffner, 1980) and represents the youngest major deformation event in the eastern Helvetic Alps.

The Glarus thrust is exposed as an exceptionally sharp horizon over an area of about 600 square kilometers. The hangingwall is generally represented by the Verrucano formation, a clastic series of predominantly siltstones and shales with minor intercalations of conglomerates and volcanoclastic horizons. In the southernmost exposures, Verrucano is thrust over parautochthonous Late Jurassic to Early Cretaceous limestones. In the north, the footwall of the thrust is represented by an up to two kilometers thick sequence of N-Helvetic flysch primarily comprised of marly slates, sandstones and conglomerates. North of the Lochseiten locality the Glarus thrust plunges below topography. It is interpreted to merge with the basal Helvetic Säntis thrust (Schmid et al. 1996), where higher Helvetic nappes are thrust over Late Oligocene to Early Miocene Molasse. Balanced cross sections

indicate, that the Glarus thrust extends to mid crustal levels some 20 kilometers south of the southernmost exposures (Pfiffner, 1985). It may be rooted behind either one of the Aare-, Tavetsch-, and Gotthard crystalline massifs (e.g. Burkhard et al. 1992).

Metamorphic grade ranges from "anchizonal" (i.e. $\geq 200^{o}$C) in the north and in the footwall flysch to lower greenschist facies (i.e. 350^{o}C) in the south and in the hangingwall Verrucano. The "anchi/epi zone" boundary is offset along the Glarus thrust by about two kilometers due to post metamorphic thrusting (Rahn et al. 1995), and an inverse metamorphic gradient is documented across the thrust contact (Frey, 1988). The Glarus thrust probably developed at a crustal depth of 10 to 15 kilometers corresponding to lithostatic pressures of about 300 to 450 MPa. Metamorphism in the hangingwall Verrucano was dated by Hunziker et al. (1986) and Hunziker (1987) at 30 Ma. Concordant K/Ar and Rb/Sr ages of "illite" ($< 2\mu$m) from the Lochseite locality indicate that thrusting was active till at least 23 Ma.

The thrust contact at Grauberg

The Grauberg section is located about two kilometers northwest of Segnashütte (Swiss coordinates 736.250/192.700), at an elevation of 2300 meters above sea level. There, about five meters vertical section of footwall limestones, a 25 centimeter thick layer of Lochseiten calc-mylonite and over 100 meters vertical section of the hangingwall Verrucano are exposed. The footwall consists of Upper Jurassic to Lower Cretaceous massive grey limestones comprised of calcite (> 95vol%) and minor amounts of quartz and muscovite. A pronounced foliation dipping about 30 to 40^{o} SSE is ascribed to the pre-thrusting Calanda phase (Milnes and Pfiffner, 1980). In the uppermost meter below the thrust contact, this foliation is progressively rotated parallel to the thrust. Within this shear zone, the limestones are transformed to grey calc-mylonites with a planar millimeter scale

banding defined by the alternation of pure carbonate layers with more mica rich layers and by layer parallel calcite veins (see figure 2a). Within the mica rich layers dolomite occurs as a second carbonate phase. The H_2O and CO_2 contents of selected samples are shown in figure 3. The CO_2 content systematically decreases from close to 44 wt% to about 41 wt% within the uppermost two meters of the footwall limestones. At the same time, the water content increases from about 0.15 to 0.4 wt%.

A 25 centimeter thick yellowish calc-mylonite layer sandwiched between the grey footwall limestones and the hangingwall Verrucano represents the Lochseiten calc-mylonite. It shows a planar mylonitic banding defined by an alternation of calcite veins, a fine grained calcite matrix and stylolites comprised of muscovite. In the matrix the grain size is generally less than 5 μm, within veins, the calcites may be up to 100 μm in diameter. The CO_2 content of the calc-mylonite is between 38 and 41 wt% (see figure 3b) testifying to the presence of a significant fraction of silicate phases. The contact to the Verrucano is sharp.

The hangingwall Verrucano is primarily comprised of quartz, albite, muscovite, chlorite, and calcite. It has a mylonitic texture, where layers rich in albite and quartz alternate with muscovite-chlorite rich layers. It shows an intense thrust parallel foliation with frequent northward dipping shear bands indicating thrusting with top to the north. The bulk of the quartz-albite matrix is recrystallized at a grain size of generally less than 50 μm. At distances of more than two meters above the thrust, quartz and albite occasionally occur as up to one millimeter sized clasts. The bulk rock water content progressively increases from about 2 wt% at 20 meters above the thrust to 4.5 wt% at the calc-mylonite/Verrucano contact (see figure 3). The hangingwall Verrucano has a "background" carbonate content of about 5 to 10 wt% $CaCO_3$-equivalent. In the lowermost 10 centimeters of the Verrucano the carbonate content is significantly increased to about 20 wt% $CaCO_3$-equivalent (see

figure 3). Calcite usually occurs as late phase in fracture fillings. Locally ankerite is found as a second carbonate phase. It occurs as well crystallized idiomorphic grains in textural equilibrium with the mylonitic quartz-albite matrix. At distances of more than two meters above the thrust haematite and ilmenite are the dominating opaque phases. Towards the thrust, ilmenite is replaced by titanite and the main opaque phase is pyrite.

The thrust contact at Lochseite

The Lochseiten locality is situated some two kilometers east of the village of Schwanden at Swiss coordinates 725.860/206.400 at an elevation of 600 meters above sea level. There a vertical section of about one meter of footwall flysch, an about 50 centimeter thick layer of Lochseiten calc-mylonite and a 20 meter vertical section of the hangingwall Verrucano are exposed.

The footwall flysch is comprised of marly slates with shale layers alternating with impure sandstone layers on a millimeter scale. The common mineral assemblage is illite - chlorite - albite - quartz- calcite - organic material. Close to the strongly lobate-cuspate contact with the calc-mylonite the flysch is intensively folded and has a chaotic structure. Further down it shows a more regular slaty cleavage.

The about 50 centimeter thick layer of Lochseiten calc-mylonite is characterized by a high density of millimeter thick veins, which are intensely folded, refolded and disrupted. They give a "turbulent" appearance to the rock referred to as "knead structure" by Heim, (1921). A planar, thrust parallel brittle structure referred to as the "septum" crosscuts all internal structures. This feature has been interpreted as a cataclasite that formed during the last stages of thrusting (e.g. Funk et al. 1983).

The hangingwall Verrucano is comprised of massive siltstone and conglomerate horizons alternating with subordinate shale layers. The main constituents of Verrucano are quartz,

albite, muscovite, calcite, and chlorite. In the lowermost one to two meters above the thrust the Verrucano is partially mylonitized, and obtains a green colour. Further away from the thrust, the mylonitic foliation dies out and the rock obtains a reddish colour, which is characteristic for unaltered Verrucano from the northern section of the Glarus Alps. Quartz and albite clasts have a size of up to five millimeters at distances of more than 10 meters above the calc-mylonite/Verrucano contact. Towards the thrust, they are progressively transformed into fine-grained quartz-albite aggregates, and albite clasts show progressive alteration to sericite. The bulk rock water content increases from about 2.5 wt% at eight meters above the thrust to 4 wt% at the calc-mylonite/Verrucano contact (see figure 3). In the lowermost two meters above the thrust abundant fractures in quartz- and albite clasts are sealed with newly formed fibrous quartz, ankerite and calcite (see figure 2b). Newly formed quartz is also observed in pressure fringes around pyrite (see figure 2c). At distances of more than two meters above the thrust albite and quartz occur at about equal proportions. In the lowermost two meters above the thrust albite is significantly less abundant than quartz with molar albite to quartz ratios generally less than 0.15. As in the Grauberg rocks, calcite occurs as the prime carbonate phase in cracks and fissures. The "background" carbonate content is, however, only 1 to 5 wt% $CaCO_3$-equivalent (see figure 3). At the contact to the thrust, the carbonate content increases to about 10 wt% $CaCO_3$-equivalent.

Sampling and analytical methods

Sampling

Profiles across the Glarus thrust were sampled at the Grauberg- and the Lochseite localities. At Grauberg, samples were taken with a rock saw to ensure recovery of unweathered material. At the Lochseiten locality samples were taken with the permission of the "Direktion für Landwirtschaft, Wald und Umwelt" of the Kanton of Glarus. Due to natural heritage regulations, samples could only be taken with a hammer. Samples were taken at decimeter intervals in the first meter below and above the thrust contact and at metric intervals further away. An aliquot of 40 grams of each sample was crushed in a jaw crusher and ground to a powder with a grain size $< 40\mu$m in a tungsten carbide mill. Rock powders were used for bulk rock analyses and for mineral separation.

Stable isotope analyses

For stable isotope analysis of carbonates bulk rock powders with an equivalent 0.1 to 0.3 milligrams carbonate content were loaded into individual glass vials. CO_2 was extracted by reaction with 102% H_3PO_4 at 70°C for four minutes on a Finnigan Kiel II device. The CO_2 was analyzed on line with a Finnigan-MAT Delta^{plus} isotope ratio mass spectrometer. Reproducibility of replicate measurements was better than $0.1^o/_{oo}$ (1σ) for both δ^{18}O and δ^{13}C. In addition to bulk rock samples we analyzed carbonate microsamples taken with a dentist drill from polished rock surfaces.

Quartz-albite separates were obtained from the Verrucano samples by means of chemical purification techniques (Kiely and Jackson, 1964; Syers et al., 1968). For the analysis of quartz about 2 mg of quartz-albite concentrate were loaded into a nickel sample holder. Albite was removed quantitatively by fluorination in a BrF_5 atmosphere for 12 hours at

room temperature. The purity of the remaining quartz was routinely checked by XRD analysis. To test for possible influence of the purification procedure on the oxygen isotope composition of quartz, two standard quartz samples were run through an identical procedure as the samples. Oxygen isotope analysis showed no significant alteration of the ^{18}O values of quartz. As albite could not be separated from quartz, its oxygen isotope composition was determined from the oxygen isotope composition of quartz-albite mixtures with known albite/quartz ratios and the oxygen isotope composition of quartz. To minimize loss of albite pre-fluorination was done for 9 minutes only. The quartz/albite proportions of the samples after prefluorination were determined by XRD.

Oxygen was extracted from mineral separates on a laser fluorination line of the design described by Sharp (1990). Samples of one to two milligrams were reacted in a BrF_5 atmosphere under a slightly defocused 25 W CO_2 laser beam. The liberated oxygen was separated from excess reagent and reaction by-products cryogenically and by means of a 20 centimeter KBr column kept at 120^oC. O_2 was collected on a molecular sieve at liquid nitrogen temperatures and finally expanded into the variable volumes of a Finnigan Delta^{plus} isotope ratio mass spectrometer. UWG-2 garnet (Valley et al., 1995) was used as an internal standard. Reproducibility of replicate measurements was better than $0.15^o/_{oo}$ (1σ). Oxygen isotope compositions are given in the conventional δ-notation relative to V-SMOW.

Strontium isotope analyses

The $^{87}Sr/^{86}Sr$ ratios of the carbonate fraction of 20 selected samples were analyzed. The mechanical separation of the carbonate- and silicate fraction was impossible. To minimize contamination of the carbonate derived strontium by silicate derived strontium granulates with a grain size of 500 μm were used for acid leaching. The granulates were initially

treated with 2.5M HCl at room temperature. Strontium was isolated using standard ion exchange technique. The $^{87}Sr/^{86}Sr$ ratios were normalized to NBS-987 = 0.71022. Analytical precision was better than 0.000011 (2σ). Because of the young age of the tectonic activity along the Glarus thrust (Hunziker et al. 1986) age corrections for radiogenic strontium are negligible (Burkhard et al. 1992).

Determination of water- and carbonate contents

H_2O and CO_2 contents were determined on a Leco RC-412 elemental analyzer. The samples were roasted at 1000°C under excess oxygen. The H_2O and CO_2 gases produced were monitored simultaneously on infrared cells. Reproducibility of measurements was better than 0.04 wt% (1 σ) for both H_2O and CO_2.

Stable isotope data

^{18}O- and ^{13}C-variations across the thrust

The oxygen and carbon isotope compositions of carbonates from the two sampling profiles across the thrust contact at the Grauberg and Lochseite localities are shown in figure 4. At the Grauberg locality a smooth transition from relatively ^{18}O enriched compositions with δ^{18}O values of about 25 $^{o}/_{oo}$ relative to SMOW in the footwall carbonates to relatively ^{18}O depleted compositions of about 8.5 $^{o}/_{oo}$ in the hangingwall Verrucano is observed. At Lochseite, a similarly smooth transition from about 20 $^{o}/_{oo}$ in the footwall flysch to 17 $^{o}/_{oo}$ in the hangingwall Verrucano is documented.

There are two fundamental differences between the oxygen isotope profiles of Lochseite and Grauberg: Firstly, the oxygen isotope compositions of the footwall grey limestones of Grauberg are systematically depleted beginning about five meters below the thrust. In contrast, the uppermost flysch carbonate samples at Lochseite do not show any oxygen isotope alteration. Their δ^{18}O values are similar to the δ^{18}O values of carbonate from the unaltered flysch (18.5 to 20.5 $^{o}/_{oo}$ according to Burkhard and Kerrich, 1990; Badertscher et al. 2001). Secondly, above the thrust contact at Grauberg, the oxygen isotope compositions of calcite in Verrucano level out at about 8.5 $^{o}/_{oo}$ at a distance of 2.5 meters from the thrust. On the contrary, at Lochseite, the corresponding ^{18}O values gradually decrease from about 20 $^{o}/_{oo}$ at the calc-mylonite/Verrucano contact to 17 $^{o}/_{oo}$ at 20 meters above the thrust. The "background" composition of carbonates from the Verrucano is about 13 $^{o}/_{oo}$ as determined in samples from about 100 meters above the thrust (Badertscher et al. 2001). This composition is not attained in the first 20 meters above the thrust.

The carbon isotope compositions are δ^{13}C(PDB) $\approx 2^{o}/_{oo}$ in unaltered footwall rocks of both the Grauberg and Lochseite localities. At Grauberg, a steep systematic deple-

tion trend from $\delta^{13}C \approx 2^{o}/_{oo}$ at 25 cm below the calc-mylonite/Verrucano contact to $\delta^{13}C \approx -0.9^{o}/_{oo}$ at the contact is observed within the calc-mylonite. In the hangingwall Verrucano, this trend flattens and declines, and the $\delta^{13}C$ values level out at a composition of about -5 $^{o}/_{oo}$ at about 1.5 meters above the thrust contact. At Lochseite, a ^{13}C depletion trend is only observed within the Verrucano, where $\delta^{13}C$ values decrease from about 2 $^{o}/_{oo}$ at the calc-mylonite/Verrucano contact to a "background" composition of -6 $^{o}/_{oo}$ two meters above the thrust.

Small scale ^{18}O variations in the footwall limestones at Grauberg

The oxygen isotope compositions of the footwall limestone at Grauberg are shown in figure 5. Whereas the bulk carbonate samples define a relatively smooth ^{18}O trend, the oxygen isotope compositions of microsamples taken from veins and matrix may vary considerably on a small scale. The veins may be both depleted or enriched in ^{18}O relative to the bulk sample carbonate by up to 2 $^{o}/_{oo}$. Small scale oxygen isotope heterogeneities may be even more pronounced within the fine grained matrix. Relatively ^{18}O enriched layer parallel domains with $\delta^{18}O$ of 21 to 23 $^{o}/_{oo}$ alternate on a millimeter scale with more depleted domains, where $\delta^{18}O$ is between 11 and 13 $^{o}/_{oo}$ (see figure 5). Oxygen isotope gradients of about 10 $^{o}/_{oo}$ are documented over distances as small as two millimeters. The isotopically relatively "heavy" domains correspond to pure calcite layers. The relatively ^{18}O depleted domains coincide with layers, which contain abundant micas and dolomite grains.

Quartz-calcite oxygen isotope systematics

The oxygen isotope compositions of quartz, albite and calcite and the corresponding intermineral fractionations from the sampling profiles at Grauberg and Lochseite are shown in figure 6. At Grauberg, quartz shows a subtle trend of ^{18}O enrichment from about 11.5 $^{o}/_{oo}$ at more than 10 meters above the thrust to about 13.5 $^{o}/_{oo}$ at the calc-mylonite/Verrucano

contact. The concomitant ^{18}O enrichment in calcite is more pronounced, especially within the lowermost 50 centimeters of the Verrucano (see figure 6). As a consequence, the quartz-calcite fractionations decrease from about 4 $^{o}/_{oo}$ at 2.5 meters above the thrust to less than 2 $^{o}/_{oo}$ at the calc-mylonite/Verrucano contact.

At Lochseite, quartz shows a pronounced trend of ^{18}O enrichment from about 15 $^{o}/_{oo}$ at eight meters above the thrust, to about 23 $^{o}/_{oo}$ at the calc-mylonite/Verrucano contact (see figure 6). Albite shows a similar trend, which is less well established due to the absence of albite in the lowermost two meters above the thrust. The concomitant ^{18}O enrichment in calcite is less pronounced, and the quartz-calcite fractionations increase from about -2.5 $^{o}/_{oo}$ at more than two meters above the thrust to 3.5 $^{o}/_{oo}$ at the calc-mylonite/Verrucano contact (figure 6).

Strontium isotope data

The $^{87}Sr/^{86}Sr$ ratios of calcite analyzed in selected samples from the two vertical profiles at the Grauberg and the Lochseite localities are shown in figure 4. At Grauberg the $^{87}Sr/^{86}Sr$ values range from 0.708 in the footwall limestones to 0.716 in the hangingwall Verrucano with a smooth transition in a narrow zone along the thrust contact. The $^{87}Sr/^{86}Sr$ values of the footwall limestones are well within the range of the strontium isotope ratios typical for marine carbonates of Mesozoic to Early Miocene age (0.707 to 0.7089 according to DePaolo, 1986; Burke et al. 1992). The $^{87}Sr/^{86}Sr$ values of the Verrucano samples are similar to those obtained by Hunziker et al. (1986) (0.7136 to 0.7211 at 30 to 20 Ma). The transition between these two strontium reservoirs is confined to a narrow zone ranging from about 25 centimeters below to about 15 centimeters above the calc-mylonite/Verrucano contact. The $^{87}Sr/^{86}Sr$ gradient is steepest within the Lochseiten calc-mylonite where the $^{87}Sr/^{86}Sr$ are 0.710 at the contact to the footwall carbonates and 0.714 at the contact to

the Verrucano. A small but readily detectable shift in the $^{87}Sr/^{86}Sr$ values from 0.7148 to 0.7158 is identified in the lowermost 15 centimeters of the hangingwall Verrucano.

At the Lochseite locality the $^{87}Sr/^{86}Sr$ values of calcite vary from 0.709 in the footwall flysch to 0.714 in the Verrucano. The flysch values agree well with the range of 0.7089 to 0.713 given by Hunziker et al. (1986) for the carbonate fraction of low grade metasediments of the Infrahelvetic complex. There is a smooth transition between the Verrucano and flysch strontium reservoirs. In contrast to the Grauberg profile, at Lochseite most of the strontium isotope variation occurs within the hangingwall Verrucano. Within the Verrucano the $^{87}Sr/^{86}Sr$ ratios range from 0.710 at the calc-mylonite/Verrucano contact to 0.714 at 3.5 meters above the thrust. The Lochseite calc-mylonite shows $^{87}Sr/^{86}Sr$ ratios of 0.710 with only minor internal variation (also compare Burkhard et al. 1992).

Discussion

Mineralogical changes associated with thrusting

In the unaltered hangingwall Verrucano of both localities the major minerals are quartz, oligoclase, potassium feldspar, muscovite and chlorite with some biotite and calcite. As the thrust is approached from some 50 meters distance, albite, quartz, chlorite and muscovite/illite gradually become the dominant silicate phases and the bulk rock water content increases from about two up to about five weight percent (see figure 3). This suggests that hydration reactions occurred near the thrust that led to the replacement of oligoclase, potassium feldspar and biotite by albite, quartz, sericite, and chlorite. Assuming that aluminum was conserved the corresponding reactions may be written as:

$$3\,KAlSi_3O_8 + 12\,H_2O + 2\,H^+ = KAl_3Si_3O_{10}(OH)_2 + 2\,K^+ + 6\,H_4SiO_4$$

$$3\,CaAl_2Si_2O_8 + 2\,H_2O + 2\,K^+ = 2\,KAl_3Si_3O_{10}(OH)_2 + 3\,Ca^{2+}$$

$$2\,KMg_3AlSi_3O_{10}(OH)_2 + 6\,H_2O + 4\,H^+ = Mg_5Al_2Si_3O_{10}(OH)_8 + 3\,H_4SiO_4 + 2\,K^+ + Mg^{2+}$$

Newly formed sericite and chlorite are frequently found as fracture fillings and in pressure shadows of rigid objects (also compare Arkai et al. 1997). The liberated silica was precipitated as quartz, whose syntectonic growth is well documented for the lowermost two meters of Verrucano by fibrous aggregates in fractures and in pressure fringes (see figures 2b,c). At Grauberg, the occurrence of partially syntectonically grown dolomite along stylolites and mica rich layers in the uppermost meter of the footwall limestone suggests introduction of magnesium bearing species that were probably derived from the biotite to chlorite transformation in the hangingwall Verrucano.

The fact that the carbonate content of unaltered Verrucano is relatively constant and

does not show any systematic variation with distance from the thrust suggests that it is due to pre thrusting diagenetic and metamorphic processes. The occurrence of calcite as fracture fillings indicates that it was remobilized and recrystallized during deformation. Syntectonic calcite metasomatism in the Verrucano due to the introduction of Ca- and carbonate bearing species from the footwall was restricted to the lowermost 10 centimeters above the thrust (compare also Burkhard and Kerrich, 1990).

In the footwall limestone and in the calc-mylonite material transfer in the course of ongoing dissolution and precipitation is suggested by abundant stylolites and veins. A net decrease of the carbonate content in the uppermost meter towards the thrust contact at Grauberg (Figure 3) suggests a net carbonate loss in the course of this process.

Oxygen- and carbon isotope profiles across the thrust

The isotopically contrasting footwall and hangingwall lithologies are regarded as two distinct carbon and oxygen reservoirs, which may exchange material by diffusive/dispersive and advective transport in the pore fluid. The oxygen- and carbon isotope transitions at both the Grauberg and Lochseite localities are characterized by monotonic enrichment/depletion trends across the thrust and are interpreted as isotopic fronts. The isotopic composition of the calc-mylonite is never outside the range between the compositions of the footwall and hangingwall lithologies in neither of the three isotope systems investigated.

The propagation of a reactive tracer isotope in a one-dimensional system, where transport occurs by diffusion/dispersion in the pore fluid and by fluid advection, may be represented by (e.g. Bear, 1972):

$$D\frac{\partial^2 R_f}{\partial x^2} - v\frac{\partial R_f}{\partial x} = \frac{\partial R_f}{\partial t} + \sum_{k=1}^{M} \frac{X_k}{X_f}\frac{\partial R_k}{\partial t}, \qquad (1)$$

where R_f and R_k are the isotopic compositions of the pore fluid and of mineral k. x

and t are distance and time, D and v are the effective diffusion/dispersion coefficient of the isotopic species and the mean interstitial particle velocity. X_k and X_f are the mole fractions of the isotopic element contained in mineral k and in the fluid, respectively.

Oxygen and carbon isotope fronts at the Lochseite locality

The fact that the footwall flysch does not show any sign of isotopic alteration at the Lochseite locality suggests that upward material transport was particularly efficient within this lithology. As a consequence the isotopic composition at the calc-mylonite/Verrucano contact was largely buffered by the pore fluid of the flysch. For this situation the initial and boundary conditions may be stated as:

$$\begin{aligned} R_f &= R_f^h \quad at\ t = 0 \quad for\ x > 0 \\ R_f &= R_f^f \quad for\ t > 0 \quad at\ x = 0, \end{aligned} \tag{2}$$

where R_f^h is the isotopic composition of the pore fluid in equilibrium with the unaltered hangingwall Verrucano and R_f^f is the isotopic composition of the fluid infiltrating from the footwall. Provided local isotopic equilibrium is maintained during alteration, the solution to equation 1 subject to the initial and boundary conditions in equation 2 is given by (e.g. Lapidus and Amundson, 1952):

$$R_f(x,t) = R_f^h + 0.5(R_f^f - R_f^h)\left(1 + F(x,t) + e^{\frac{v\,x}{D}}\,G(x,t)\right), \tag{3}$$

with

$$\begin{aligned} F(x,t) &= erf\left(\frac{v\sqrt{t}}{2\sqrt{D}} - \frac{x}{2\sqrt{Dt}}\right) \\ G(x,t) &= erfc\left(\frac{v\sqrt{t}}{2\sqrt{D}} + \frac{x}{2\sqrt{Dt}}\right) \end{aligned} \tag{4}$$

The relevant transport parameters, namely $\sqrt{D \cdot t}$ and $(v \cdot t)$ that may explain the oxygen and carbon isotope pattern at the Lochseite locality were obtained by minimizing the variance, σ^2, of the model predictions with respect to the observational data[4]:

$$\sigma^2 = \sum_N \frac{(R^{obs} - R^{mod})^2}{N}, \tag{5}$$

where R^{obs} and R^{mod} are the observed and modeled isotopic compositions and the sum is over N observations. The corresponding model curves are shown in figure 7. The transport parameters obtained are $\sqrt{D^O \cdot t} = 0.70$ m and $v^O \cdot t = 1.63\ m$ for oxygen and $\sqrt{D^C \cdot t} = 0.53$ m and $v^C \cdot t = 1.42\ m$ for carbon[5].

To obtain time integrated volumetric fluxes the retardation of the tracer front with respect to the physical infiltration front must be considered. Provided that local equilibrium is maintained, the retardation factor, R_d, may be expressed as (e.g. Abart and Pozzorini, 2000):

$$R_d = \left(1 + \sum_{k=1}^{M} \frac{X_k}{X_f} \alpha_k\right), \tag{6}$$

where α_k is the equilibrium fractionation factor for isotopic exchange between mineral k and the pore fluid. R_d may be expressed as a function of the volumetric porosity ϕ:

$$R_d = \left(1 + \frac{1-\phi}{\phi} \kappa\right), \tag{7}$$

with

[4] $\sqrt{D \cdot t}$ has dimensions of length and is usually referred to as the characteristic length of diffusion.
[5] Upwards directed flow has a positive, downwards directed flow a negative sign.

$$\kappa = \frac{n^{\epsilon}_{rock}\bar{v}_{fluid}}{n^{\epsilon}_{fluid}\bar{v}_{rock}} \cdot \alpha_k, \tag{8}$$

and n^{ϵ}_{rock} and n^{ϵ}_{fluid} are the numbers of moles of the isotopic element ϵ per mole of rock and fluid and $\bar{v}_{rock}$ and $\bar{v}_{fluid}$ are the corresponding molar volumes. For small porosities the retardation factor may be approximated by:

$$R_d \approx \frac{\kappa}{\phi}. \tag{9}$$

The time integrated volumetric fluid flux, $TIFF$ is related to $(v \cdot t)$ by:

$$TIFF = (v \cdot t) \cdot \phi, \tag{10}$$

scaling for the retardation using equation 9 yields:

$$TIFF = (v \cdot t) \cdot \kappa. \tag{11}$$

Since α_k is close to unity, κ is merely a function of the fluid/solid partitioning of the isotopic element (see equation 8). The carbon and oxygen contents and molar volumes of the relevant rock forming minerals and possible pore fluids are given in table 1. The fluid/solid partitioning estimated for the different rock types are given in table 2.

The effective fluid/solid partitioning and the extent of retardation will be diminished, if some minerals of a rock fail to react in exchange equilibrium with the pore fluid (e.g. Abart and Pozzorini, 2000). Kinetically controlled mineral-fluid exchange is indicated by the systematics of the inter-mineral fractionations in the Verrucano from the Lochseite locality. At 220°C, the quartz-calcite oxygen isotope fractionation is 2.06 (Matthews et al. 1983) to 3.87 $^{o}/_{oo}$ (Chiba et al. 1989), depending on the calibration used. The fact that at Lochseite the quartz-calcite oxygen isotope fractionation is reversed at distances

of more than about one meter above the thrust indicates departure from equilibrium. At Lochseite, the calcite-albite oxygen isotope fractionations vary between 3 and $6^o/_{oo}$. They are generally larger than the calcite-albite equilibrium fractionation, which is predicted to be 1.14 (Zheng, 1993) to $2.30^o/_{oo}$ (Chiba et al. 1989) at 220°C. At distances of more than one meter above the thrust, calcite is too isotopically enriched to be in oxygen isotope equilibrium with quartz and albite. In the course of recrystallization during thrusting calcite attained isotopic equilibrium with the local pore fluid. At distances of more than about two meters above the thrust, oxygen isotope exchange between quartz and albite and the fluid was insignificant and quartz and albite preserved their original (pre-thrusting) oxygen isotope compositions. Only within the lowermost one to two meters above the thrust, they were both shifted to higher ^{18}O values. Textural forms such as fibrous quartz in pressure fringes and as fracture fillings (see figure 2b,c) suggest that oxygen isotope exchange was facilitated by syntectonic, stress induced recrystallization within this zone of the Verrucano. However, these recrystallization effects quickly die out upwards after about one meter. The effect of varying rates of mineral fluid exchange may be considered in a semiquantitative way by accounting for the presence of slow exchanging phases in the calculation of the fluid-solid partitioning. In table 2 the κ^O factors for the Lochseite Verrucano are given for three different scenarios regarding the mineral-fluid exchange rates. In the "local equilibrium" scenario all minerals are regarded to be in oxygen isotope equilibrium with the pore fluid. Although not justified in light of the systematics of the inter-mineral fractionations, this scenario may be considered as a conservative maximum estimate of the κ^O factors. In the "inert quartz and albite" scenario all phases except for quartz and albite were assumed to be in exchange equilibrium with the local pore fluid. This is considered as the most realistic scenario, because a significant fraction of muscovite (illite) and chlorite was newly formed and calcite was remobilized during

thrusting and most likely attained oxygen isotope equilibrium with the pore fluid. The "only calcite reactive" scenario treats all phases except for calcite as inert with respect to oxygen isotope exchange. This scenario yields minimum estimates for the κ^O factors.

Considering the entire range of feasible fluid/solid oxygen partitioning, the corresponding κ^O factors may vary from 0.08 to 1.60 at the Lochseite Locality (see table 2). The corresponding time integrated, upwards directed volumetric fluid fluxes are 0.13 to 2.6 m^3/m^2. Given the fact that time integrated fluid fluxes derived from the oxygen- and carbon isotope fronts must be the same suggests that $\kappa^O/\kappa^C \approx (v^C \cdot t)/(v^O \cdot t) = 0.87$. For the local equilibrium scenario and for the "quartz-albite inert" scenario, this corresponds to fluid compositions with $0.005 < X_{CO_2} < 0.05$, and the corresponding time integrated volumetric flux is 1.0 to 2.6 m^3/m^2. The corrected $\sqrt{D \cdot t}$ parameters are 0.55 to 0.9 m for oxygen and 0.39 to 1.2 m for carbon.

Oxygen and carbon isotope fronts at the Grauberg locality

At Grauberg, both the footwall and the hangingwall rocks are isotopically altered. A fixed concentration boundary condition is thus not applicable and mass transport must be modeled explicitly in both the Verrucano and in the footwall limestones. The initial and boundary conditions may be stated as:

$$\begin{aligned} R_f = R_f^h \; for \; x > 0, \quad R_f = R_f^f \; for \; x < 0 \quad at \; t = 0 \\ R_f = R_f^h \; for x = \infty, \quad R_f = R_f^f \; for x = -\infty \quad at \; t > 0 \end{aligned} \tag{12}$$

Uniform flow model: One possibility to model material transport at Grauberg is then to consider diffusion/dispersion and fluid advection across the thrust contact, and to treat

effective diffusivities and fluid flow velocities as being uniform throughout the system (uniform flow model of Bickle and Baker, 1990). For this model, equation 1 may be reduced to a pure diffusion equation by transforming the x-coordinate to account for the displacement of the tracer front by fluid advection. If the new space coordinate is taken as $x + vt$, the solution to equation 1 as subject to the initial and boundary conditions in equations 12 is given by (e.g. Crank, 1975, eq. 2.14):

$$R_f(x,t) = R_f^f + 0.5(R_f^f - R_f^h) \cdot erfc\left(\frac{x+vt}{2\sqrt{Dt}}\right) \tag{13}$$

The curves obtained from fitting this model to the isotope data from Grauberg are shown in figure 7. The transport parameters obtained are $\sqrt{D^O \cdot t} = 2.6$ m and $v^O \cdot t = -3.8\ m$ for oxygen and $\sqrt{D^C \cdot t} = 0.17$ m and $v^C \cdot t = 0.08\ m$ for carbon.

For the footwall carbonates the fluid/solid partitioning was calculated assuming local isotopic equilibrium (see table 2). Even if mineral-fluid oxygen isotope exchange may have been kinetically controlled for quartz and muscovite, this would have but a negligible effect on the fluid/solid partitioning due to the small amount of quartz and muscovite present. Burkhard et al. (1992) presented oxygen isotope data for albite, chlorite, and muscovite from the hangingwall Verrucano of the Grauberg locality that indicate that all phases except for quartz were in exchange equilibrium during thrusting. The quartz-calcite inter-mineral fractionations show a systematic decrease towards the thrust. This indicates that quartz-fluid oxygen isotope exchange was slow compared to the exchange of the other minerals. This is why a "local equilibrium" and an "inert quartz" scenario are considered for the Verrucano at Grauberg (see table 2).

In the uniform flow model the effective retarded diffusivities/dispersivities and effective retarded fluid flow velocities are regarded as constant throughout the system. For a given

fluid composition, the carbon fluid/solid partitioning is smaller in the footwall than in the hangingwall (see table 2). Thus the retardation of a carbon isotope front with respect to the physical infiltration front will be larger in the footwall than in the hangingwall. This is incompatible with the model assumption of constant retarded effective diffusivities and retarded fluid flow velocities as inherent in the uniform flow model. Therefore only the oxygen isotope front may be interpreted in the framework of this model. Regardless of the fluid composition the κ^O factor is about 1.6 and the downward directed time integrated fluid flux is estimated at 6.1 m^3/m^2. The corresponding corrected $\sqrt{D^O \cdot t}$ parameter is 3.3 m.

Diffusion/dispersion in a composite system: In an alternative model, the fronts at Grauberg may be interpreted as being due to diffusive/dispersive isotope exchange between footwall and hangingwall, whereby the effective diffusivities/dispersivities are considered to be different in the two lithologies. For the initial and boundary conditions stated in equations 12 the solution for this model is given by (e.g. Crank, 1975):

$$\begin{aligned} R_f^h(x,t) &= \frac{1}{1+\sqrt{D_f/D_h}}\left(1+\sqrt{D_f/D_h}\, erf(\frac{x}{2\sqrt{D_h t}}\right) \quad footwall \\ R_f^f(x,t) &= \frac{1}{1+\sqrt{D_f/D_h}}\, erfc(\frac{\|x\|}{2\sqrt{D_f t}} \quad hangingwall \end{aligned} \tag{14}$$

D_f and D_h are the effective diffusivities/dispersivities in the footwall and hangingwall, respectively. The corresponding model curves are shown in figure 7. The transport parameters obtained are $\sqrt{D_h^O \cdot t} = 45.6$ m and $\sqrt{D_f^O \cdot t} = 4.1$ m for oxygen and $\sqrt{D_h^C \cdot t} = 0.14$ m and $\sqrt{D_f^C \cdot t} = 0.1$ m. The $\sqrt{D^O \cdot t}$ parameters corrected for the fluid/solid oxygen partitioning are 5.2 m for oxygen diffusion/dispersion in the footwall carbonates and 50 to 57.6

m for oxygen diffusion/dispersion in the hangingwall Verrucano. Given that the effective diffusivity is on the same order of magnitude for carbon and oxygen bearing species in an aqueous fluid, the $\sqrt{D \cdot t}$ parameters obtained from the oxygen- and carbon fronts should be comparable. For the footwall carbonates, the relation $\kappa^O/\kappa^C \approx (D^C \cdot t)/(D^O \cdot t) = 1/1720$ indicates very low carbon contents of the infiltrating fluid with $0 < X_{CO_2} < 0.005$ (see table 2). The corrected $\sqrt{D^C \cdot t}$ parameter is hence > 0.96 m in the footwall and, provided that X_{CO_2} was uniform throughout the system, $\sqrt{D^C \cdot t} > 0.3$ m in the hangingwall. Even if no advection in the direction perpendicular to the thrust contact is allowed in this model, it indicates, that material transport was significantly more efficient in the hangingwall Verrucano than in the footwall limestones. The Verrucano again probably acted as a source of isotopically light oxygen that caused alteration of the footwall limestone.

Effective diffusivities/dispersivities

Effective oxygen diffusivities calculated from $\sqrt{D^O \cdot t}$ for geologically meaningful time scales are given in table 3. The effective diffusivity of a species in the pore fluid of a porous medium is related to the diffusivity of the same species in the free fluid, D_0, by:

$$D = \tau \phi D_0, \tag{15}$$

where τ is the tortuosity of the porous medium. The experimentally determined diffusivity of the H_2O species in water is about $5 * 10^{-8} m^2/s$ at 250°C (Frank et al. 1996). In geologic materials the porosity may vary considerably from about 10^{-4} to 10^{-2} The tortuosity may vary between 0.1 and ≤ 1. If ϕ were 10^{-2} and τ were 0.1, an effective diffusivity of $5 * 10^{-11} m^2/s$, and if ϕ were 10^{-4} and τ were 0.1, an effective diffusivity of $7.3 * 10^{-13} m^2/s$ would be calculated from the experimental data. Comparison with the values obtained from curve fitting (see table 3) shows that molecular diffusion of H_2O in the pore fluid

may well explain the inferred diffusive/dispersive contribution to oxygen transport at the Lochseite and Grauberg localities even for the short time scenario. Only the rates of diffusion/dispersion as derived from the composite medium model for the hangingwall Verrucano at Grauberg is too fast to be explained by molecular diffusion of H_2O in the pore fluid. In this case the contribution of hydrodynamic dispersion may explain the enhancement of diffusion/dispersion. As there is no advective flow component allowed in the direction perpendicular to the thrust surface in this model, this is interpreted as transversal dispersion associated with thrust parallel flow.

Strontium isotope variations

The Sr-isotope profiles from the Grauberg and Lochseite localities qualitatively show the same features as the carbon- and oxygen isotope patterns. At both localities the $^{87}Sr/^{86}Sr$ ratios show a monotonic enrichment/depletion trend across the thrust. No local $^{87}Sr/^{86}Sr$ minima/maxima at the thrust surface that would testify to the introduction of externally derived strontium by flow along the thrust could be identified. The observed patterns may be explained by strontium exchange between the more radiogenic strontium reservoir of the hangingwall and the less radiogenic strontium reservoir of the footwall lithologies. The major difference between the two profiles is that at Grauberg most of the alteration occurs below the thrust contact, whereas at Lochseite most of the alteration occurs in the hangingwall.

The fact that at Grauberg the Sr-isotope values at the thrust contact (0.714) are closer to the presumed background values of the Verrucano (0.7136 to 0.7211; Hunziker et al. 1986) than to the presumed background composition of the footwall carbonates (0.707 to 0.7089; DePaolo, 1986; Burke et al. 1992) and that the strontium isotope alteration is more pronounced in the footwall limestones suggests net strontium transfer form the

hangingwall to the footwall.

At Lochseite the strontium isotope values at the calc-mylonite/Verrucano contact (0.710) are closer to the presumed "background" compositions of the footwall flysch (0.7089 to 0.713; Hunziker et al. 1986) than to the presumed strontium isotope compositions of the Verrucano, and strontium isotope alteration is essentially confined to the hangingwall. This indicates upwards directed strontium transfer across the thrust. The fact that the Lochseiten calc-mylonite is practically identical to the flysch with respect to its $^{87}Sr/^{86}Sr$ ratios is compatible with a derivation of its carbonate matrix from the footwall flysch. The veined nature of the calc-mylonite and its relatively constant $^{87}Sr/^{86}Sr$ ratios (0.7096 to 0.7103; Burkhard et al. 1992) suggest precipitation from a flysch derived strontium bearing fluid.

Fluid regimes at the Glarus thrust

A qualitative model of the regional flow pattern associated with the active Glarus thrust is illustrated in figure 8. Mineralogical alteration such as the carbonatization of the lowermost 10 to 20 centimeters of the hangingwall Verrucano and the partial dolomitization of the uppermost footwall limestones at Grauberg as well as the oxygen, carbon and strontium isotope patterns in the two vertical profiles at the Grauberg and Lochseite localities give unambiguous evidence of material transport across the thrust. With respect to the vertical transport components, the southern section of the Glarus thrust, where the footwall is represented by Mesozoic limestones, behaved fundamentally different from the northern section, where the footwall is represented by Tertiary flysch. Both the uniform flow model and the composite medium model suggest that, at the Grauberg locality in the south, net mass transport was from the hangingwall Verrucano into the footwall limestones. In contrast, the front geometries at the Lochseite locality in the north indicate

net transport from the footwall flysch into the hangingwall Verrucano. As a consequence, the oxygen isotope composition at the calc-mylonite/Verrucano contact, and, in particular, the composition of the Lochseiten calc-mylonite, was buffered towards the Verrucano composition in the south and towards the flysch composition in the north (see inserts in figure 8). The position of the regional scale oxygen isotope front postulated by Burkhard and Kerrich (1990), Bowman et al. (1994) and more recently by Badertscher et al. (2001) for along thrust flow approximately coincides with the lithologic boundary between Mesozoic limestone and Tertiary flysch in the footwall of the thrust (see figure 1b). In the light of the vertical transport components shown by the cross thrust oxygen, carbon and strontium isotope profiles we suggest that the regional south to north ^{18}O enrichment trend was simulated by cross thrust transport.

At the Lochseite locality the water required for the observed hydration of the lowermost Verrucano may be locally derived from the underlying flysch. This is corroborated by upwards directed flow as inferred from the stable and strontium isotope patterns at Lochseite. Dewatering of the flysch during regional low grade metamorphism involving the illite to muscovite transition and compaction during thrusting are likely scenarios that may explain upwards migration of flysch derived fluids. In contrast, at the Grauberg locality there is no obvious local water source nor any isotopic indication for upwards directed flow. There the water required for the observed hydration of the bottom of the Verrucano was probably introduced by flow along the thrust. If externally derived fluids indeed migrated along the thrust, then the contrasting effective oxygen diffusivities/dispersivities in the footwall and hangingwall derived from the "composite medium model" indicate that thrust parallel flow primarily occurred within the Verrucano. A minimum estimate for the horizontal flow component may be derived from the fact that the bulk rock water content of Verrucano increased by about two weight percent (see figure 3). Given that the density

of Verrucano is approximately 2700 kg/m^3 this corresponds to an introduction of about 54 kg or 0.06 m^3 H_2O per m^3 of rock. In a south to north cross section, the portion of the Glarus thrust with Mesozoic limestone in the footwall is exposed over a distance of about four kilometers. Based on the assumption, that the hydration of hangingwall Verrucano occurred at local fluid-rock equilibrium and that it is exclusively due to the northwards migration of aqueous fluids along the thrust, a horizontal flux on the order of 240 m^3/m^2 is derived[6].

The isotopic alteration of the footwall in the southern section of the thrust may be interpreted as "lateral" fronts that developed by diffusive/dispersive exchange between footwall and hangingwall and possibly by a small vertical flow component due to lateral seepage from the Verrucano aquifer into the relatively less permeable footwall limestones. Pronounced small scale oxygen isotope variations in the footwall limestones (see figure 5) indicate a heterogeneous permeability structure. Transport along discrete high permeability structures contributed to transversal hydrodynamic dispersion. The isotopic and chemical alteration of the lowermost Verrucano at Grauberg are interpreted as a result of such transversal dispersion. Due to the low X_{CO_2} of the pore fluid, carbon isotope alteration is restricted to the uppermost 50 centimeters of the footwall limestones.

In the north, where the footwall is represented by Tertiary flysch, along thrust flow was probably deflected upwards by fluids ascending form the flysch. The Verrucano appears to have been less permeable to upwards directed flow than the footwall lithologies. Ascending fluids in the flysch were ponded below the Verrucano leading to near lithostatic fluid pressures at the thrust. This provoked brittle failure, minimized normal stress and facilitated motion along the thrust (Price, 1988).

[6] This estimate is about one order of magnitude lower than integrated fluxes derived from the regional south to north ^{18}O enrichment trend of calcites from the Lochseiten mylonite by Bowman et al. (1994) and by Badertscher et al. (2001).

The Lochseiten calc-mylonite has been interpreted as an extremely smeared out infra-helvetic limestone (Schmid, 1975). Alternatively it has been regarded as a secondary mineralization of the thrust surface (Rothpletz, 1883; Burkhard and Kerrich, 1990). At the Lochseiten locality, the Lochseiten calc-mylonite is characterized by an extremely high density of calcite veins, and it is in carbon, oxygen and strontium isotope equilibrium with the underlying flysch. Therefore at Lochseite we concur with a significant contribution to the carbonate content of the Lochseiten calc-mylonite by secondary "hydrothermal" calcite precipitation. The carbonate was probably introduced into the thrust surface via the pore fluid migrating upwards from the calcite saturated footwall flysch. The solubility of calcite was probably controlled by the reaction :

$$CaCO_3 + CO_2 + H_2O = Ca^{2+} + 2\,HCO_3^-$$

In a low salinity aqueous solution the solubility of calcite decreases with decreasing CO_2 partial pressure and with increasing temperature (e.g. Rimstidt, 1997). An increase in metamorphic grade from the footwall to the hangingwall has been documented by Frey (1988). A sharp temperature step at the thrust surface is, however, unlikely. The pronounced localization of calcite vein formation within the thrust plane is probably due to syn-tectonic pressure perturbations. Thrusting probably occurred by an alternation of brittle and ductile mechanisms (Badertscher and Burkhard, 2001). Fracturing that occurred in episodes of relatively high, close to lithostatic fluid pressure may have caused short time pore-pressure reductions. During such events CO_2 may have unmixed from the pore fluid leaving behind an aqueous solution supersaturated with respect to calcite. Subsequent calcite precipitation in veins and fractures gave the Lochseiten calc-mylonite its veined nature.

Summary and Conclusions

The ^{18}O, ^{13}C and $^{87}Sr/^{86}Sr$ variations along two vertical profiles across the Glarus thrust at the Grauberg locality in the south and at the Lochseiten locality in the north reveal fundamentally different flow regimes during deformation. In the southern section of the thrust, where the footwall is represented by Mesozoic limestones, net material transport across the thrust was directed downwards. In the northern section of the thrust, where the footwall is represented by Tertiary flysch, net material transport across the thrust was directed upwards. In the southern section of the thrust a horizontal flow component is inferred from the hydration of the lowermost ten to twenty meters of the hanging-wall Verrucano. In the south horizontal flow mainly occurred within the Verrucano, and the isotopic alteration of the footwall carbonates is ascribed to transversal hydrodynamic dispersion associated with horizontal flow and/or to lateral seepage from the Verrucano aquifer into the footwall lithologies. If at all present in the north, horizontal flow was deflected upwards by fluids ascending from the dewatering and compacting flysch. Even if the vertical components of flow were at least two orders of magnitude smaller than horizontal flow, material transport across the thrust was sufficient to largely control the ^{18}O signature of the Lochseiten calc-mylonite. The "apparent one-dimensional front geometry" of the regional south to north ^{18}O enrichment trend in the Lochseiten calc-mylonite may largely be explained by the differences in the vertical flow components in the southern and northern sections of the thrust. In the south downwards directed material transfer lead to the imprint of the Verrucano isotopic signature on the Lochseiten calc-mylonite. In the north upwards directed material transfer lead to the imprint of the flysch isotopic signature on the Lochseiten calc-mylonite. In the south the calc-mylonite at the thrust surface is largely derived from the underlying Mesozoic carbonates, only a small fraction is represented by "secondary" calcite precipitates. In the north the Lochseiten calc-mylonite

supposedly has obtained a significant fraction of its carbonate content by precipitation of calcite from ascending fluids in chemical and isotopic equilibrium with the footwall flysch.

Acknowledgements

This manuscript greatly benefited from perceptive reviews by P. Blattner, A. Skelton and S. Schmid. We want to thank H. Eppel and T. Widmer for their help in field and laboratory work. Financial support by the Austrian National Bank "Jubiläumsfonds" grant 7133 is gratefully acknowledged.

References

Abart, R. & Pozzorini, D. (2000): Implications of kinetically controlled mineral-fluid exchange on the geometry of stable isotope fronts. Europ. Journ. Mineral., **12**, Eur. J. Mineral., **12**, 1069-1082.

Abart, R., Sperb, R. (1997): Grain-scale stable isotope disequilibrium during fluid-rock interaction I: analytical solutions for advective-dispersive transport and coupled first-order kinetic mineral-fluid exchange. Am. J. Sci., **297**, 679-706.

Arkai, P., Balogh, K., Frey, M. (1997): The effects of tectonic strain on crystallinity, apparent mean crystallite size and lattice strain of phyllosilicates in low-temperature matamorphic rocks. A case study from the Glarus overthrust, Switzerland. Schweiz. Min. Petrogr. Mitt., **77**, 27-40.

Badertscher, N. & Burkhard, M. (2001): The role of fluids in thrusting of the Helvetic Glarus overthrust. in press.

Badertscher, N., Abart, R. and Burkhard, M. (2001): Fluid flow pathways along the Glarus overthrust derived from stable and Sr-isotope patterns. in review.

Baumgartner, L. & Rumble III, D. (1988): Transport of stable isotopes: I: development of a kinetic continuum theory for stable isotope transport. Contrib. Mineral. Petrol., Vol. 98, 417-430.

Bear, J. (1972): Dynamics of fluids in porose media. Elsevier, 764 p.

Bickle, M. (1992): Transport mechanisms by fluid-flow in metamorphic rocks: oxygen and strontium decoupling in the Trois Segneurs Massif - a consequence of kinetic dispersion. Am. Journ. Science, Vol. 292, 289-316.

Bickle, M. & Baker, J. (1990): Advective-diffusive transport of isotopic fronts: an example from Naxos, Greece. Earth and Planetary Science Letters, Vol. 97, 78-93.

Bickle, M. & McKenzie (1987): The transport of heat and matter by fluids during metamorphism. Contrib. Mineral. Petrol., Vol. 95, 384-392.

Bowman, J.R., Willett, S.D., Cook, S.J. (1994): Oxygen isotopic transport and exchange during fluid flow: One-dimensional models and applications. Am. J. Sci., **294**, 1-55.

Burke, W.H. Denison, R.E., Hetherington, E.A., Koepnik, R.B., Nelson, H.F., Otto, J.B. (1982): Variation of seawater $^{87}Sr/^{86}Sr$ throughout Phanerozoic time. Geology, **10**, 516-519.

Burkhard, M. Kerrich, R. (1988): Fluid regimes in the deformation of the Helvetic nappes, Switzerland, as inferred from stable isotope data. Contrib. Mineral. Petrol., **112**, 293-311.

Burkhard, M. Kerrich, R. (1990): Fluid-rock interactions during thrusting of the Glarus nappe - evidence from geochemical and stable isotope data. Schweiz. min. Petrogt. Mitt., **70**, 77-82.

Burkhard, M. Kerrich, R. Fyfe, W.S. (1992): Stable and Sr-isotope evidence for fluid advection during thrusting of the Glarus nappe (Swiss Alps). Contrib. Mineral. Petrol., Vol. 112, 293-311.

Chiba, H., Chacko, T., Clayton, R.N., Goldsmith, J.R. (1989): Oxygen isotope fractionations involving diopside, forsterite, magnetite and calcite: application to geothermometry. Geochim. Cosmochim. Acta, **53**, 2985-2995.

Cox, S.F., Etheridge, M.A., Wall, V.I. (1986): The role of fluids in syntectonic mass

transport, and the localization of metamorphic vein-type ore deposits. Ore Geology Rev., **2**, 63-86.

Crank, J. (1975): The Mathematics of Diffusion. Oxford, Clarendon press, 347 p.

Crespo, B.A., Masson, H., Sharp, Z.D., Cosca, M., Hunziker, J. (1995): A stable and (super 40) Ar/ (super 39) Ar isotope study of a major thrust in the Helvetic nappes (Swiss Alps); evidence for fluid flow and constraints on nappe kinematics. Geol. Society America Bulletin, **107**, 1129-1144.

DePaolo, D.J. (1986): Detailed report of the Neogene Sr isotopic evolution of seawater from DSDP site 590b. Geology, **14**, 103-106.

Eppel, H., Abart, R. (1997): Grain-scale stable isotope disequilibrium during fluid-rock interaction II: an example from a Penninic-Lower Austroalpine tectonic contact in eastern Switzerland. Am. J. of Sci., **297**, 707-728.

Etheridge, M.A., Wall, V.J., and Vernon, R.H. (1984): The role of the fluid phase during regional metamorphism and deformation. J. Metamorph. Geol., **1**, 205-226.

Franck, E.U. Wiegand, G. Dalmen, N. (1996): Water. In Ullmann's Encycopedia of Industrial Chemistry, **28A**, pp. 12, Verlag Chemie, Weinheim.

Frey, M. (1988): Discontinuous inverse metamorphic zonation, Glarus Alps, Switzerland: evidence from illite crystallinity data. Scweiz. Mineral. Petrogr. Mitt., **68**, 171-184.

Fyfe, W.S. & Kerrich (1985): Fluids and thrusting. Chem. Geol., **49**, 353-362.

Fyfe, W.S., Price, N.J., Thompson, A.B. (1978): Fluids in the earth's crust. Elsevier Scientific Publications, Amsterdam, Oxford, New York, 383p..